Ecological Tradeoffs to an Agricultural Amazonia: Investigating the effects of increased agricultural production on Amazonia's contribution to global climate and nitrogen cycling

A Dissertation
SUBMITTED TO THE FACULTY OF
UNIVERSITY OF MINNESOTA
BY

Christine Sierra O'Connell

IN PARTIAL FULFILLMENT OF THE REQUIREMENTS
FOR THE DEGREE OF
DOCTOR OF PHILOSOPHY

Advisers: Sarah Hobbie and Stephen Polasky

November 2015

Acknowledgements

I am eternally humbled by the wonderful, dedicated and wise mentoring I received during graduate school. Sarah Hobbie and Steve Polasky have been amazing advisors, as was Jon Foley during the first four years of my graduate work. Jennifer Powers and Rod Venterea, both phenomenal committee members, have been crucial to my development and went above and beyond when they took me under their wings. I wouldn't have made it through the wild ride that is graduate studies without these five wonderful mentors.

Just as importantly, I owe an enormous debt to the many, many mentors I worked with during my field training. Mike Coe at the Woods Hole Research Center has been crucial in helping me learn how to tackle a scientific question. Chris Neill (Marine Biological Laboratory) ushered me through my first trial-by-fire field campaign and Eric Davidson (University of Maryland Center for Environmental Science) was indefagitable in the face of my questions. A huge thanks to Marcia Macedo, Paul Lefebvre, Chelsea Nagy, Paulo Brando, Wendy Kingerlee, Gillian Galford, Ciniro Costa Jr., KathiJo Jankowski and the Cerri laboratory for being colleagues and inspirations during Tanguro adventures.

I could not have dreamed of conducting research in the Amazon without the support of Instituto de Pesquisa Ambiental da Amazônia (IPAM). Wanderley Rocha da Silva, Claudinei Oliveira-Santos, Adilson Ribeiro Coelho, Darlisson Nunes da Costa,

Ebis Pinheiro do Nascimento, Maria Lúcia Nascimento, Raimundo Mota Quintino, Sandro Rocha Pereira and Sebastião Aviz do Nascimento: muito, muito obrigada.

At the University of Minnesota, I was very fortunate to have great colleagues and collaborators: Jamie Gerber, Paul West and the Global Landscapes Initiative at the Institute on the Environment, the Polasky, Powers and Hobbie lab groups, my graduate cohort, and countless professors, researchers, postdoctoral scholars and fellow graduate students who provided key insight and support along the way. The Department of Ecology, Evolution and Behavior was my home at Minnesota, and I will proudly call myself an EEB-er into the future. I am grateful to the following funding sources: the National Science Foundation, the Mellon Mays Fellowship Program, the University of Minnesota Doctoral Dissertation Fellowship Program, the Bell Museum of Natural History, the Institute on the Environment and the Gordon and Betty Moore Foundation.

To the many friends who were my adopted Midwestern family, thank you for everything. To friends elsewhere around the world who got to witness the madness, huge hugs. I am lucky to be a member of the world's greatest community.

Finally, graduate school is temporary, but family is forever. Thank you, familia, for your endless love and support! I love you!

Dedication

For my dad. We love you and miss you.

Abstract

The Amazon rainforest is experiencing widespread land-use/land-cover change, much of which is driven by agricultural expansion and shifts in agricultural management. These changes have contributed to high annual greenhouse gas emissions, changing regional climate due to shifts in energy balance, and disruptions to nutrient cycles, occurring on a scale large enough to have ramifications for the larger earth system. This dissertation investigates how human land use for agriculture affects Amazonia's contribution to climate regulation and nitrogen cycling and the tradeoffs between agricultural production and ecosystem ecology.

First (**Ch1**), I model the impact of agricultural *expansion* on four important ecosystem services (agricultural production, carbon storage, biodiversity, and regional climate regulation) using data from a combination of remote sensing, model output, and geostatistical datasets. I find that different regions within Amazonia are of primary importance for each non-agricultural ecosystem service, suggesting that using complementary conservation strategies that target a collection of environmental goals could minimize the ecological impacts of expanding agriculture. Second (**Ch2**), I show that at the site-level, patterns of trace gas concentrations throughout the soil column differ between eastern Amazonian forest and deforested soybean fields, indicating that agricultural *expansion* can affect the carbon (C) and nitrogen (N) cycles at depth in Amazonian soils.

Amazonia's current croplands are also undergoing management *intensification*. I conduct a multi-year field campaign to measure how emissions of nitrous oxide (N_2O), a powerful greenhouse gas, carbon dioxide (CO_2) and methane (CH_4) change after fertilizer addition on an industrialized farm in Mato Grosso, Brazil. I find (**Ch3**) only modest increases in N_2O emissions on intensified croplands in comparison to Amazon forest, suggesting that cropland intensification may not necessarily lead to increased greenhouse gas emissions in southeastern Amazonia.

These projects use multiple spatial scales, multiple ecosystem response variables, and multiple approaches to quantify the ecological consequences of agricultural expansion and intensification in the Amazon rainforest. As global change continues, determining how to utilize dynamic tropical landscapes while minimizing ecological disruption will be key to tropical sustainability.

Table of Contents

List of Tables

List of Figures

Introduction

Perhaps more than any other terrestrial ecosystem on the planet, the Amazon rainforest is simultaneously responding to, and driving, global environmental change. Amazonia's[1] influences on the earth system are multiple: as the world's largest contiguous tropical forest, it is an enormous stock of sequestered carbon (Malhi *et al.*, 2006; Saatchi *et al.*, 2011), a hotspot of terrestrial biodiversity (Dirzo & Raven, 2003; Hubbell *et al.*, 2008), and a dynamic part of global hydrologic and nutrient cycles (Foley *et al.*, 2007). But these links are all vulnerable to changes in climate, atmospheric chemistry, and especially land use/land cover change: land use change has contributed to high annual greenhouse gas emissions (Malhi *et al.*, 2008; Davidson *et al.*, 2012a), changed the amount and timing of water flow out of Amazonian watersheds (Coe *et al.*, 2009; Stickler *et al.*, 2013), and is projected to lead to substantial species losses (Hubbell *et al.*, 2008; Feeley & Silman, 2009). Critically, the changes wrought in Amazonia could occur on a scale that would have global ramifications.

Like tropical forests writ large, much of Amazonia's land use change is caused by the pressure that growing needs for agricultural products have put onto forested landscapes (Soares-Filho *et al.*, 2006; Davidson *et al.*, 2012b). In the eastern Amazon, the so-called 'arc of deforestation,' deforestation is driven largely by the expansion of pasture (for cattle) and cropland (for soybean) (Morton *et al.*, 2006; Macedo *et al.*, 2012), both of which are increasingly in demand on international commodity markets (Rudel *et al.*, 2009; DeFries *et al.*, 2010). Further, as deforestation rates in Amazonia have slowed

[1] Henceforth, Amazonia will refer to tropical forest within the Amazon and Tocantins River basins.

since their peak in the mid-2000s, agricultural intensification[2], particularly of soybean croplands operated by large producers (Galford *et al.*, 2008; DeFries *et al.*, 2013), has becoming a dominant pattern of secondary land use change. Many agricultural systems in Amazonia now match the industrialized, intensive agricultural production generally seen in temperate, wealthy nations.

Though the biogeochemistry of Amazonia is more studied than that of many other tropical forest systems, there remain many unknowns surrounding the ecological consequences of agricultural expansion and intensification. Where are tradeoffs between agricultural yield and environmental impacts relatively large or small? What effects does cropland intensification have on trace gas emissions? On soil nutrient pools? Are there patterns at the site and landscape level that can refine our ability to manage one of the most critical ecosystems on the planet?

In this dissertation, I investigate how human land use for agriculture affects Amazonia's contribution to climate regulation and nitrogen cycling and the tradeoffs between agricultural production and ecosystem ecology. Chapter 1 takes a modeling approach to balancing non-agricultural ecosystem services and agricultural production across Amazonia as agriculture's footprint expands. In it, I develop a simple quantitative model to explore the tradeoffs between conservation goals and apply the model to Amazonia using high-resolution spatial ecological and agricultural data. This chapter uses the largest spatial scale in this dissertation, and considers Amazonia as a system that crosses ecotones and political boundaries. Chapter 2 also considers agricultural

[2] Intensification here meaning increases in agricultural productivity facilitated by management (e.g. via nutrient and water additions, seed technology and/or mechanization).

expansion, but at the smallest spatial scale considered in this dissertation (Figure 0.1). Working at Tanguro Ranch ("Fazenda Tanguro," in Portuguese), a large industrialized farm in eastern Amazonia (Mato Grosso, Brazil) in which approximately 65% of the landscape remains mature Amazon forest, while the remainder is high-productivity cropland, I look at the top 10 meters of the soil profile and ask whether deforestation and subsequent cropping systems have changed the carbon and nitrogen cycles at depth. Chapter 3 also features research conducted at Tanguro Ranch, but asks questions about the effect of cropland intensification on trace gas emissions from soil and measures those emissions patterns across the landscape. Working at multiple scales – system, landscape, and soil profile scale – enables these papers to considering several angles of how carbon and nitrogen are affected by Amazonia's changing agricultural regime.

The Amazon has the most industrialized agricultural system in the tropics and is concurrently experiencing global change. It is a study system that allows us to explore the ecological costs and benefits of an intensified agricultural system occurring at a large scale, for the first time, not in the temperate zone, but within the borders of a dynamic, ecologically unique and increasingly threatened tropical forest. This dissertation explores the implications of agricultural land use change for the carbon and nitrogen cycles in Amazonia, an area of uncertainty that is critically important as our agricultural and earth systems continue to change.

Figure 0.1. This dissertation considers the landscape-level (a) and site-level (b) effects of agricultural land use change on carbon and nitrogen in Amazonia (photos: C. S. O'Connell).

Chapter 1:

Balancing tradeoffs: Reconciling multiple environmental goals when ecosystem services vary regionally

Abstract

As the planet's dominant land use, agriculture often competes with the preservation of natural systems that provide globally and regionally important ecosystem services, particularly in tropical systems (Foley *et al.*, 2012; Nepstad *et al.*, 2013; Lapola *et al.*, 2014). How ecosystem service delivery is impacted by agriculture varies geographically, among services being considered, and across spatial scales. Thus, strategies to reconcile disparate land use goals are essential (Daily *et al.*, 2009; Davidson *et al.*, 2012b; Foley *et al.*, 2012; Nepstad *et al.*, 2013; Oliveira *et al.*, 2013; Lapola *et al.*, 2014). But when ecosystem services are not aligned in space, conservation decisions become reliant on human valuation (Goldstein *et al.*, 2012). Here, we explore solutions to this tension, using as a case study the Amazon, a key ecosystem and agricultural frontier. We show that different regions within Amazonia are of primary importance for agricultural production, carbon storage, habitat for biodiversity, and regional climate regulation. We then present a model that compares the impact of different agricultural expansion patterns on multiple ecosystem services and integrates human preferences into those deforestation patterns simply and transparently. Even under efficient, optimal conditions, we show that, as land use expands, small increases in the stated environmental priority for one

ecosystem service can lead to reductions in spatially offset ecosystem services by as much as 140%. Our results highlight the difficulty of managing land for multiple environmental goals in cases where ecosystem properties do not geographically vary in concert; the model presented here can guide value-laden conservation decisions and identify potential solutions that balance priorities. As agricultural production increases globally, carefully considering the regional ecosystem context alongside socio-economic priorities will be essential to designing complementary conservation strategies that achieve multiple desired environmental outcomes.

Keywords: conservation, Amazonia, land use, ecosystem services

Introduction

Increasing demand for agricultural products from a global population that is getting larger and wealthier has led to widespread conversion of natural habitat to cropland and pastureland: agriculture's footprint now covers nearly 40% of the planet's ice-free land (Foley *et al.*, 2012). This demand is projected to increase in the coming decades (Tilman *et al.*, 2011). Alongside sustainable intensification, expanding croplands and pasturelands is one way in which humanity can produce more agricultural output.

But land provides many other things of value beyond food, in particular suites of ecosystem goods and services (Daily *et al.*, 2009; Tallis & Polasky, 2009). Large-scale land use change from natural vegetation to agricultural lands affects several key aspects of the earth's environmental systems, including the standing stocks of biomass and soil carbon (Harris *et al.*, 2012), biodiversity (Pimm *et al.*, 2014), and the global hydrologic and nutrient cycles (Vitousek *et al.*, 1997a; Bonan, 2008). Agricultural expansion leads to attendant environmental impacts and the loss of ecosystem service delivery.

The environmental tradeoffs associated with land use conversion for agriculture are often framed as a case of food 'versus' natural systems. But the situation can be far more complicated – land resources provide multiple ecosystem services of interest, only one of which is agricultural production. Not all of these non-agricultural ecosystem service benefits are provided in the same place or in the same way (Nelson *et al.*, 2009), and conversion of intact ecosystems to agriculture can diminish the delivery of some non-

agricultural ecosystem services more than others depending on the landscape's ecological context (Stickler *et al.*, 2009; Goldstein *et al.*, 2012). Thus, continued land-use change for agriculture can put two (or more) non-agricultural ecosystem service goals in tension with each other due to a lack of alignment among different services across space or time.

These points lead to a fundamental challenge: can conservation strategies designed to increase agricultural production with one environmental goal at the fore (e.g., carbon storage) adequately address a second, third, or fourth environmental goal (e.g., biodiversity protection, provision of water resources, or pollination services)? If not, thinking carefully about which services to emphasize makes for difficult decisions and raises the importance of the relative value, financial or otherwise, of different ecosystem services.

Here, we use a general approach to illustrate the environmental challenges associated with the provision of multiple ecosystem services in the Amazon. Amazonia is a vitally important region that provides ecosystem services of regional and global importance and is a dynamic agricultural frontier (Foley *et al.*, 2007; Davidson *et al.*, 2012b; Nepstad *et al.*, 2014), making it a useful case study of multiple environmental tradeoffs. We take advantage of recently developed high-resolution, spatially-explicit ecological datasets (Del Grosso *et al.*, 2008; Powers *et al.*, 2011; Anderson-Teixeira *et al.*, 2012; Baccini *et al.*, 2012; Hiederer & Kochy, 2012; Feeley *et al.*, 2012a; Aide *et al.*, 2012; Mueller *et al.*, 2012a; Clark *et al.*, 2012; INPE (Brazilian National Institute for Space Research)) to assess the geographic variation in how agricultural expansion affects the delivery of four ecosystem services or properties associated with environmental goals

in Amazonia: agricultural production, carbon storage, high-biodiversity habitat, and biophysical climate regulation. We then quantify tradeoffs between increased agricultural production via agricultural expansion and each individual environmental goal. Finally, we conduct a series of simulations of "least harm" agricultural expansion while shifting the priority placed on different environmental goals to explore alternate strategies for protecting multiple ecosystem services in tandem.

We use spatially-explicit data in combination with a simple optimization model to show that, in geographically heterogeneous systems including Amazonia, land-use decisions that aim for the provision of multiple ecosystem services hinge on value-laden tradeoffs not only between food and the environment, but between different ecosystem services. Sustainable land use strategies will increasingly require a multi-dimensional, quantified approach to explicitly account for these tradeoffs as the earth system remains under pressure to provide agricultural and environmental output across the planet (Nelson *et al.*, 2009; Tallis & Polasky, 2009; Goldstein *et al.*, 2012).

Study system

The Amazon is host to a multitude of important environmental properties that are important to protect and are vulnerable to increasing land-use pressures (Davidson *et al.*, 2012a; Nepstad *et al.*, 2014). Amazonian agricultural expansion has substantial impacts on individual ecosystem services: carbon emissions (Soares-Filho *et al.*, 2010; Baccini *et al.*, 2012; Harris *et al.*, 2012), habitat for biodiversity (Soares-Filho *et al.*, 2006; Feeley &

Silman, 2009; Lenzen *et al.*, 2012), hydropower services and freshwater availability (Coe *et al.*, 2009; Stickler *et al.*, 2013) and climate-agriculture feedbacks (Oliveira *et al.*, 2013). Over the last 30 years, Amazonia has experienced rapid growth in agricultural production (INPE (Brazilian National Institute for Space Research)). Croplands and pasturelands expanded, and some areas now experience intensive management and dramatically higher cropland yields (Ray *et al.*, 2013). Notably, deforestation in Amazonia has slowed dramatically in recent years, after targeted policy and economic interventions (Nepstad *et al.*, 2014).

In this analysis, we do not make predictions about how land use in Amazonia might change; others have done so using sophisticated statistical techniques (Soares-Filho *et al.*, 2006; 2010). Rather, we ask how to weigh potential tradeoffs between environmental goals if land is managed in certain ways. The Amazon can serve as an effective exemplar of the challenges of addressing multiple environmental goals in the face of land use expansion: Amazonia spans several ecological gradients (e.g., precipitation and elevation), but functions hydrologically and climatically as an interconnected system (Davidson *et al.*, 2012a). The Brazilian Legal Amazon, which covers a majority of the Amazon River's watershed, is a cohesive management unit under pressure from diverse stakeholders (Soares-Filho *et al.*, 2014), with similar stakeholder dynamics between agriculturalists/developers and environmental interests playing out in the portion of Amazonia outside of Brazil's boundaries. This combination leads to an ecologically heterogeneous system of great global importance that is under pressure to

increase agricultural output as well as the production of a variety of ecosystem services – and makes it an ideal system to explore the tradeoffs among multiple ecosystem services.

Results

Agricultural production. We estimate the potential attainable agricultural yield for soybeans and cattle, key Amazonian commodities, on lands currently in agriculture and extend these estimates to regions of the Amazon not currently in agriculture (Figure 1.1, Supplemental Methods). Our estimates of attainable agricultural yields are optimistic because they assume that lands not currently in production but with similar climatic conditions to land currently in agriculture will generate similar yields (Figure 1.1). It is unclear whether western Amazonia can support high yields due to rainfall and topographic limitations (Supplemental Methods). Attainable soybean yields are estimated to be nearly uniform across Amazonia provided that producers have access to management technologies that enable them to realize these attainable yields (Foley *et al.*, 2012; Ray *et al.*, 2013). We estimate annual soybean yield to be 10.755 ± 0.837 million kilocalories (kcal) hectare^{-1}, which are on par with those of top global producers. For pasturelands, we estimate annual yields 0.053 ± 0.009 million kcal hectare^{-1} (Supplemental Discussion), though substantial uncertainty surrounds the upper limits on cropland-pastureland mixed-use intensification. As with cropland production, we make the conservative assumption that agricultural management practices that maximize yields will proceed without constraint.

Carbon storage. Land-use change releases carbon dioxide stored in vegetative biomass and soil organic matter. We estimate that agricultural expansion leads to the mean release of 214.0 ± 98.0 tonnes of carbon per hectare (Mg C ha^{-1}, Figure 1.1, Supplemental Figure S1.1, Supplemental Methods). The tradeoff between the carbon lost and agricultural yield gained from agricultural expansion (Mg C $kcal^{-1}$, Figure 1.2) shows a distinct spatial pattern across Amazonia, driven primarily by variation in the standing forest carbon stocks. There is less release of carbon per unit increase in agriculture in some flooded forests in the central Amazon and in the southeastern Amazon transition zone from forest to cerrado (tropical savannah). Because western and northeastern forests are carbon-rich and still relatively intact, additional food production in these regions generates disproportionately large impacts on carbon storage.

Habitat for biodiversity. The loss of biodiversity-rich habitat impacts ecotourism and global genetic diversity, among other ecosystem services (Chazdon, 2008). We use mapped ranges of Amazonian plant, mammal and bird species to estimate relative local diversity (the number of species ranges present in a given location, Supplemental Methods). Average relative diversity in a 5 arc-minute by 5 arc-minute area is 1026 ± 560 species represented (Figure 1.1) (499 ± 505 for plants, 79 ± 16 for mammals, 449 ± 91 for birds, Supplemental Figure S1.2). Relative species diversity we use here as a proxy for the quality of different habitats across a landscape. The largest tradeoff between habitat for biodiversity and increased agricultural production (species $kcal^{-1}$, Figure 1.2)

is in the Andes-Amazon region. The pronounced importance of Andes-Amazon habitat for biodiversity becomes more marked when we take into account not only the number of overlapping species ranges but also the size of each range using a rarity index (Supplemental Text S1.4. Full methods: Biophysical climate regulation Supplemental Figure S1.3). Species with smaller ranges are likely to be more rare and more vulnerable to extinction due to habitat loss.

Regional climate regulation. Agricultural expansion can also drive changes in regional climate (Anderson-Teixeira *et al.*, 2012) through changes in the flows of heat and water from the land to the atmosphere, potentially affecting local (Oliveira *et al.*, 2013) and downwind (Bagley *et al.*, 2012) ecosystems. We simulated the effects of replacing natural vegetation (i.e., forest or cerrado) with agricultural lands on local atmospheric temperature and moisture using the land surface model Agro-IBIS (Anderson-Teixeira *et al.*, 2012) (Supplemental Methods, Supplemental Figure S1.4). We estimate that deforestation leads to a regional warming of 0.33 ± 0.29˚C (annual mean) and a regional atmospheric drying (due to a decrease in atmospheric moisture loading from vegetation) of 0.84 ± 0.31 mm H_2O per day (Figure 1.1). The spatial pattern in the tradeoffs between regional climate regulation and agricultural production (change in (delta) ˚C $kcal^{-1}$ and change in (delta) mm H_2O day^{-1} $kcal^{-1}$, Figure 1.2) is driven by strong climate seasonality in the east, where relatively short-rooted crops have dramatically reduced evapotranspiration rates during the lengthy dry season relative to more deeply rooted forests that they replaced (Supplemental Figure S1.5). Notably, eastern Amazonia, the

region that currently has the highest levels of deforested land (Figure 1.2) has the least efficient climate regulation tradeoff with agriculture, implying that substantial impacts on regional climate regulation could already be underway. Precipitation extremes in Amazonia are increasingly common (Gloor *et al.*, 2013), and the interaction of drought and landscape level changes to energy balance could have large effects on forest functioning (Gatti *et al.*, 2014) and fire regimes (Alencar *et al.*, 2015).

Regional atmospheric warming and drying could have significant impacts on agriculture and ecosystems in Amazonia (Oliveira *et al.*, 2013), northern Argentina and southeastern Brazil (Bagley *et al.*, 2012), as well as on hydropower (Stickler *et al.*, 2013) and urban water supplies (Setälä *et al.*, 2013), suggesting that regional biophysical climate disruption is an environmental tradeoff that ought to be considered in tandem with the biogeochemical effects of greenhouse gas emissions on the global climate. Our modeled estimates of the tradeoff between agriculture and regional climate regulation are conservative, incorporating neither climate-agriculture feedbacks (i.e., any post-clearing reduction in agricultural yields due to local climatic disruption) nor the influence of larger regional circulation changes, which likely make some areas more prone to regional climatic disruption than our results indicate (Malhi *et al.*, 2008; West *et al.*, 2011; Oliveira *et al.*, 2013) (Supplemental Discussion).

Single- and multi-service tradeoffs. To detect locations where preventing deforestation would secure *multiple* environmental benefits, we identified locations with the greatest potential to store carbon, provide species-rich habitat, and regulate regional climate per

unit of agricultural production foregone (Figure 1.2, highest quartile of ratios between agricultural production and each ecosystem service, where a large ratio indicates a large agricultural gain per unit of environmental harm). The top performing areas for each of the three non-agricultural ecosystem services are clustered, indicating that particular regions within Amazonia would be effective at preserving a particular ecological function independently.

However, the top performing areas for the delivery of each non-agricultural service are not geographically aligned: protecting eastern Amazonia is most important if the conservation priority is regulating regional climate, but protecting western Amazonia is most important if the conservation priority is maintaining biodiversity. Consequently, there are limited opportunities to simultaneously protect *both* regional climate and biodiversity in the same location. Protecting carbon stocks provides more opportunity for cobenefit protection. If left in forest, areas with large carbon stocks cover a swath from western to eastern Amazonia that intersects with areas of high relative biodiversity in the west and some portions of high-performing climate regulation areas in the northeast (Figure 1.2). Qualitative comparison indicates that a targeted land conservation strategy can be effective at limiting a single environmental tradeoff in the face of agricultural expansion.

Limiting the tradeoffs for multiple ecosystem services at once in geographically variable regional contexts will require difficult decisions about how to balance different environmental goals. The relative priority of environmental goals may alter where that land expansion occurs, and thus the associated impacts. To explore this tension, we use

land-use optimization simulations to assess (1) the effects of different geographic patterns of deforestation and (2) how prioritizing environmental goals in relation to one another shifts ecosystem service delivery, even under efficient, "best-case-scenario" land use expansion (Supplemental Methods). In each simulation (n=882), we experimentally double Amazonia's agricultural footprint at the least combined environmental harm while varying the conservation priority given to carbon storage, habitat provision, and regional climate regulation. We use a simple model to determine where land conversion leads to the "least combined environmental harm":

$$V_{ij} = \sum_{k=1}^{N} w_k D_{kij} p_{ij}$$

Here, V is the value placed on a parcel of land remaining in natural vegetation, w_k is the weight, or human preference given to each ecosystem property, D_{kij} is the delivery of the ecosystem property, k is an index for each ecosystem property (e.g., potential agricultural yield, carbon storage, etc.) being incorporated into V, p_{ij} indicates whether locations are to be *a priori* protected, and ij points to the grid cell.

Each grid cell is assigned a combined environmental value V, which depends on the relative weights (w) assigned to each ecosystem service and maps of potential agricultural yield and non-agricultural ecosystem service delivery (D_{kij}, Figure 1.1); deforestation is simulated with perfect efficiency (i.e., cells with low V values are converted to agriculture in rank order). The relative weights (w) between factors was

varied across each simulation systematically in 5% increments ($w_1 = (1.0, 0, 0), w_2 = (0.95, 0.5, 0)$, ...) for an n=441. Finally, each simulation was run where current Amazonian protected areas were not eligible for conversion to agriculture (via p_{ij}). For instance, in one simulation lowering carbon emissions could receive 55% of the priority, protecting high numbers of species could receive 30% priority and limiting changes to regional climate regulation could receive the final 15% priority. One optimization would be run without regard to protected areas, showing the theoretical boundaries of efficient land-use change. A second simulation would not allow any land-use change within protected areas, to approximate efficiency within current bounds. While these simulations were not mean to be realistic future Amazon land use scenarios, they do allow us to explore broad patterns in balancing multiple landscape goals in heterogeneous systems as prioritization varies.

These simulations deliver similar amounts of additional agricultural output by design, but their environmental impacts vary considerably (Figure 1.3). As higher priority is placed on either carbon storage, habitat provision, or regional climate regulation (from 0% to 100% priority for each), agriculture expands optimally into areas that emit less carbon, affect fewer species, or cause less disruption to regional climate after land-use change, leading to lower overall levels of carbon emissions, destruction of high-quality habitat or regional climate disruption (Figure 1.3a,e,i). The Pearson's correlation coefficients (ρ) between carbon storage priority level and total TgC emitted, habitat priority level and species ranges affected and regional climate priority level and the regional climate index are -0.78, -0.57 and -0.93, respectively (p-values all < 0.001),

indicating strong negative correlations. By contrast, the impacts on services not targeted rise as the priority is shifted increasingly towards a single environmental goal: as carbon priority increases from 25% to 75%, the mean regional climate index increases from 0.43 to 0.58 (Figure 1.3c). Similarly, as regional climate priority rises, the carbon emitted as agriculture expands increases by >100% and the number of species ranges affected rises by 35% (Figure 1.3g-h).

Linear trends belie the wide spread in outcomes for the two "non-prioritized" ecosystem services. Balancing more than two ecosystem service goals requires placing value judgments on, here, the second and third service under consideration. Those relative priorities in some cases lead to large variation in how impacted secondary and tertiary environmental goals are. For instance, even when habitat conservation is given 75% of the environmental priority, simulations that value regional climate regulation highly have a regional climate index ~40% lower than simulations that value carbon storage highly (Figure 1.3f). Explicit conservation goals can produce sizeable positive environmental impacts for the primary environmental goal under consideration, as well as secondary goals.

3-dimensional efficiency frontier. Land use expansion simulations indicated that, at a given priority level for each ecosystem service, there could be large variations in the delivery of the balance between the remaining services. We plotted each land use simulation as a point on a 3-dimensional efficiency frontier (Figure 1.4), which shows the upper limit service delivered from the landscape given defined constraints (here, the

footprint of agriculture). We see that a swath of "Goldilocks" land use arrangements do appear on the frontier: simulations where a medium amount of species ranges are affected, regional climate is moderately disrupted and a relatively small amount of C is emitted. By contrast, there are few clear "win-win-win" land use arrangements, where a simulation with low total C emissions appears along the efficiency frontier between habitat and climate regulation (i.e., points towards the upper right quadrant, Figure 1.4). Instead, isoquants indicate that land use simulations that perform well for carbon storage appear densely bundled in efficiency space away from simulations that perform well for regional climate regulation.

Discussion

Our results suggest that even if agricultural lands were to be increased via a "least harm" pathway, in ecologically heterogeneous regions, large and differential effects on the earth system can result depending on the particular environmental goals. Including additional ecosystem services, such as those related to disruptions to water or nutrient cycles, further complicates our ability to design land-use strategies that maximize both agricultural and multiple environmental benefits. For this reason, a "one-size-fits-all" land conservation strategy in the Amazon that attempts to simultaneously achieve multiple environmental goals by managing for any particular ecosystem service is unlikely to be effective. Instead, a "portfolio" approach that strategically targets different regions of Amazonia to achieve different environmental outcomes could be a way forward; the current arrangement of protected areas in Brazil approaches this strategy in

portions of the Amazon (Soares-Filho *et al.*, 2010), likely why simulations that consider or do not consider protected areas are qualitatively similar (Figure 1.3).

Here, we explore how balancing multiple ecosystem services can be navigated despite spatial heterogeneity in a context relatively free from socio-governance constraints. Exploring tradeoffs under efficient, optimal conditions allows us to determine the outer bounds of what is possible were environmental goals determined, stated, and pursued without inefficiencies. Notably, even under these unimpeded conditions balancing multiple ecosystem services proves a challenge at the regional scale. In actually, several realities of modern conservation, and the associated challenges, merit discussion.

Quantifying competing interests. We imagine this as a first-pass effort towards developing quantitative tools to reconcile environmental goals that differ across space and time. In this case study, we consider ecosystem service delivery across space, but our approach, which combines prioritization weights and estimates of ecological properties before and after a given landscape change (here, conversion to agriculture), could be applied to service delivery across time, as well as to any landscape with heterogeneous ecological properties.

In cases where delivery of different ecosystem services do not align in space, subjective decisions about environmental and land-use priorities must be made when setting land-use and road-building policies, expanding private land holdings, etc. Directly incorporating these subjective preferences for particular environmental priorities

allows us to measure how varying human preferences can influence the environmental outcomes associated with land use expansion. Indeed, shifts in preference lead to significant differences in earth system impacts: which environmental priorities are valued in the face of land-use change may have far-reaching effects on incurred environmental impacts. This approach and similar analyses can be used at the regional scale to explore land conservation approaches and inform the balance between environmental priorities.

The framework above can flexibly incorporate disparate meanings of "human preference." Here we apply qualitative priorities, varying priorities between 0-1 to indicate the relative attention and importance placed on a particular service. Alternatively, a financial valuation approach could be substituted into our prioritization model (e.g., prices in place of weights w_k), with alternate discount rates for each service being considered if applicable to the study system. We declined to set weights using prices in this case study in order to investigate the full suite of simulations irrespective of uncertainties in ecosystem service pricing. Using prioritization weights could be beneficial for conducting theoretical cost-benefit analyses or considering alternate policy approaches, where weights integrate across stakeholder groups. Alternatively, where we compared sets of simulations with and without the potential *a priori* importance of protected areas, the same approach could be used to quantify who wins and loses under different land use regimes. For instance, p_{ij} could be defined not as a protected area metric, but instead as a specific portion of the landscape of particular importance to the livelihood of a given stakeholder group.

Incorporating uncertainty. Incorporating uncertainty into the land use optimization approach could strengthen this framework. We used a Monte Carlo approach to integrate uncertainty in plant biomass carbon stocks, soil carbon stocks, and soil carbon stock loss factors which was effective in setting bounds on our spatial estimates (Supplemental Figure). A similar Monte Carlo approach could be employed to estimate the sensitivity of the simulated land use patterns to uncertainty in the underlying data: the efficient agricultural expansion pattern for each set of priority weights could be calculated for many spatialized datasets that are perturbed based on the underlying uncertainty of carbon stock, regional climate and biodiversity effects of deforestation. A less computationally intensive approach would be to run each optimized land use simulation for the mean value of each service estimate in each cell (as we have done here) and also for +/- one standard deviation for each service in each cell. This would lead to an overestimate and an underestimate of ecosystem service delivery that could define the boundaries of land use impacts across a study system. Further improvements include using models that consider how ecosystem services interact during and after land use change (Isbell *et al.*, 2014).

Land conservation and governance context. While ecological explorations like the above can be useful to investigate conservation possibilities and their implications, in reality the land conservation and governance context of regions like Amazonia are the driving forces behind the relative priorities given to different environmental goals. Comparing the social and political context of a system to efficient land use outcomes

such as those generated above can help define what environmental priorities are relatively underserved.

In the case of Amazonia, large protected areas in the Brazilian states of Pará and Mato Grosso (World Database on Protected Areas, Supplemental Figure) overlap extensively with the high-delivering areas for biophysical climate regulation highlighted in Figure 1.2. Western Amazonas state (Brazil) and two large protected areas in Peru overlap extensively with areas of biodiversity-rich habitat, and in some cases with both high performing biodiversity-rich habitat areas and high-performing carbon storage areas. Protected areas in northwest Amazonas also protect carbon-rich forests. Broadly, current protected areas, in the north and west of the Brazilian Legal Amazon particularly (Soares-Filho *et al.*, 2010), are distributed well in space and do overlap with portions of all three high-delivering ecosystem service regions (Figure 1.2). Indeed, the Brazilian Amazon's protected areas are key to ecosystem service protection (Soares-Filho *et al.*, 2010) and Brazil's protected areas maintain low deforestation rates because of a multi-pronged set of government, private sector and non-governmental organization initiatives to limit Amazonian deforestation (Nepstad *et al.*, 2014). That said, Lapola et al. (Lapola *et al.*, 2014) note that the eastern Amazon region and cerrado biomes in Brazil have a less extensive protected area network; this portion of Amazonia is highly important for regional climate regulation. In this case, comparing strictly efficient land use simulations with the current strengths and weaknesses in Amazonia's protected lands can highlight a potential area of focus for environmental stakeholders.

Not all landscapes that may be managed synthetically for ecosystem service delivery will have the robust and relatively holistic public policy infrastructure of Amazonia. In cases where landscapes under consideration do not necessarily have a current and ongoing conservation context, data on revealed or stated preferences for avoiding environmental impacts can be used to put this exploratory model into perspective. In the absence of a targeted conservation agenda for a landscape, or when exploring the implications on future land use decisions on multiple ecosystem services, we see our optimization model of the efficient outcomes from a wide variety of preferences as a comprehensive first effort that can supplement careful consideration of the social and political context on top of the local ecology.

Balancing multiple ecosystem services must be an explicit, targeted environmental goal as land resources become increasingly valuable. A purposefully-adopted scheme of complementary conservation strategies across large, interconnected ecosystems would be a massive conservation undertaking. In this case, coordination among the multiple nations with Amazonian land holdings and other governance structures could overcome some political and economic constraints. Given the dual pressures on Amazonia and other heterogeneous landscapes to provide increased agricultural production and maintain multiple ecosystem services, determining how to balance multiple human benefits on constrained land resources is of critical importance to conservation practitioners, decision-makers, and stakeholders across the globe.

Methods Summary:

Potential agricultural yield. We estimate the attainable yield of soybean cultivation across Amazonia using a yield gap approach (Mueller *et al.*, 2012b) with extended climate bins that encompassed the study region. We estimate attainable pasture yield across Amazonia by linking a model of non-tree aboveground net primary productivity (Del Grosso *et al.*, 2008) to intensified stocking densities (head of cattle per hectare of pasture) reported in the literature for Amazonian pasture systems. Cropland and pasture attainable yields are converted to kilocalories per hectare for direct comparison.

Carbon stock losses. We derive a map of above-ground carbon contained in natural vegetation by combining a year 2008 map of live woody biomass carbon (Baccini *et al.*, 2012) with a year 2008 map of natural vegetation developed by combining three high-resolution land cover datasets (Aide *et al.*, 2012; Clark *et al.*, 2012; INPE (Brazilian National Institute for Space Research)). We estimate soil carbon emissions post-clearing using a map of soil organic carbon stocks (top 30cm) (Hiederer & Kochy, 2012) and a spatially-explicit map of soil carbon stock change factors (Powers *et al.*, 2011). We calculate a bootstrapped 95% confidence interval around the mean carbon loss from vegetation and soil carbon post-land use change across Amazonia.

Relative species richness. We use online databases of vascular plant, mammal and bird herbarium and museum collections tied to georeference data to compile presence/absence

observations for Amazonian plant, mammal and bird species. Those geolocated presence/absence data are combined with mean annual temperature, Maximum Climatological Water Deficit (a measure of water stress and precipitation regime), and ecoregion identity (serving as a proxy for non-climatic factors such as soil type) to model the distribution of each species using a simple species distribution model (Feeley *et al.*, 2012b). We define relative species diversity as the number of overlapping species ranges in each 5 arc-minute by 5 arc-minute grid cell.

Biophysical climate regulation. We use Agro-IBIS, a process-based ecosystem land-surface model, to model the net radiation, latent heat flux and sensible heat flux across Amazonia for three land use types: natural vegetation, grass and soybean cultivation. Agro-IBIS has previously been calibrated for use in Amazonia (Anderson-Teixeira *et al.*, 2012). We calculate the effects of land use change on energy balance as the difference in energy fluxes between the natural vegetation and the agricultural simulations. We then convert the energy balance impacts of land use change into impacts on air temperature and impacts on atmospheric moisture *sensu* West et al. (West *et al.*, 2011)

Tradeoffs associated with agricultural expansion. We experimentally double the land in non-natural vegetation as of 2008. New hectares of agriculture are allocated to locations where land clearing would lead to the least environmental harm, defined as a composite index of harm via carbon emissions, loss of habitat with high relative species richness, and potential disruption to local biophysical climate regulation. The general

equation is printed below, where V is the synthetic value placed on a parcel of land remaining in natural vegetation, w_k is the weight, or human preference, given to each ecosystem property, D_{kij} is the delivery of the ecosystem property, k is an index for each ecosystem property being incorporated into V, p_{ij} indicates whether locations are to be *a priori* protected, and ij points to the grid cell.

$$V_{ij} = \sum_{k=1}^{N} w_k D_{kij} p_{ij}$$

The relative weight between those factors was varied across each simulation systematically in 5% increments ($w_1 = (1.0, 0, 0), w_2 = (0.95, 0.5, 0)$, ...) for an n=441, and simulations were run with or without regard to current protected areas (thus, total n=882). Maps of potential agricultural yield and non-agricultural ecosystem service delivery are used to estimate the number of calories and environmental impacts of each spatial pattern of agricultural expansion.

Figures:

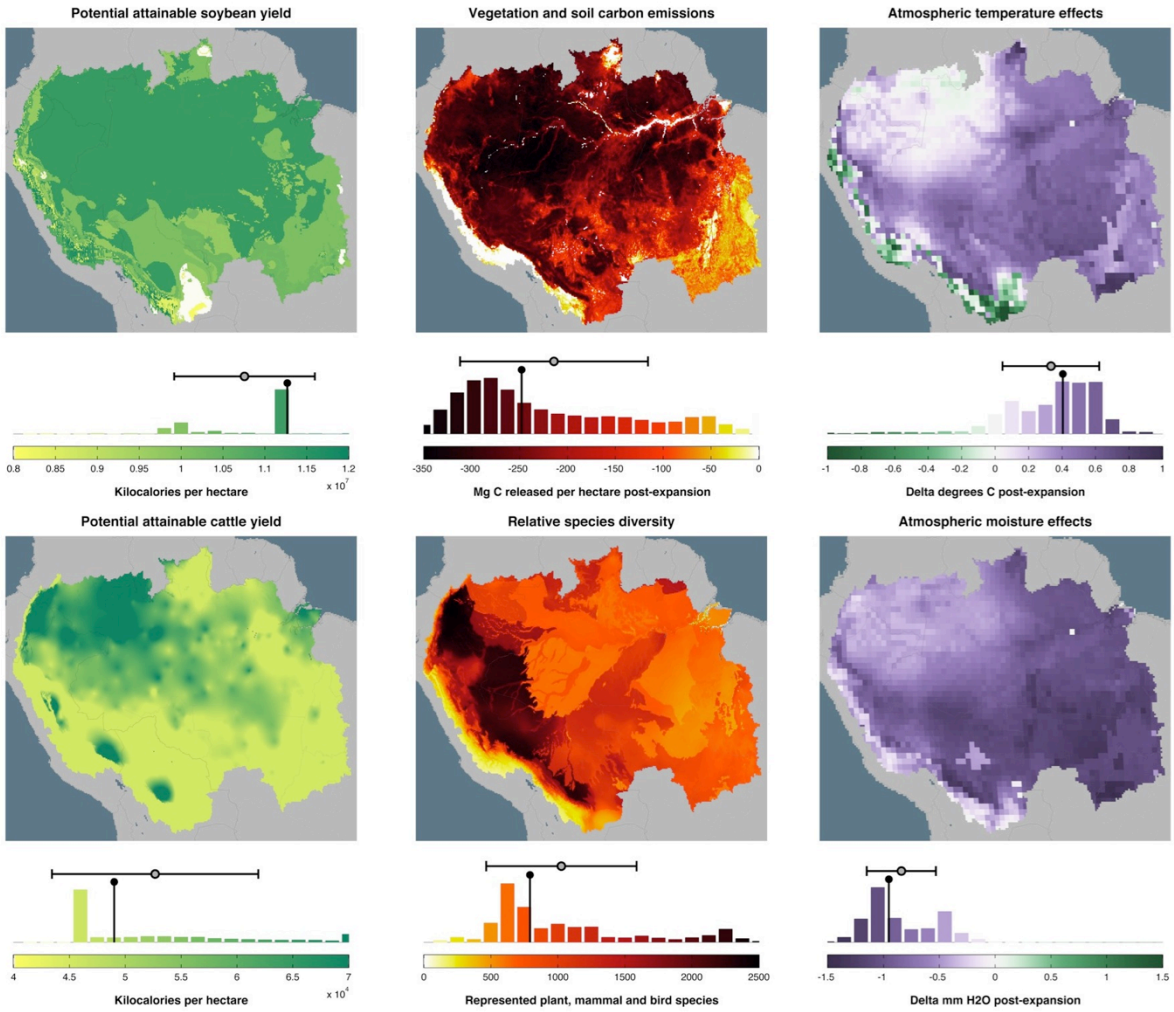

Figure 1.1. Spatial pattern, landscape mean (grey open dot), standard deviation (whisker lines), and median (vertical stem plot) of the agricultural benefits and environmental costs associated with future agricultural expansion. See Supplemental Methods and Supplemental Figure S1.1 for uncertainty measures.

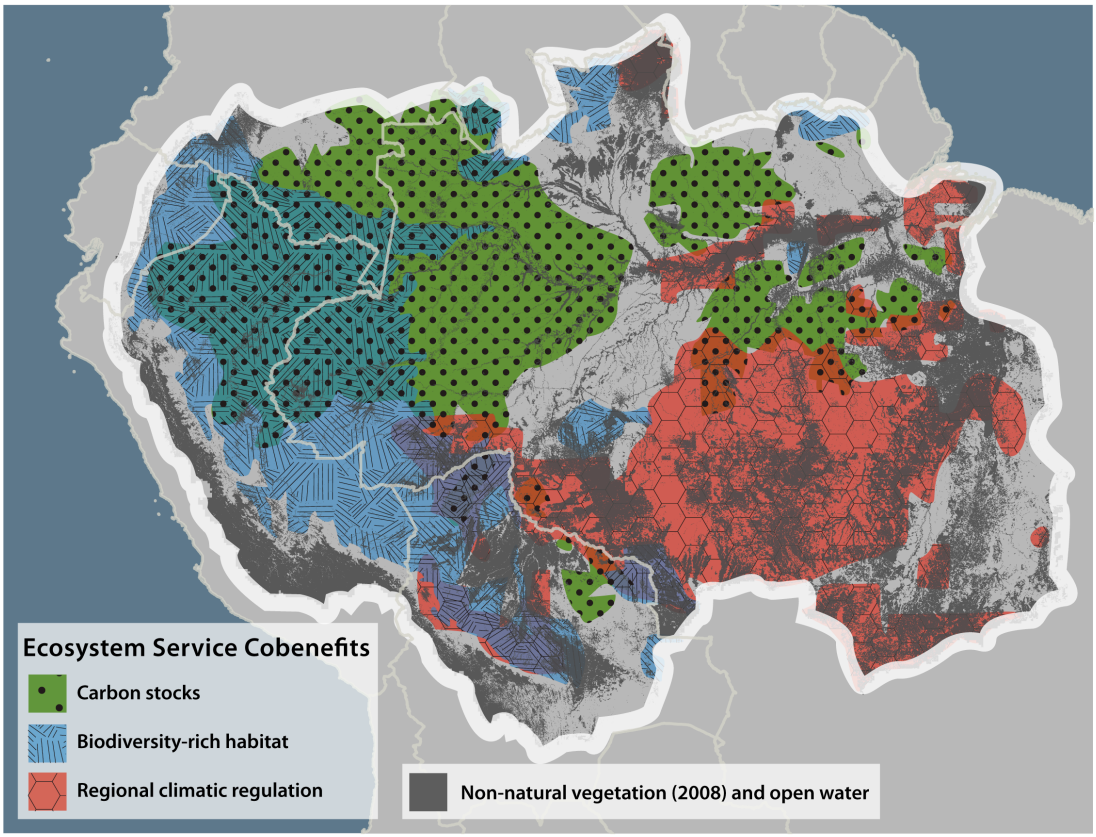

Figure 1.2. Potential ecosystem service cobenefits to avoided agricultural expansion. Highlighted areas are locations that store vegetative and soil carbon, provide biodiversity-rich habitat or regulate biophysical climate in the top 25% of cells for each ecosystem service (Figure 1.1). Non-natural vegetation as of 2008 or areas of open water are indicated in grey (Supplemental Methods).

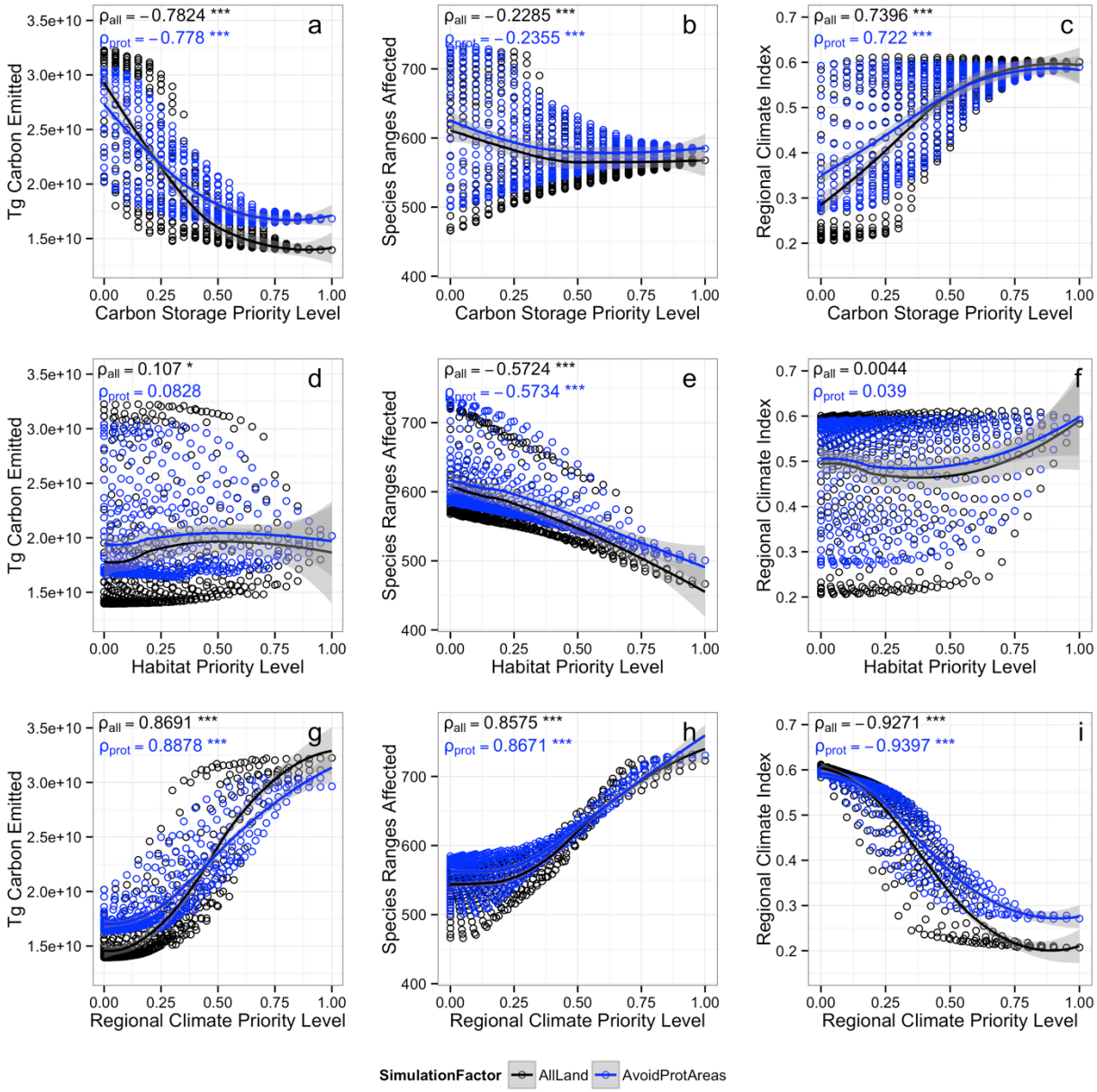

Figure 1.3. Variation in environmental impacts for land-use simulations in which Amazonia's land-use footprint was doubled at the least combined environmental harm; simulations apply different levels of environmental priority to the three ecosystem services of interest: minimizing impacts to carbon storage, habitat provision and regional

climate regulation is balanced according to priority "weights" which add up to 100% (Supplemental Methods). As the priority given to a given service rises (x-axis), the impact of agricultural expansion on that service decreases while the impacts on the remaining services rise, though often with substantial spread (e.g., panel 3a (C emitted decreases when C priority increases) versus panel 3i (regional climate stabilization decreases as C priority increases). Agricultural "optimal expansion" scenarios were optimized when strictly avoiding protected areas (blue data points, ρ_{prot}) and without avoiding protected areas (black data points, ρ_{all}); qualitative trends hold regardless. Trend lines are Loess local regressions with a 95% confidence interval. ρ is Pearson's linear correlation coefficient (measures correlation on a -1 to +1 scale) which is marked as significantly different from zero as *** when p-value <0.001, ** when p-value <0.01 and * when p-value <0.05. Regional climate index is the mean of the normalized deviations in heat and moisture regulation after land use change where +1.0 is a large amount of biophysical climatic deviation.

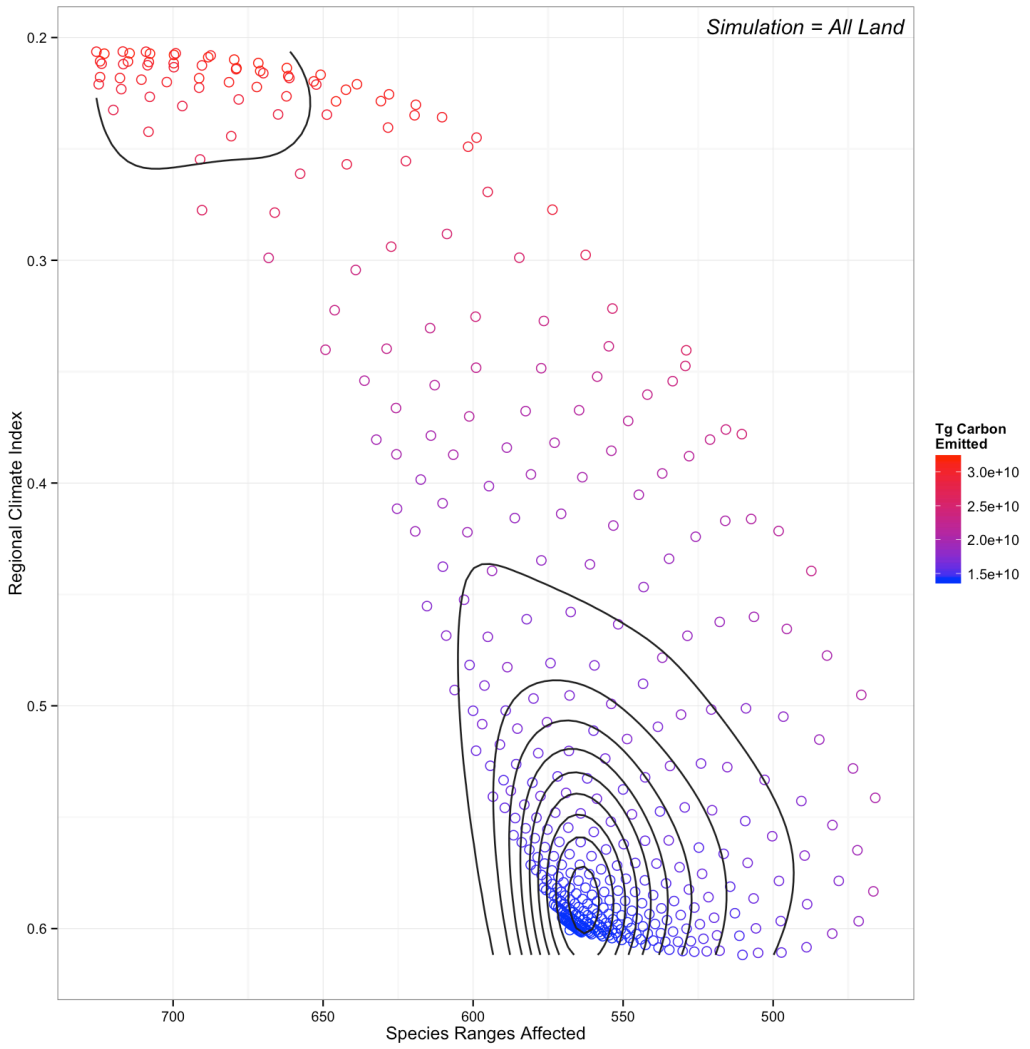

Figure 1.4. The 3-dimensional efficiency frontier defined by the efficient land use simulations (All Land simulations, n=441, e.g., those without avoidance of protected areas; results are similar under both conditions). Points towards the upper right of the figure represent a traditional, 2-dimensional ecosystem services "efficiency frontier" (here, habitat trading off with regional climate regulation). Since each land use simulation was fully efficient, including carbon storage (color bar) creates a 3-

dimensional tradeoff surface. Lines are topographic isoquants to aid with data visualization.

Supplemental Figures:

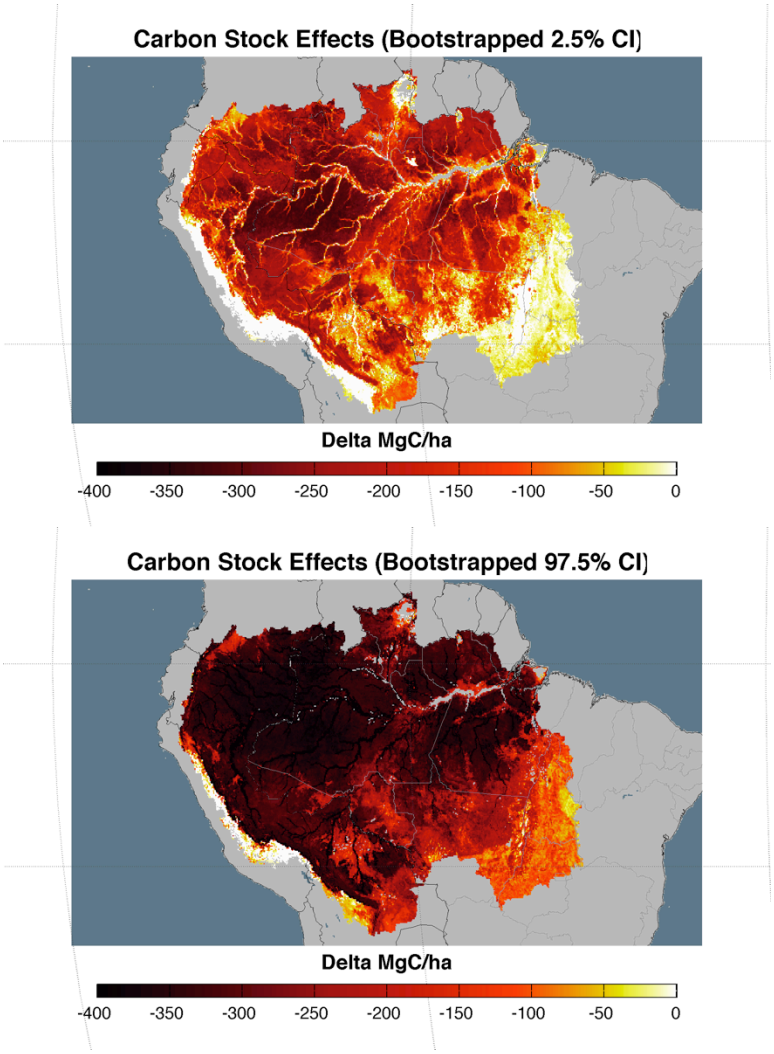

Supplemental Figure S1.1. Bootstrapped 95% confidence interval of carbon emissions ha^{-1} post-land use change from loss of vegetation and soil carbon stocks. The mean value of carbon stock effects is the value reported in Figure 1.1 in the main text of this paper.

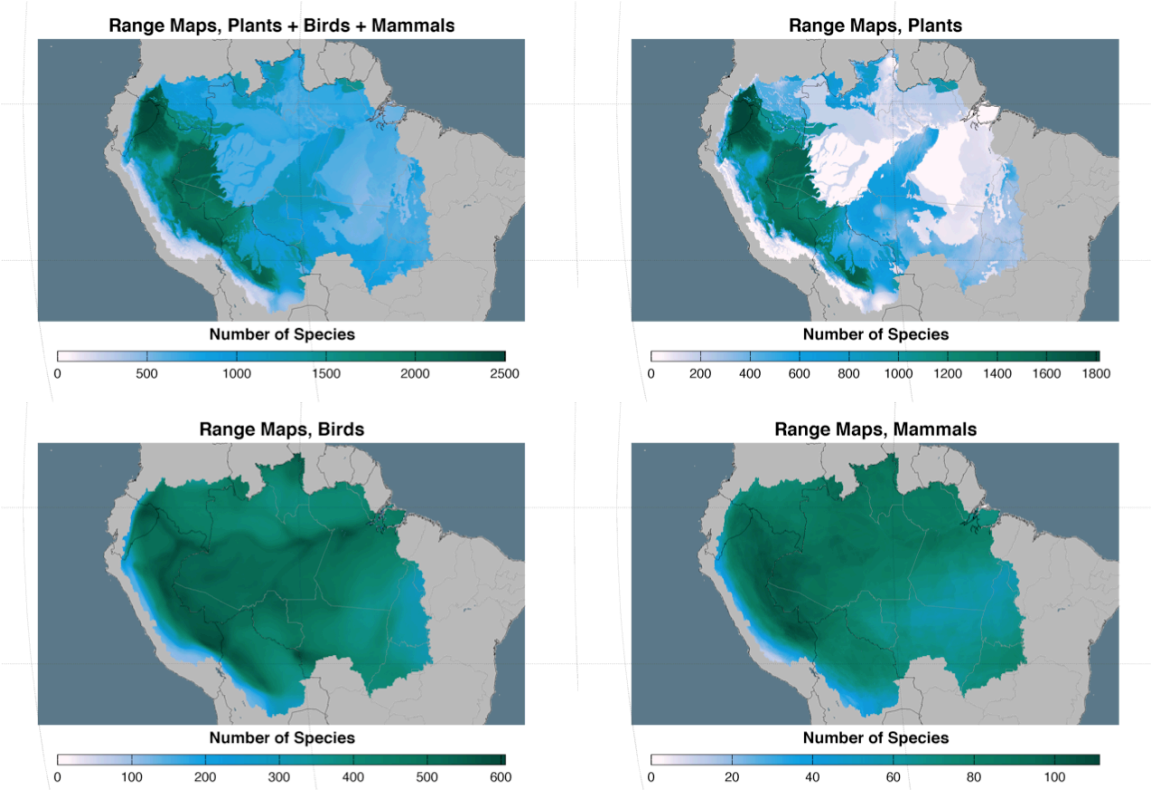

Supplemental Figure S1.2. Relative species diversity for the three taxa groups considered: plants, birds, and mammals. The combination map above is reported in Figure 1.1 in the main text of this paper.

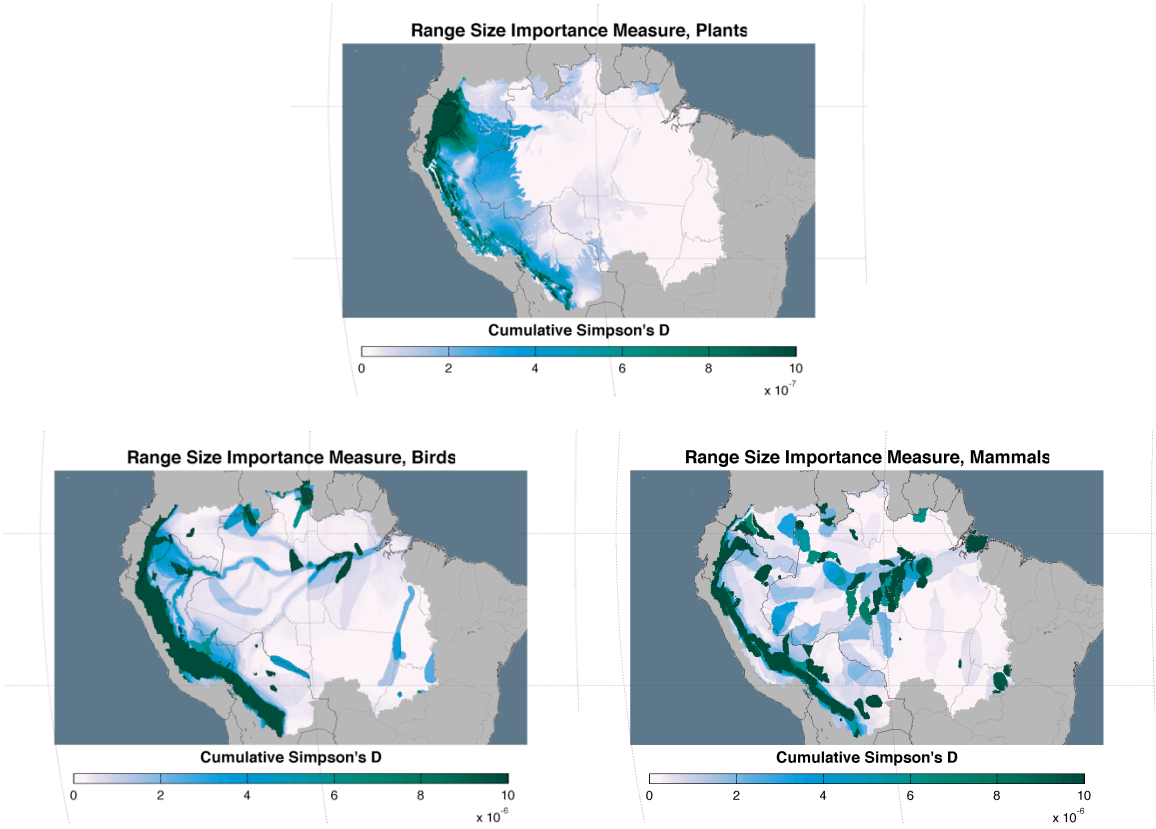

Supplemental Figure S1.3. We used a cumulative rarity index that accounts for range size, based on the formula for Simpson's D (a biodiversity index that measures species evenness in a community), for the three taxa groups considered. Our rarity index was defined as:

$$D = \sum_{i=1}^{n} 1/p_i^2$$

where n is the number of species of plants, birds or mammals, and p_i is the number of cells in our estimated range for that species.

Using a range-weighted biodiversity metric shows a similar pattern as Supplemental Figure S1.3 much more starkly. If the priority is on protecting natural

landscapes that are home to many small-ranged species, then the Andes draw attention even moreso as high-priority lands. This isn't surprising when you consider that biodiversity in areas with sudden topographic changes is high because habitat type is changing very suddenly with elevation. Those sudden changes act to restrict potential habitat. The same effect is not present on Amazonia's flat floodplain for plants, but habitats adjacent to major waterways are here associated with higher range-adjusted habitat priority.

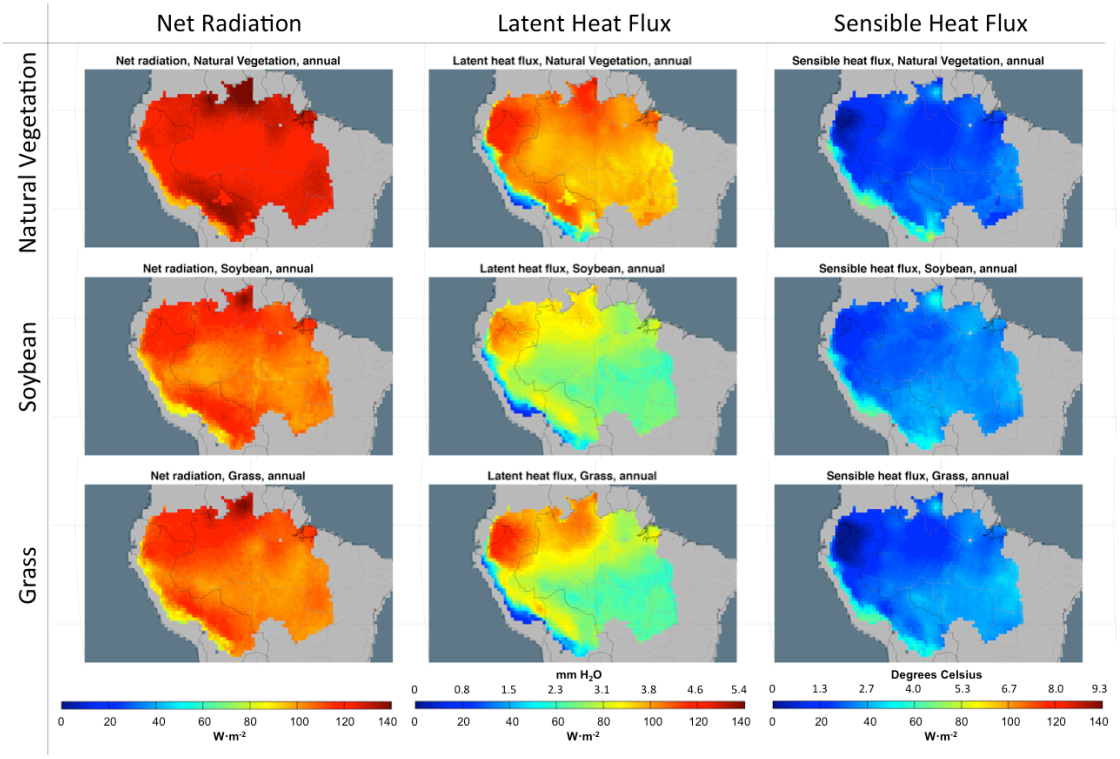

Supplemental Figure S1.4. Energy balance simulation results (annual mean) for natural vegetation, soybean cultivation, and grass (representative of pastureland).

Net radiation (R_{net}) is higher in the natural vegetation simulation than in the soybean or grass simulations. Grass and soybeans both have higher albedo than moist tropical forest or cerrado, the two dominant natural vegetation types in Amazonia, resulting in more incoming solar radiation being absorbed by natural vegetation than either of the two alternate land cover categories and explaining the higher R_{net} values.

How excess absorbed energy (the portion of R_{net} not used in photosynthesis) is balanced – by some combination of latent and sensible heat flux – also differs between

different land uses. The natural vegetation simulation sees excess energy balanced primarily by latent heat flux. In contrast, the agricultural simulations emit much larger proportions of the landscape's excess energy as sensible heat. These results are consistent with previous work using different models (West *et al.*, 2011) and with theory (Bonan, 2008; Jackson *et al.*, 2008).

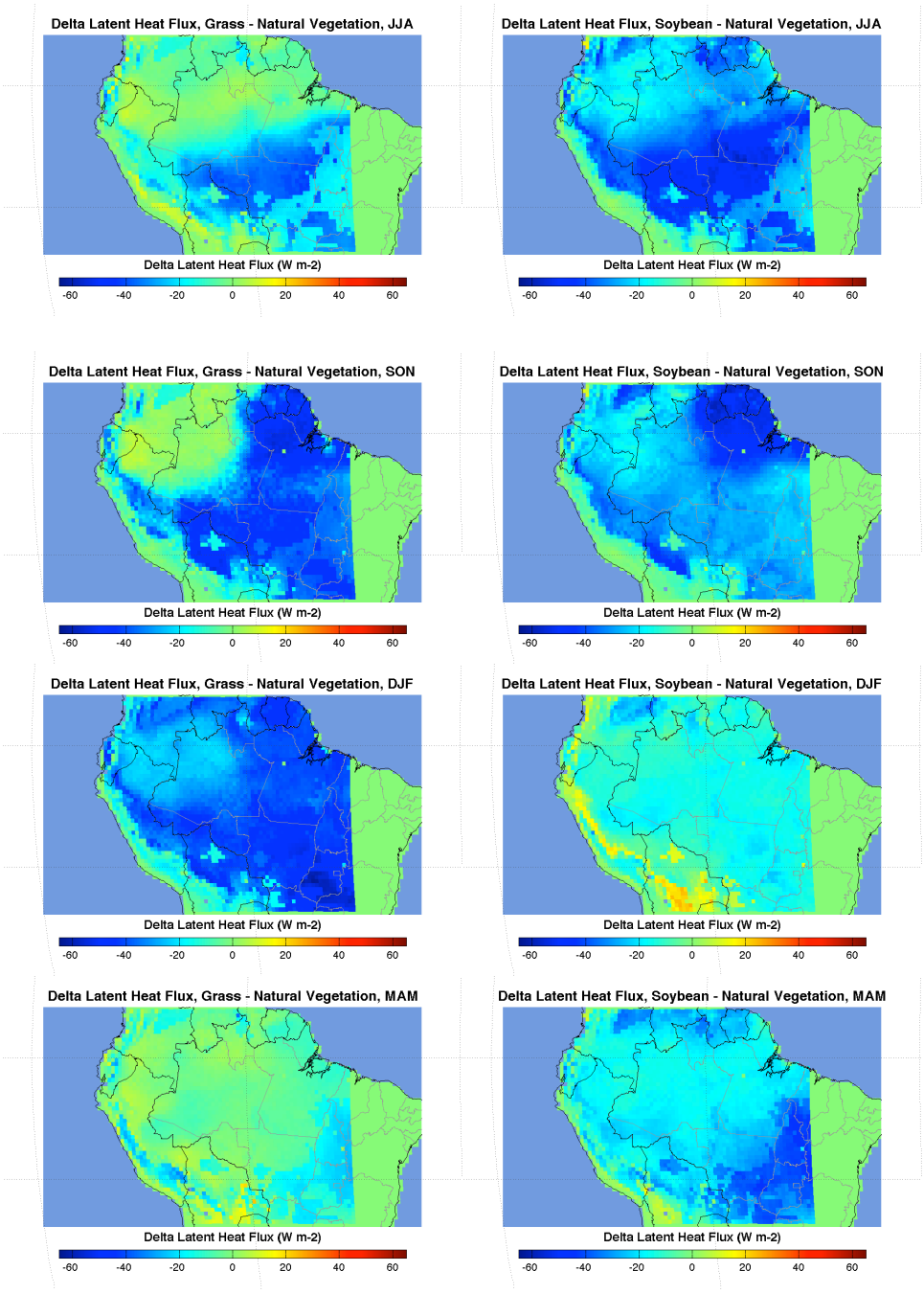

Supplemental Figure S1.5. Seasonality of changes to biophysical climate regulation post-agricultural expansion. Simulated changes in latent heat flux after conversion to

grass (representative of pastureland) or soybean cultivation from natural vegetation for each season (designated in common 3-month increments, JJA = June, July, August, etc.).

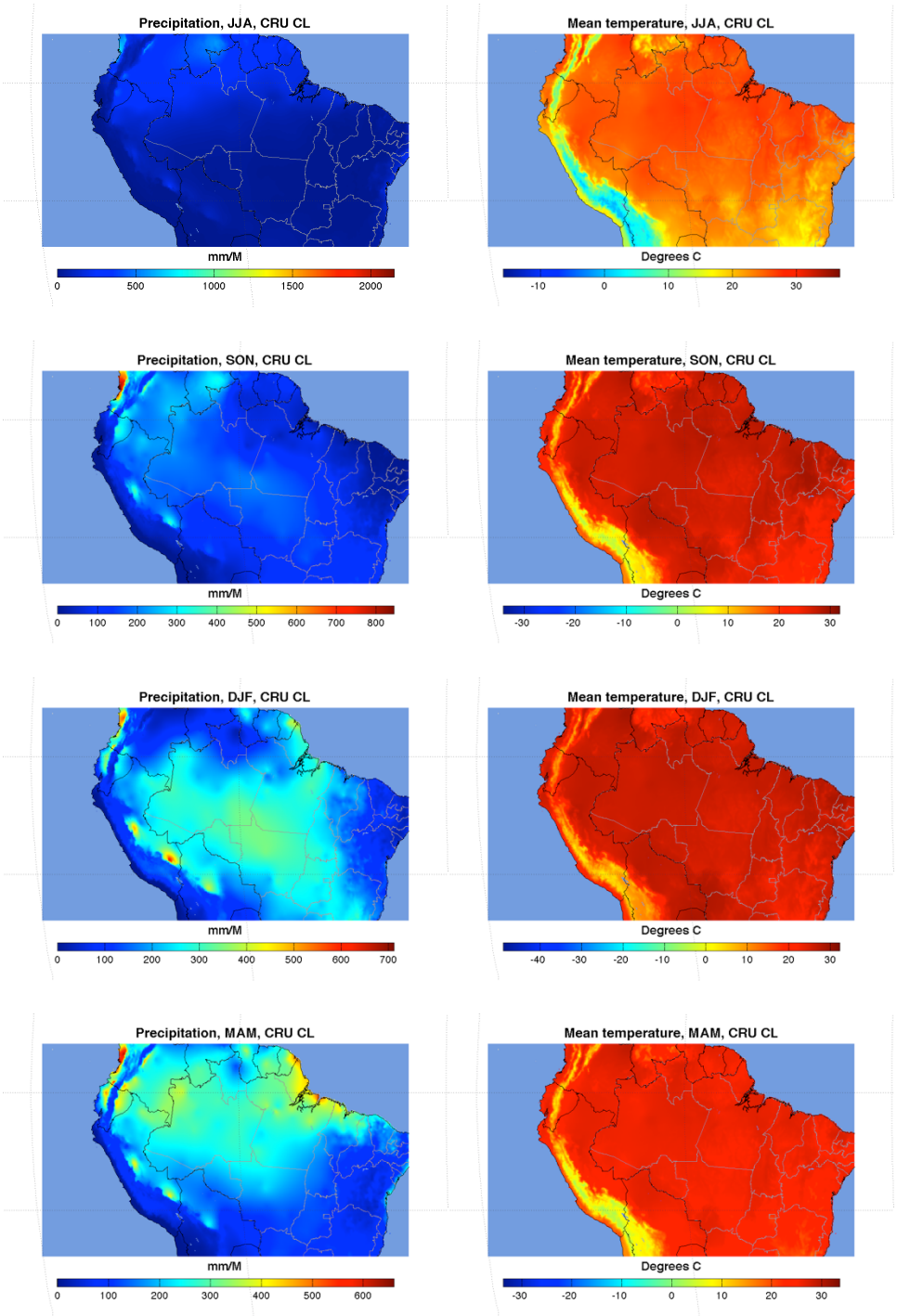

Supplemental Figure S1.6. Reference climate in Amazonia (temperature and precipitation). Seasonal precipitation (mean millimeters per month) and mean

temperature (degrees Celcius) reported by season (designated in common 3-month increments, JJA = June, July, August, etc.). Data from the CRU Global Climate Dataset, available through the IPCC DDC (http://www.cru.uea.ac.uk/cru/data/hrg/ and http://www.ipcc-data.org/observ/clim/get_30yr_means.html). The mean climatology dataset (labeled CRU CL in figures above) provides monthly mean climate over a 30-year period, 1961-1990, as a measure of average climate in the recent past.

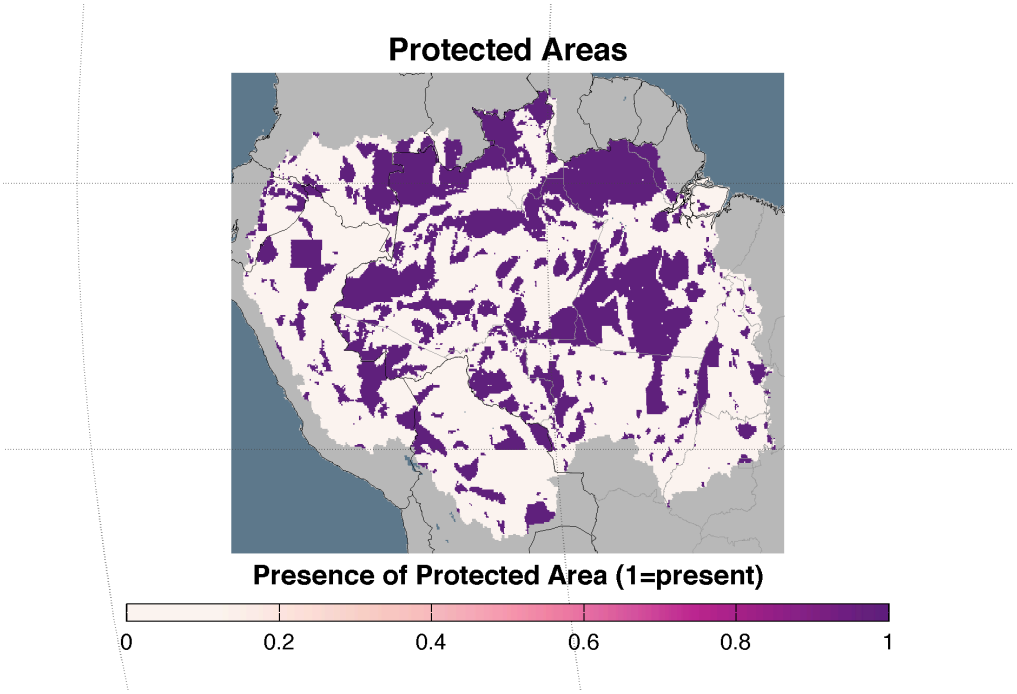

Supplemental Figure S1.7. For qualitative reference of how current protected areas align with a "portfolio" conservation approach, we downloaded all data for Amazonia from Protected Planet, the online interface for the World Database on Protected Areas (WDPA, http://www.protectedplanet.net/).

Supplemental Methods:

Supplemental Text S1.1. Full methods: Potential agricultural yield

Cropland (soybean) attainable yield

We calculate the attainable yield of soybean cultivation across Amazonia using a yield gap approach *sensu* Mueller et al. and Foley et al. (Foley *et al.*, 2012; Mueller *et al.*, 2012a). This yield gap approach only applies to areas climatically similar to 95% of the global soybean cropland circa 2000, a limited portion of Amazonia:

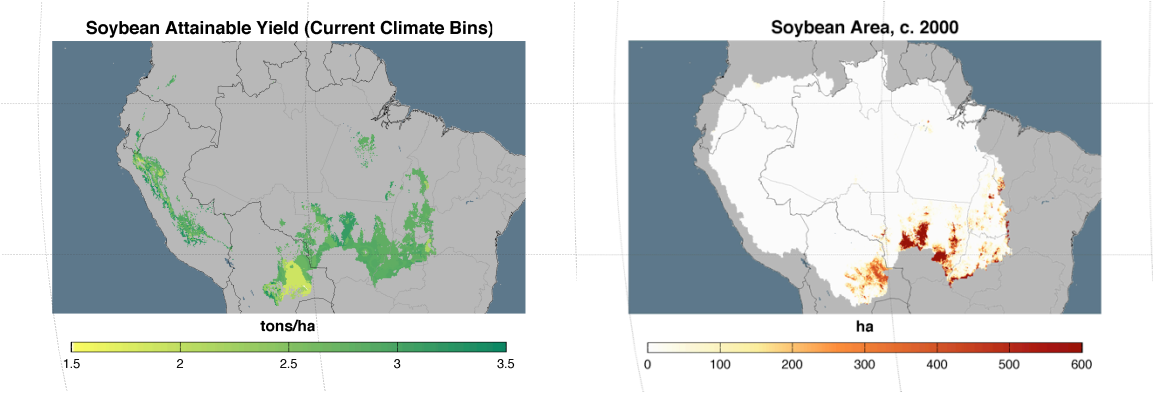

Climate bins are based on precipitation and a measure of temperature (growing degree days, GDD). In order to model soybean yields outside of the current climate bin limits, we extended climate bins to fill the entire climate space across the study system by holding GDD steady and expanding the upper precipitation limits of each climate bin. Across the areas in this study system included in the non-extended climate bins areas, we find that GDD is more influential than precipitation on crop yields. As such, we felt justified in extending climate bins beyond the observed data by holding the limits of GDD constant and allowing climate bins to extend into areas of higher precipitation.

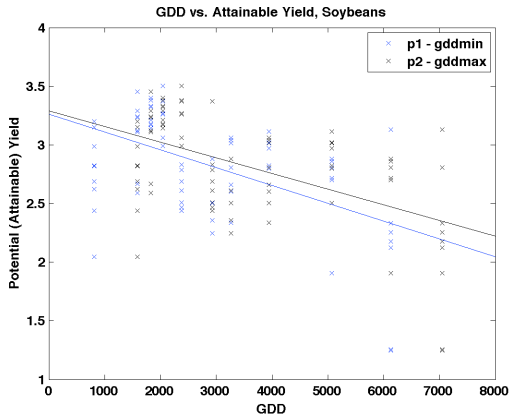

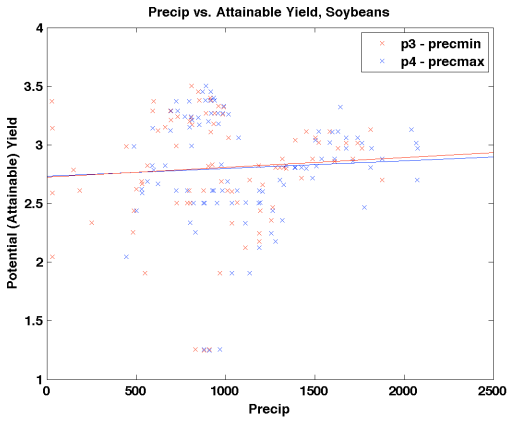

After extending climate bins based on precipitation and defining the associated attainable yield, 4.29% of the study area was left without an attainable soybean yield assignment as capturing that climate space would require extension of a combination of both GDD and precipitation bin edges. We used a nearest-neighbor interpolation algorithm to assign an attainable soybean yield to 3.54% of the study area. The remaining 0.75% of cells that did not have an assigned attainable yield (near the edge of the study system, rendering nearest-neighbor interpolation ineffective) were assigned Amazonia's average attainable soybean yield of 3 tons/hectare (ha).

Cropland (soybean) attainable yield uncertainty

Uncertainty was not estimated quantitatively (Foley *et al.*, 2012; Mueller *et al.*, 2012a), but according to Ramankutty et al. (Ramankutty *et al.*, 2002), the vast majority of Amazonia is suitable for agriculture (based on climatic and soil characteristics). Locations that Ramankutty et al. point to as less suitable (low index values in the figure below) can be qualitatively given less certainty.

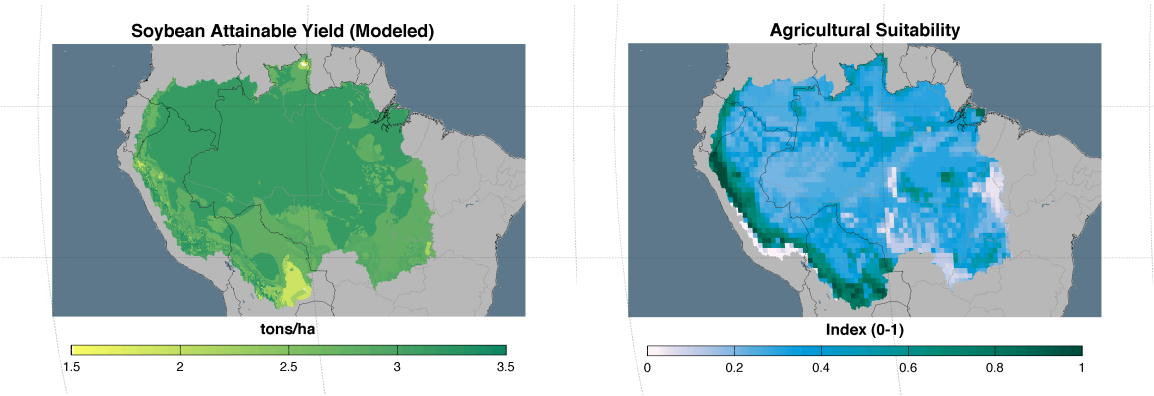

That said, in general there is good reason to believe that cropland productivity in Amazonia (and the Brazilian Amazon particularly) can reach its attainable yield. Ramankutty et al. note that the acidic soils of Amazonia can be fertilized and given lime additives – at a cost – to overcome suitability issues. Soybean, the crop we consider here, performs well inside of the Brazilian Amazon boundaries: 31% of Brazilian production is produced in the Brazilian Legal Amazon with yields (tons/ha) that are 106% of the national average yield. We presume that since Amazonia cropland, even in the eastern Amazon that Ramankutty suggests might be unsuitable for agriculture, is keeping even with yields elsewhere in Brazil, a global cropland powerhouse, that cropland across Amazonia could also be managed for high soybean yields.

Pastureland (cattle) attainable yield

We modeled attainable pasture yield across Amazonia by linking a model of non-tree aboveground net primary productivity (NTANPP) (Del Grosso *et al.*, 2008) to stocking densities (head of cattle per hectare of pasture) from the literature for high yielding or intensified pasture systems in Amazonia. We found a cited range of 1.5-4

cattle per hectare was the upper limit on pasture productivity, with Amazonian pastureland currently housing on average 1.17 livestock units per hectare (with 1 head/ha being a commonly used stocking density number for non-intensified pasturelands). We then scaled our NTANPP map from 0-4 and brought up the lowest locations to 1.5 so that the entire map varied from 1.5 head/ha to 4 head/ha. This approach presumes that variation in pastureland cattle that can be supported on the landscape is primarily tied to calories available to those cattle when grazing – that is, the aboveground grass stock. This approach also uses what we consider an appropriate estimate of a currently attainable best-case scenario of calorie production, as in our cropland estimates.

Both of these approaches were designed to allow the tradeoff from land use change to represent the best-case scenario – we assign grid cells to a potential soybean yield in line with the best performers from around the world in a similar climatic regime and we presume that more productive grassland ecosystems are sufficient to maintain intensified pasture systems. By avoiding assumptions about agriculture's likelihood of reaching its attainable yield (e.g., because of management or infrastructure deficiencies), our estimates of efficiencies remain conservative – the efficiencies we find are on the more efficient end of the run of possibilities.

Combining pastureland and cropland attainable yields to estimate gains to agriculture

To compare environmental impacts of land clearing to the gains to new agricultural lands generally (Figure 1.2, main text), we combined the gains from pastureland and cropland. We converted cropland gains from tons/ha to kilocalories

(kcal)/ha and pasture gains from head of cattle/ha to kcal/ha. Then our agricultural gains were all in units of consumable calories. Soybean calories were estimated as 3,596,499.11 kcal/tonne (Cassidy *et al.*, 2013). This estimate does not incorporate the fact that many of these soybeans are being used to feed animals on distal landscapes (DeFries *et al.*, 2013), which reduces the effective number of calories that a tonne of soybeans delivers to humans as food. Since the spatial pattern of calories production across Amazonia would be similar with or without this "soybeans for feed" correction, we do not account for it here.

Pastureland calories were estimated as

Livestock kilocalories per hectare per year =

(SD) * (COR) * (kilogram of beef per head of cattle) * (kilocalories per kg of beef)

where SD is the stocking density, or head of cattle/hectare, COR is the cattle offtake rate (cattle harvested/year), for which we use 8.5% (Bowman *et al.*, 2012), kilogram of beef per head of cattle is 175 kg (Bowman *et al.*, 2012), and kilocalories per kg of beef is 2034.71 (Tilman *et al.*, 2011). The offtake rate plays a role in reducing the estimated calories from pastureland. In addition, this formula does not take into account the fact that many cattle farms use a feedlot approach for some portions of the cattle lifecycles.

Finally, we combined the caloric gains of new cropland and new pasture into estimated gains to new hectares of "agriculture" by taking a simple mean between the gains to cropland and pastureland for each cell.

Supplemental Text S1.2. Full methods: Carbon stock losses

Recent radar- and lidar-based remote sensing analyses now provide wall-to-wall, high-resolution datasets of aboveground tropical carbon stocks (Saatchi *et al.*, 2011; Baccini *et al.*, 2012). We take advantage of these data to assess the potential tradeoffs between biogeochemical climate regulation via losses of above-ground carbon (AGB), and production from agricultural expansion.

To derive a map of above-ground carbon contained in natural vegetation (NV), we combine a year 2008 map of live woody biomass carbon developed by Baccini et al. (Baccini *et al.*, 2012) with a 2008 map of natural vegetation developed by combining three high-resolution land cover datasets (Aide *et al.*, 2012; Clark *et al.*, 2012; INPE (Brazilian National Institute for Space Research)). Using this carbon map, we estimate potential committed carbon flux from converting natural vegetation conversion to agriculture. Methods are described in detail here:

Natural Vegetation Maps

Brazilian Legal Amazon: PRODES is a program by the Brazilian federal government to track annual forest cover and deforestation in the Brazilian Legal Amazon; 90m digital data are freely available for download from 2000 to the present (www.dpi.inpe.br/prodesdigital/dadosn/). We downloaded PRODES maps for all dates from 2000 to 2012. Within ArcGIS (www.esri.com), we re-sampled and snapped all 90m PRODES data from various dates to the 2008 dataset. Using Dinamica EGO

(www.csr.ufmg.br/dinamica/), we used change detection techniques (e.g., if an area that was cloudy in 2008 was forest in 2009, the 2008 pixel was assigned the value of "forest") to classify the 2008 scene into NV, non-natural vegetation (NNV; including water), and unknown (e.g., clouds).

Brazilian cerrado: The Laboratory of Image Processing and GIS at the Federal University of Goias in Brazil (LAPIG) produces annual 2002-2012 deforestation maps in the cerrado biome (www.lapig.iesa.ufg.br/lapig/index.php/lapig-database). These maps are based on a 2002 30m land cover map derived from Landsat 5 data(Sano *et al.*, 2009). We classified the 2002 map so that protected areas, remaining cerrado, and secondary forest were considered NV; water, reforestation, agriculture, pasture, mining and urban area were all NNV. Then, deforestation polygons from 2003 to 2008 were added to the 2002 dataset as NNV, and converted to raster format to match PRODES.

Non-Brazilian Amazon: To assess 2008 land use outside Brazil, we used a land change dataset derived from 250m MODIS data (Clark *et al.*, 2012). We first re-sampled and snapped these data to match the PRODES data, and then reclassified the data as follows: woody and mixed woody classes were classified as NV, while water, plantation, herbaceous, agriculture, built up and bare classes were defined as NNV. Because the herbaceous class was difficult to distinguish from pasture (M. Aide, pers. comm.), we treated it as a pasture analog.

Merging into a simple land cover dataset: We used Dinamica EGO to merge all datasets, with LAPIG taking precedence over PRODES, which took precedence over the

MODIS-derived dataset. Finally, these 90m data were clipped and resampled to 500m to match the live woody carbon maps.

Using carbon and vegetation maps to determine carbon stocks in NV

Using these 2008 vegetation and carbon maps, we then calculated the mean and standard deviation of carbon stocks (MgC ha^{-1}) contained within NV and NNV for every 5 arc-minute grid cell. Our derived mean natural vegetation carbon stock values are consistent with previous work that collected empirical carbon stock data in undisturbed Amazon forest (Malhi *et al.*, 2006) and simulated biomass values for undisturbed vegetation (Castanho *et al.*, 2013).

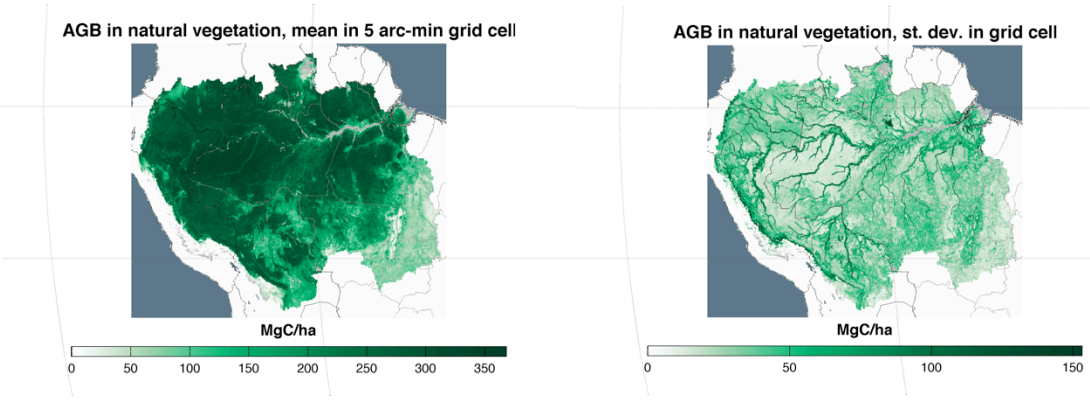

We also generated a file representing natural vegetation fraction in each grid cell. These values scale from 0-1.

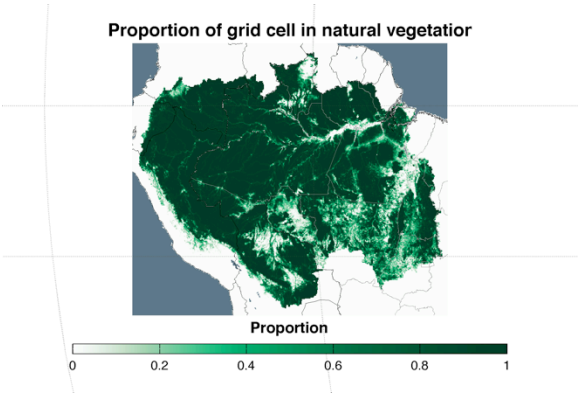

Estimating carbon stock losses upon conversion from natural vegetation to agriculture

To estimate carbon emitted after agricultural expansion, we calculate the difference between the mean vegetative carbon stock in NV and the carbon stock in either grassland (representative of pasture systems) or soybean cultivation (representative of cropland). Cropland vegetative carbon stocks were derived by taking the attainable soybean yield dataset and using a series of conversion factors (*sensu* West et al. (West *et al.*, 2010)) to convert from yield to AGB values, with a value across the region of 2.9 +/- 0.23 MgC/ha. Vegetative carbon stock values for pasture were presumed equal to the IPCC reported value (Verchot *et al.*, 2012) for biomass values on grasslands in wet and moist tropical ecosystems: 6.2 +/- 4.65 peak above-ground biomass (Mg dry matter/ha), which we converted to MgC/ha by multiplying by 0.5, for a 50% carbon:dry matter conversion rate.

Soil stock losses

We used the specialized "subsoil reference bulk density" (kg/dm3) and "subsoil organic carbon" (% weight) available in the Harmonized World Soil Database (HWSD)

data layers (Hiederer & Kochy, 2012; Nachtergaele *et al.*, 2012) to solve for organic carbon soil stocks in the top 30 cm of soil (MgC/ha). To estimate the MgC/ha lost from soil carbon stocks after land clearing, we spatialized the soil stock change factors reported in Powers et al. (Powers *et al.*, 2011) for conversion of natural vegetation to pasture and cropland. We multiplied those stock change factors by the HWSD soil carbon stocks to determine the soil carbon losses upon land clearing for cropland and pasture.

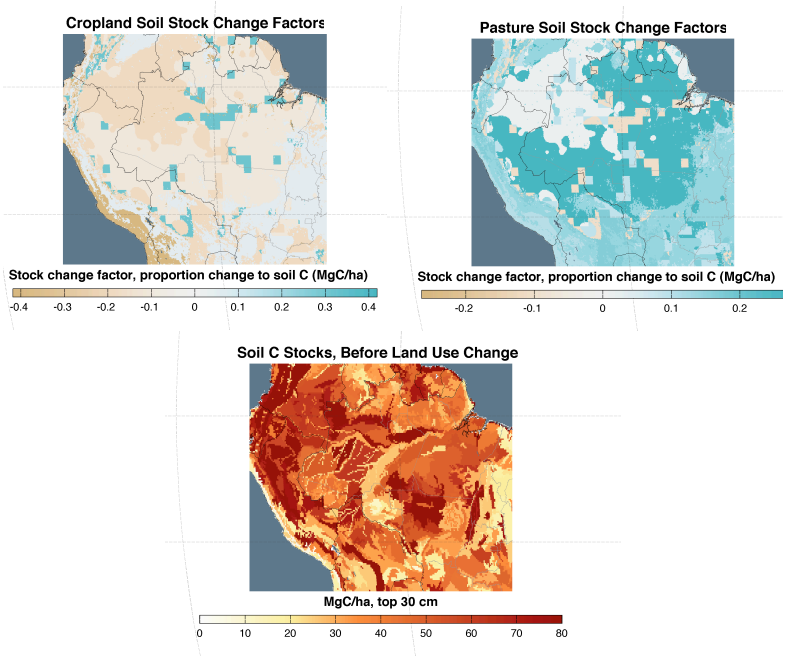

Uncertainty

We then calculated a bootstrapped 95% confidence interval around the mean delta carbon stock post-land use change for each cell in Amazonia using a Monte Carlo approach in which soil stock change factors and the AGB carbon stocks could vary over a defined standard deviation (Supplemental Figure S1.1). The AGB carbon stocks varied

over the standard deviation of natural vegetation observed within the grid cell, while we presumed that the log variance of soil stock change factors is homoskedastic and allow stock change factors to vary over the standard deviation found in Murty et al. (Murty *et al.*, 2002) of soil carbon stocks after conversion among studies which corrected for bulk density. We ran the Monte Carlo simulation for 1,500 repeats.

Supplemental Text S1.3. Full methods: Relative species richness

Relative species diversity was defined as the number of overlapping species distributions (i.e., species ranges) in each 5 arc-minute by 5 arc-minute grid cell.

We compiled species presence/absence observations for Amazonian plant, mammal and bird species by downloading georeferenced records from herbarium and museum collections available online (via the Global Biodiversity Information Facility [GBIF: http://www. gbif.org] and SpeciesLink [http://splink.cria.org.br] online data portals). Species were only considered if they had more than 20 observations in total.

Species observations were combined with mean annual temperature, Maximum Climatological Water Deficit (MCWD, a measure of water stress and precipitation regime), and ecoregion identity (serving as a proxy for non-climatic factors such as soil type) via a simple species distribution model based on BIOCLIM (Feeley *et al.*, 2012b). Mean annual temperature data was downloaded from the WorldClim database (Hijmans *et al.*, 2005), MCWD was calculated *sensu* Feeley 2012 (Feeley & Rehm, 2012) and ecoregion identifications were made using the WWF ecoregion dataset (Olson *et al.*, 2001). Estimated thermal and drought tolerances for each species were defined as the 2.5-97.5% quantiles of the temperature and MCWD values at the geolocated observations. Suitable habitat for each species was defined as the number of pixels that (1) was within currently occupied ecoregions, (2) within the estimated thermal tolerance of the species and (3) within the estimated drought tolerance of the species. More detailed discussion of these methods, including comparison of how this simple species

distribution model compares with machine learning-based species distribution models such as MAXENT, can be found in Feeley et al. 2012. We presume that upon conversion to agriculture, none of the species considered could use that same location as habitat, a simplification that discounts the persistence of generalist species in tropical agricultural zones (Karp *et al.*, 2011).

Land use change has been shown to impact biodiversity in Amazonia across scales, from the soil microbial community (Rodrigues *et al.*, 2013) to Amazonia-wide plant biodiversity (Hubbell *et al.*, 2008). These effects show pronounced differences between species depending on, among other things, their tolerance for fragmentation or mosaic landscapes. Rather than estimate these effects on a per-species basis, we opted to consider more generally the number of different species that could utilize natural vegetation as habitat in a given location. This approach provides a more generalized measure of habitat provision for biodiversity, a commonly considered ecosystem service.

See Supplemental Figure S1.2 for maps of relative species richness for the three considered taxa groups (plants, mammals and birds). See Supplemental Figure S1.3 for maps of an index of habitat for biodiversity that takes species range size into account.

Supplemental Text S1.4. Full methods: Biophysical climate regulation

Agro-IBIS (Kucharik, 2003; Cuadra *et al.*, 2011; Anderson-Teixeira *et al.*, 2012) was used to quantify the impact of clearing natural vegetation (defined per the IBIS potential vegetation dataset (Foley *et al.*, 1998)) and replacing it with either soybean cultivation (representative of cropland) or grass (representative of pasture). For the natural vegetation, soybean and grass simulations we modeled the net amount of solar radiation absorbed by the landscape (R_{net}), latent heat fluxes (LE, in which the system cools as excess energy is used to evaporate water, generally via evapotranspiration) and sensible heat flues (H, in which the system cools as excess energy heats winds as they move over the landscape). LE and H are the two key means by which excess incoming solar energy is emitted. See Supplemental Figure S1.4 for simulation results as annual averages. CRU3.0 climatology data was used to force the simulations (http://www.cru.uea.ac.uk/cru/data/hrg/). Simulations ran over the time frame 1973-2005 with a two-year spin up. The simulation area was as follows: latitude +5.4° to -20.1°; longitude -45.8° to -79.6°.

We then calculated the effects of land use change on energy balance as the difference in watts per m^2 ($W \cdot m^{-2}$) between the natural vegetation and the agricultural simulations (Supplemental Figure S1.5). In the tropics, land use change generally decreases R_{net} as surface albedo increases. In addition, replacement vegetation after land use change often has lower rates of evapotranspiration than natural vegetation; post-land use change ecosystems with lower evapotranspiration rates will emit less excess energy

as LE and emit a greater proportion of their excess energy as H. Our results are consistent with these trends.

We then converted the impacts of land use change on energy balance into more interpretable units, *sensu* West et al. (West *et al.*, 2011), for investigating tradeoffs: impacts on local atmospheric temperature (changes in degrees Celsius) and impacts on exported atmospheric moisture (changes in mm H_2O day^{-1}) (Supplemental Figure S1.5). Conversion of latent heat fluxes from $W \cdot m^{-2}$ to changes in mm H_2O day^{-1} is a straightforward unit conversion (see West et al. 2011); for conversion of sensible heat fluxes from $W \cdot m^{-2}$ to delta degrees C we assumed a boundary layer that decayed linearly from 500m high at the equator to 350m high at the poles and a 12 hour residence time of local air.

Changes to atmospheric temperature and moisture can have far-reaching effects. Drier air, when transported to downwind systems, can alter the precipitation regimes in important agricultural zones elsewhere. Bagley et al. 2012 (Bagley *et al.*, 2012) showed that the central and southeastern Amazon was an important evaporative source of water for the South American soybean "breadbasket," centered in northern Argentina and southeastern Brazil. Further, large changes to outgoing evapotranspiration, as implied by changes to LE in our simulation results, could shift the water cycle Basin-wide: under natural vegetative conditions, up to 60% of annual rainfall in the Amazon is evapotranspired and in western Amazonia between 50% and 88% of rainfall can be traced back to water that was evapotranspired from elsewhere in Amazonia (Brienen *et al.*, 2012).

As a first-order approximation of how local atmospheric temperature and moisture effects would alter the existing climatic regime, Supplemental Figure S1.6 shows the reference climate (1961-1990 seasonal averages). Note that changes in exported mm H_2O does not necessarily compare directly to precipitation locally – as mentioned, exported moisture can be transported and become precipitation elsewhere. Modeling those effects is outside of the scope of this study, but comparing local precipitation with changes to atmospheric moisture export can provide some insight into potential changes to the larger water cycle after local land-use change.

Supplemental Text S1.5. While this dissertation is written by the dissertation author, the manuscript version of this chapter will have the following authorships and affiliations:

Authors: Christine S. O'Connell[1,2]*, Kimberly M. Carlson[1], Santiago Cuadra[3], Kenneth J. Feeley[4,5], Paul C. West[1], Jonathan A. Foley[1,2], Stephen Polasky[1,2,6]

Affiliations:

[1]Institute on the Environment, University of Minnesota, Saint Paul, Minnesota, 55108 USA

[2]Department of Ecology, Evolution & Behavior, University of Minnesota, Saint Paul, Minnesota, 55108 USA

[3]Brazilian Agricultural Research Corporation - Embrapa, National Temperate Agriculture Research Center, Pelotas, RS 96010-971, Brazil

[4]Department of Biological Sciences, Florida International University, Miami, Florida 33199 USA

[5]Fairchild Tropical Botanic Garden, Coral Gables, Florida 33156 USA

[6]Department of Applied Economics, University of Minnesota, Saint Paul, Minnesota, 55108 USA

*Correspondence to: coconn@umn.edu

Chapter 2:

How does deforestation for cropland affect trace gas concentration and diffusion flux at depth in Southeastern Amazonian soils?

Abstract

Tropical soils contain large stocks of carbon (C) and nitrogen (N), but it remains poorly documented how C and N in these deep, weathered soils are affected by land use change. Evidence from the top 30 centimeters (cm) of soil indicates that land use change from forest to agriculture in the Amazon depletes C and N stocks, depresses carbon dioxide (CO_2) and nitrous oxide (N_2O) emissions and reduces methane (CH_4) uptake; how CO_2, N_2O and CH_4 change below 30 cm soil depth after deforestation remains poorly understood. Characterizing how trace gas fluxes vary down the soil profile can provide information about C and N availability below the rooting zone as well as the origin of greenhouse gases within the soil profile between land uses. In this study, we measured concentrations of CO_2, N_2O and CH_4 in soil air at equilibrium from 15 cm depth to 450 cm depth, in combination with soil temperature and volumetric water content, in 10-meter soil pits located in mature forest and monoculture soybean/maize cultivation at a research site in southeastern Amazonia. We found that CO_2 concentration differed significantly between land uses, with lower CO_2 concentration at depth (> 250 cm) in agriculture than forest. Similarly, N_2O concentration at depth (> 40 cm) was lower in agriculture than in forest, while CH_4 concentrations were higher in relatively shallow and

relatively deep agricultural soils (< 75 cm, >350 cm), suggesting that these soil depths have lower CH_4 uptake rates. In all cases, concentrations of trace gases, temperature and volumetric water content differed significantly between land uses ($p < 0.001$). We estimated trace gas flux at depth using a diffusion model that showed higher variability in trace gas fluxes in deep forest soils than in deep agricultural soils. Because deep agricultural soils had higher temperature and volumetric water content than forest soils, but lower N_2O and CO_2 concentrations, which would normally be promoted by warm and wet conditions, our results suggest that C and N availability differed between deep agricultural and forest soils in this system. Further investigation of soil solution nutrient concentrations in these soils could illuminate patterns of nutrient availability in sub-soils. Finally, trace gas patterns throughout the soil profile support indications that intensive agriculture in this system does not substantially contribute to higher landscape-level GHG emissions.

Keywords: greenhouse gases, soil profiles, land use change, Amazonia

Introduction

Tropical soils contain large stocks of carbon (C), but the size and dynamics of tropical soil C pools below 1 meter depth are poorly quantified (Jobbágy & Jackson, 2000; 2001; Harrison *et al.*, 2011; Powers *et al.*, 2011). Soil nitrogen (N) dynamics at depth are similarly under-investigated. In the past several decades, it has become clear that these sub-soils play multiple important roles in Amazonia's biogeochemistry. Amazonian trees have deep roots with high soil water uptake and influence total soil carbon dioxide (CO_2) efflux and soil C inputs (Nepstad *et al.*, 1994; Jobbágy & Jackson, 2000; Harrison *et al.*, 2011; Powers *et al.*, 2011). Soil organic carbon (SOC) pools below 1 m depth contribute up to 17% of CO_2 emissions from the soil surface, and SOC in tropical sub-soils may be more susceptible to loss than SOC in temperate sub-soils (Rumpel & Kögel-Knabner, 2010). Previous work has shown that nitrous oxide (N_2O) emissions in forest in northeastern Amazonia rises down the soil profile until approximately 2 m (Sotta *et al.*, 2007), and anion exchange at depth in these weathered soils may regulate nitrate availability (Neill *et al.*, 2006).

Historically, our understanding of tropical soils has been that nutrients cycle rapidly in shallow soils (perhaps <30 cm depth) as densely packed, shallow fine roots take up phosphorus, N and micronutrients released during decomposition. We do not have as robust an understanding of the dynamism of nutrient stocks and trace gas production in deeper soils. Variability of nutrient cycling in deep soils could be substantial: recent work has shown that the microbial communities down the soil profile

can be as heterogeneous as the communities in surface soils across local sets of sites (Neill *et al.*, 2006; Eilers *et al.*, 2012). Amazonian soils are likely subject to this same heterogeneity – in microbial activity, as well as in labile nutrient pool size – within the soil profile. Critically, investigating how sub-soil contributes to soil trace gas production can inform interpretation of greenhouse gas (GHG) emissions measured from surface soils and how deforestation and subsequent cultivation influence tropical biogeochemistry and GHG emissions.

While there exists uncertainty surrounding C and N dynamics in deep soils of tropical forests, there is additional uncertainty surrounding how global change factors may influence sub-soil C and N. Land use change is well known to alter C and N dynamics in the top meter of Amazonian soils (Neill *et al.*, 1995; Fearnside & Barbosa, 1998; Feldpausch *et al.*, 2004; Wick *et al.*, 2005), but data are still limited for deeper soils. Deforestation and conversion to pasture depresses net N mineralization and nitrification, but these effects may not manifest for a decade or more (Neill *et al.*, 1999; Eilers *et al.*, 2012). Conversion to pasture has also shown longer-term impacts on microbially mediated C cycling (Neill *et al.*, 1999; Melo *et al.*, 2012), including decreases in methane (CH_4) uptake or even a switch to net CH_4 production (Keller *et al.*, 2005; Melo *et al.*, 2012). By contrast, burning, a common means of deforestation, leads to an initial pulse of soluble ions and changes in soil fertility (Williams *et al.*, 1997; Keller *et al.*, 2005; Piccolo *et al.*, 2011). Other global change factors have also been considered. An experimental drought in eastern Amazonia showed a decrease in N_2O emissions at depth and an increase in CH_4 uptake in the drought manipulation plots. In

the temperate zone, consideration of sub-soil leads to different estimates of the effects of N fertilization on soil C than estimates based on the top 30 cm of soil alone (Williams *et al.*, 1997; Harrison *et al.*, 2011; Piccolo *et al.*, 2011). Large uncertainties remain surrounding N and C cycling in deep Amazonian soils and, moreover, whether the known biogeochemical effects of land use change in the Amazon perpetuate down the soil profile.

Elsewhere in the tropics, studies have consistently shown that C and N vary down the soil profile, but land use change for agriculture in some cases does not significantly alter C and N stocks, while in other cases does so substantially. In one Panamanian study, soils under both forest and grassland had significantly lower carbon stocks below 10 cm depth than in the top 10 cm of soil (Schwendenmann & Pendall, 2006), but did not differ in total soil carbon stocks. Conversely, Veldkamp et al. 2003 (Veldkamp *et al.*, 2003) found that land use change could mobilize C stocks at 1-3 m depths despite no significant change to soil C stocks from 0-30 cm. Work in Puerto Rico also showed decreases in total C and total N from 0-50 cm in forest, pasture and secondary forest (Marin-Spiotta *et al.*, 2009); the same pattern held for C and N concentration from 0 cm to 2.5 m depth in a cacao agroforest in Sulawesi, Indonesia (Schwendenmann *et al.*, 2010).

In this study, we detail the changes in trace gas concentrations (e.g., carbon dioxide, CO_2; nitrous oxide, N_2O; and methane, CH_4) down the soil profile in six 10-meter soil pits, located in either forest or agriculture, on a working farm in southeastern Amazonia. Trace gas concentrations can serve as markers for soil microbial activity as

well as point to whether substantial labile C or N is available; large labile nutrient pools can lead to trace gas production. Here, we use trace gas concentrations in combination with an estimate of trace gas diffusion fluxes in deep soil to point to general trends in C and N cycling from the top 15 cm of soil down to approximately 5 m depth.

We hypothesized that because the agricultural lands at this station have been deforested for several decades, soil C and N stocks would be smaller in agriculture than in forest, with associated lower CO_2 and N_2O concentration. Forests in this system have higher evapotranspiration rates than croplands, meaning more water infiltrates to deeper in the soil profile in agricultural soils. We thus hypothesized that these wetter agricultural soils would lead to CH_4 uptake at depth in agricultural soils.

Materials and methods

Site description

Sampling was conducted at Tanguro Ranch, a 32,000 hectare industrial farm located in Mato Grosso, Brazil (Figure 2.1). Tanguro Ranch is surrounded by closed-canopy tropical forest (25m height) typical of southeastern Amazonia, a region of transitional forest between cerrado (tropical savanna) to the east and more diverse, high-statured forests to the northwest. This area of Amazonia is also marked by lower precipitation and higher seasonality than central Amazonia. Mean annual precipitation (MAP) at Tanguro Ranch averaged 1900 mm/year between 1987 and 2007 and ranged from 1500

to 2500 mm y^{-1} (Tanguro Ranch, unpublished results). The wet season extends from September to April with a dry season between May and August. Mean annual temperature (MAT) is 27 °C, but temperatures vary between forested areas and cropland areas both diurnially and on average over the year. Tanguro Ranch is located on the Brazilian Shield and the underlying parent material is Precambrian gneisses (Projeto Radambrasil, 1981). Upland soils are ustic Oxisols (55% sand, 2% silt, and 43% clay mean texture, Oliviera et al., 1992, Soil Survey Staff, 1999) with high infiltration rates and little lateral water movement in upper soil horizons (depth to water table estimated to be between 20-40m (Harrison *et al.*, 2011; Hayhoe *et al.*, 2011)). The site features little topographic variation and is generally flat plateaus interspersed with stream channels (Nagy et al., *in press*).

Originally deforested to support a pasture ranch (cleared between 1982-83), Tanguro now primarily plants soybeans, a nitrogen-fixing legume (conversion from pasture to soy occurred between 2003-8). Highly intensively managed, Tanguro's croplands receive multiple applications per year of fertilizer (phosphorous [P] and potassium [K]; nitrogen [N] on some double-cropped fields), pesticide, herbicide, fungicide and soil additives (lime) to moderate soil pH (Grupo A. Maggi, pers. comm.). A subset of soybean fields is double-cropped late in the wet season with maize, which receives additional P and N fertilizer. The transition from low intensity pasture to intensive, mechanized cropland is representative of the land use trajectories taking place across eastern Amazonia (Hayhoe *et al.*, 2011; Macedo *et al.*, 2012; DeFries *et al.*, 2013). There have been numerous previous projects in this system, all with the logistical

cooperation of farm leadership (Balch *et al.*, 2008; Hayhoe *et al.*, 2011; Macedo *et al.*, 2012; DeFries *et al.*, 2013; Brando *et al.*, 2014).

Trace gas measurements

Six 10 m soil pits were permanently installed across Tanguro Ranch between 2010 and 2015. C2, K4 and M8 were located in intact forest, while Mutum (MU), Area3 and APP1 pits were located in the center of soybean fields or soybean/maize fields (Area3 pit). We installed 7 brass tubes horizontally into the side of each soil pit at depths of 15, 40, 75, 150, 250, 350 and 450 cm. Each tube was fitted with a swage and septum for gas sampling. One week after installation, we withdrew between 24 and 96 mL of gas (depending on tube length), which we subsequently discarded as a flushing protocol; tubes equilibrated for at least 48 hours before the first sampling. Sampling was conducted on December 17-18, 2013, February 25-26, 2014 and January 27-28, 2015; all three sampling periods took place during the height of the wet season.

Gas sampling tubes were between 50 and 200 cm long in order to ensure that gas samples were drawn from soil pore space beyond the zone affected by the exposed pit wall (based on measured temperature and soil moisture pilot data, P. Lefebvre, personal communication). Tubes lengths were chosen in order to limit the trace gas infiltration from the exposed pit walls to the point of sampling: 50 cm tubes were installed horizontally at 15 and 40 cm depth, for instance, so that the soil pore space at the end of the tubes was at least as far from the pit wall by horizontal distance as from the soil

surface by vertical distance. For the 250, 350, and 450 cm depth samples, the gas sampling tubes were only 200 cm long. While this means that some of the gas sampled at these depths had likely diffused horizontally from the soil pit itself (i.e., we can not assume that vertical diffusion is solely responsible for trace gas concentrations at each depth), there is evidence from a similar study in northeastern Amazonia that beyond 200 cm into a soil pit wall, the rate of change of soil CO_2 concentrations across horizontal space saturates (Davidson & Trumbore, 1995).

At each sampling date, three samples per depth were collected using a 12mL polypropylene syringe (Monoject) that withdrew 12mL of gas which was then injected into a 9mL glass vial (Grace Davidson) that had been pre-sealed with butyl rubber septa (Grace Davidson). Samples 1-3 generally had good agreement (Supplemental Figure S2.1), but we eliminated samples 1 and 2 in February 2014 based on systematic patterns based on vial order for CO_2 and CH_4. We used un-evacuated vials containing ambient (lab) air (*sensu* Venterea 2005 (Venterea *et al.*, 2005; Balch *et al.*, 2008; Hayhoe *et al.*, 2011; Brando *et al.*, 2014)). Sets of vials containing ambient air included four replicate vials with ambient air that were later analyzed for concentrations of CO_2, N_2O and CH_4, which were then used to calculate trace gas concentration without dilution. Un-evacuated vials were preferred over evacuated vials in this study because evacuated vials sitting at ambient pressure for several weeks, as they would have been under field conditions in the absence of a reliable means to evacuate vials on site, have a high risk of inward air leakage.

Gas samples were analyzed by gas chromatography using a headspace autosampler at the University of Minnesota (Teledyne Tekmar, Mason, OH). The autosampler was modified to fill multiple sample loops from each vial. Sample loops fed into a flame ionization detector for CH_4, an electron capture detector for N_2O and a thermal conductivity detector for CO_2. Standard curves and system calibration were done using analytical grade standards (Scott Specialty Gases, Plumsteadville, PA).

Soil temperature measurements

Thermocouple sensors were installed at soil pit depths of 15, 40, 75, 150, 250, 350 and 450 cm, also buried into the soil pit wall in order to avoid artifacts associated with the exposed soil pit interior. Temperature was recorded every 6 hours and temperature data the result of the average temperature over a short sensor period (variable, ~20 uS). Data were recorded by dataloggers (Campbell Scientific) and downloaded weekly. Temperature and moisture data are reported as averages over a single week in December, January and February. These months were chosen to complement gas samples taken during December, January and February, which were in turn chosen because soils are more dynamic in this system during the wet season (September-April).

Soil volumetric water content measurements

Time domain reflectometry (TDR) soil moisture meters were installed at 0, 30, 50, 100, 200, 300, 400, 500, 600, 700, 800 and 900 cm depths in each soil pit. Data were collected using the same datalogger as was used to record thermocouple data (Campbell Scientific) and were downloaded weekly. Data were calibrated and converted to volumetric water content (VWC).

Due to the limited space along soil pit walls, and the need to keep sensors apart, TDR sensors were not placed at the same depths as thermocouple sensors or gas sample tubes. To have fully comparable datasets, we estimated VWC at 15, 40, 75, 150, 250, 350 and 450 cm depth, using the simple assumption that the VWC at the midpoint between two sensors would be the mean of the two. We report both the measured data and the estimated data in depth figures (e.g, Figure 2.4), but statistical analyses using VWC as a predictor variable use the estimated, depth-matched VWC data.

Modeling diffusivity and trace gas diffusion flux by depth

We modeled trace gas fluxes down the soil profile by taking advantage of Fick's first law of diffusion, which states that the diffusion flux is a function of both the concentration gradient of a gas species across space and the diffusivity of that gas through the medium (in this case, soil). We modeled Fick's first law as:

$$diffusion\ flux = D_p * \frac{dC}{dz} * \frac{52{,}700}{T}$$

in which D_p is the effective diffusivity of either N_2O, CO_2 or CH_4 in soil ($cm^2\ s^{-1}$), $\frac{dC}{dz}$ is the change in concentration of N_2O, CO_2 or CH_4 across soil depth ($ppm\ cm^{-1}$), and T is

soil temperature in Kelvin with data available from pit-specific temperature measurements (*sensu* Davidson et al. 2006). The value 52,700 is used for unit conversion. D_p was modeled as:

$$D_p = P_A^{\frac{4}{3}} * \left(\frac{P_A}{P_T}\right)^2 * D_o$$

where P_A is the air-filled porosity (cm^3 air-filled pore space cm^{-3} bed space), P_T is total porosity (cm^3 pore space cm^{-3} bed space) and D_o is the diffusion coefficient of each gas in air (0.122 for N_2O, 0.136 for CO_2, 0.81 for CH_4 (Davidson & Trumbore, 1995)). We solved for P_T and P_A using information about bulk density (BD), average particle density of soil minerals (PD), and P_W, water-filled pore space (*sensu* Davidson and Trumbore 1995):

$$P_T = 1 - \frac{BD}{PD} = P_A + P_W$$

Bulk density values were based on bulk density measurements taken at 7 Tanguro forest sites and 28 agricultural sites at depths of 0-10, 10-20, 40-50, 90-100 and 190-200 cm (Nagy et al., *in prep*). From that dataset, bulk density values were extrapolated using regression out to 450 cm depth (R^2 value for forest model = 0.289, R^2 value for cropland model = 0.163). Particle density (PD) was assumed to be 2.65 g cm^{-3} (Davidson *et al.*, 2006). P_W was defined by measured, pit-specific volumetric water content data.

The concentration gradient between each depth at which we sampled trace gas concentrations ($\frac{dC}{dz}$) can be determined by solving for the first derivative of the curve fit to the plot of depth by μg C cm^{-3}. To determine that derivative, i.e., the change of concentration with change of depth, we fit a curve to the data using LOESS curve fitting

(local polynomial regression). We chose a non-parametric, local regression technique because in many cases trace gas concentrations across the first 30 cm of soil created large concentration gradients that switched directions rapidly in space and thus were not well characterized by linear or polynomial regressions. Diffusivity models require robust representation of concentration gradients, with changes across depth being better captured by local curve fitting techniques. We then solved for the derivative of that LOESS curve from 15 to 450 cm depth (Supplemental Figure S2.2). The first derivative values at 15, 40, 75, 150, 250, 350 and 450 cm were used as $\frac{dC}{dz}$ values for a given depth, pit and sampling month.

Estimates diffusion flux values that were positive can be interpreted as a downward flux: diffusion flux is positive when moving to a depth with a higher absolute value (e.g., 150 cm from 75 cm), or moving further down in the soil column.

After solving for the diffusion flux at each depth for each pit and sampling month, we converted units of g C m^{-2} h^{-1} or g N m^{-2} h^{-1} to units of μg C cm^{-2} h^{-1} or ng N cm^{-2} h^{-1}. Soil pits that did not have directly measured temperature or moisture data for a given month were excluded from the modeled flux analysis, as accurate and site-specific estimates of effective diffusivity through the soil (D_p) are critical to robust diffusion flux estimates.

Statistical analysis

Gas concentration, temperature and VWC data were analyzed using a two-way nested analysis of variance (ANOVA). Each response variable (e.g., trace gas concentration, soil temperature or volumetric water content) was analyzed in a nested ANOVA design where soil pit was nested within land use (e.g., forest or agriculture). The second ANOVA factor other than land use was sample depth down the soil profile. One interaction term, sample depth by land use, was included in the model; a soil pit by land use interaction was not included because, since pit was nested within land use, their interaction was confounded by the nested pit effect. Since this experimental design had unbalanced sample sizes between subgroups (e.g., soil pit), normally a Satterthwaite approximation is needed to calculate accurate p-values from a nested ANOVA. However, the R statistical software's base ANOVA function handles unbalanced sampling internally and manual corrections for unbalanced sample sizes were unnecessary. All statistical tests were conducted with R statistical software. Two-way nested ANOVA diagnostic tests for all models are available in Supplemental Figure S2.3. Models were deemed statistically significant at $p<0.05$.

ANOVA tests were not conducted on modeled diffusion flux rates. Our diffusion model only yielded a single flux value per depth per pit because gas concentration measurements were combined to quantify the concentration gradient down the soil profile ($\frac{dC}{dz}$). We preferred to show the modeled results as stand-alone estimates rather than conduct an analysis of variance without the inclusion of within-pit variation, which would have led to problematic pseudoreplication.

To compare surface trace gas fluxes during the same time period as these measured deep soil trace gas concentrations, surface fluxes at Tanguro measured during the wet season (O'Connell et al., Chapter 3) were analyzed using a one-way analysis of variance (ANOVA), in which wet season fluxes of N_2O, CO_2 or CH_4 were compared between forest, soybean/maize fields and soybean sites. See Chapter 3 of this volume for further information on sampling methods and experimental design. All ANOVA assumptions were met and models were considered significant when $p<0.05$. Statistical tests were performed using R statistical software (R version 3.1.2, packages "nlme" for model construction and "multcomp" for posthoc tests).

Results

Temperature and moisture results

In two forest soil pits (K4 and M8), soil temperature at depth followed a consistent pattern, increasing between 15cm and 1m depth, before remaining steady at lower depths (Figure 2.2). Forest pit C2 also had higher temperatures at depth, but the increase continued after 1m depth and the temperature pattern was more variable, decreasing at 45cm then increasing at 75cm depth, before decreasing at 1.5m, after which temperatures continue to rise down the soil column. Mutum, APP1 and Area3 pits (agriculture) had soil temperatures that had larger standard error values at each depth – the forest pits, by contrast, had variable surface soil temperatures, but relatively small standard errors for

deeper temperatures (e.g., temperatures varied less over the course of the week). Further, agricultural soil temperatures were significantly warmer than the soil temperatures in forest pits ($p < 0.001$, Table 2.1), and were similar across sampling month and depth, remaining between 25.5 and 27.5 °C, higher than all but 3 weekly average temperatures in any of the forest pit sites or depths. None of the months considered (December-February) had distinct soil temperature patterns; month was not a significant predictor of temperature.

Month was a significant predictor of VWC (Figure 2.3), with pits C2, K4 and M8 having higher VWC values when sampled later in the wet season (which begins in approximately September and continues to approximately April). The lone exception is that C2's moisture values were larger during December 2013 than January 2015. As with temperature, K4 and M8 pits were distinct from C2, which had generally higher VWC values (Table 2.2). Depth in all three cases was positively related to VWC ($P<0.001$). Agricultural pits, in contrast to the forest pits, showed a pronounced decrease in VWC from 15cm to 40cm and VWC remained low through 75cm depth, after which there was a positive relationship between VWC and depth.

Trace gas concentrations

Forest had significantly higher N_2O concentrations than agriculture throughout the profile; concentrations did not differ significantly with depth (Table 2.3, Figure 2.4, Figure 2.5). Standing concentration values were routinely well above ambient values

(~0.32 ppm (Venterea *et al.*, 2005; Blasing, 2009)). Not only were measured N_2O concentrations higher in forest soil pits, they were also more variable between pits and with depth: in some cases concentrations changed radically with depth (Figure 2.4) while in other forest pits they remained steady across depths.

Carbon dioxide values differed significantly between land use types (Table 2.4), with higher CO_2 concentrations in forest (Figure 2.4, Figure 2.5). Again, there were not significant differences in concentration by depth. Some qualitative differences exist for CO_2 concentrations between forest and agriculture below 250 cm depth, at which point forest concentrations are higher than agriculture concentrations (Figure 2.6).

As with N_2O and CO_2, nested ANOVA results found that while CH_4 concentrations differ significantly between land uses (Table 2.5, $P<0.001$), they do not differ significantly by depth (Table 2.5, $P=0.09$). In linear models, however, the inclusion of sample depth as a predictor variable for CH_4 concentrations increased R^2 by nearly 40%, which wasn't the case for the other trace gases measured. Qualitatively, CH_4 was higher in shallow (< 75 cm) and very deep (> 350 cm) agricultural soils in comparison to forest (Figure 2.6).

Trace gas diffusion flux

Modeled N_2O diffusion flux was highly variable in forest sub-soils in comparison to agricultural sub-soils (Figure 2.4). Further, N_2O flux appeared highest in forest soils at less than 150 cm depth. CO_2 diffusion flux was also more variable in forest sub-soils

than in agricultural sub-soils, with large negative fluxes seen in some cases at depths less than 150 cm. Higher variability in forest sub-soils than in agricultural sub-soils was also modeled for CH_4 diffusion fluxes down the soil profile. Two of the modeled pits, K4 and M8 (both forest), showed starkly patterns of CH_4 diffusion flux: in pit M8, there were large, positive methane fluxes in the top 75 cm of soil, while in pit K4 there were large, positive methane fluxes below 250 cm.

Discussion

Abiotic context of temperature and moisture patterns

Cropland soils were hotter, wetter and more homogeneous than forest soils (Figure 2.2, Figure 2.3), a broad abiotic pattern between the two land uses. One distinct difference between forest and cropland soil pit results is that sub-soil underneath cropland was less variable in temperature down the soil profile, and statistically indistinguishable from month to month. Mutum, the cropland soil pit, was also wetter than most of the forest pits. Moisture results were also less variable in cropland than in forest.

What could be leading to this relative homogeneity of temperature and moisture in cropland sub-soils? Several inter-related factors could explain these patterns. First, cropland soils in this system are exposed to more net radiation than forest soils: solar radiation in forests is absorbed in part by high photosynthetic rates and in part by latent heat flux, the energy used for evapotranspiration (ET), both of which absorb less of the

incoming energy in croplands, thus allowing greater soil heat flux and explaining the higher soil temperatures in cropland sub-soils. Because net radiation in croplands is disproportionately heating the air and soil, and net radiation varies less across months than ET, energy balance could also explain the consistency in cropland sub-soil temperatures. Similarly, croplands are likely to have a more consistent rooting depth and lower root water uptake than forests – Tanguro's croplands are monocultures with soya plants that root to approximately 1-2 m, whereas eastern Amazonian forests have many tree species that are very deep rooting, drawing water from more than 8 m below the surface (Nepstad *et al.*, 1994; Blasing, 2009). Cropland VWC was low between 1-2 m, where soybean water uptake may have been focused, but rose below that presumed rooting depth. Forests, on the other hand, had more inconsistency in VWC down the profile, perhaps as different species' roots utilized water at different depths. Finally, the VWC consistency in croplands may have been stabilizing soil temperatures: if infiltration rates were higher because ET was lower under soybean, surface water would have been percolating relatively rapidly through the soil profile, keeping temperatures relatively homogenous.

Additionally, there were bulk density and mineralogical differences between forest and cropland soils in this system. Base saturation, aluminum saturation and pH all differ between land uses down to 200 cm in this system and bulk density differs at least to 20 cm (Nepstad *et al.*, 1994; Riskin *et al.*, 2013): cropland soils have higher base saturation, lower aluminum saturation, are less acidic, and have higher bulk density than

forest soils, with important implications for nutrient availability and sub-soil C and C transformation rates.

Trace gas concentration in deep soils

We found that, throughout the soil profile, CO_2 and N_2O concentrations were significantly higher in forest soils than in agricultural soils. In contrast, deep agricultural soils had significantly higher temperature and volumetric water content than forest soils. Generally, warmer and wetter conditions promote both CO_2 and N_2O production, all else being equal. As such, that CO_2 and N_2O concentrations were lower in deep agricultural soils suggests that that C and N availability differed between deep agricultural and forest soils in this system: smaller labile C and N pools could explain the trace gas differences between land uses. If this is the case, it may be that changes to C and N availability after land use change that have been documented in surface soils may reverberate down the soil profile (Jobbágy & Jackson, 2001; Powers *et al.*, 2011).

Perhaps there is less SOC in these deep agricultural soils, a hypothesis that would be consistent with observed decreases in soil C concentrations down to 20cm after deforestation for pasture elsewhere in Amazonia (Melo *et al.*, 2012; Riskin *et al.*, 2013), elsewhere in the neotropics (Veldkamp *et al.*, 2003; Marin-Spiotta *et al.*, 2009), in soil C loss meta-analyses considering deforestation for cropland in Amazonia (Melo *et al.*, 2012; Fujisaki *et al.*, 2015) and across the tropics (Powers *et al.*, 2011). Alternatively, changes to the microbial community that resulted from land use conversion could have

influenced the microbial community in both deep and shallow soils, leading to different soil C cycling regimes. Past work (Rodrigues *et al.*, 2013) has shown that deforestation in Amazonia leads to a loss of microbial diversity, which could in turn influence fundamental biogeochemical cycling (Madsen, 2011). Lower N_2O concentrations at depth in agriculture could be explained by a similar decrease in labile N, but could also be explained by smaller C pools: N_2O production can be limited by soil C availability (Venterea *et al.*, 2012). If labile N pools are in fact smaller, high infiltration rates in agricultural soils and lower ET rates could be flushing labile N from the system more rapidly than in forest.

Our ability to connect methane concentrations and the soil C cycle from these data is limited: CH_4 concentrations were similar between land uses and across soil depths, and statistical significance is largely driven by a single sampling month (January 2015). Figure 2.6 shows that variability in CH_4 is higher in agriculture. This variability is larger that seen for N_2O or CO_2 (Figure 2.6). It is notable that most of the recorded CH_4 ppm values are below the current ambient concentration of CH_4 (1.8 ppm), suggesting that net CH_4 uptake is taking place across soils and depths, despite hotspots on the landscape where soil surface CH_4 fluxes are positive (O'Connell et al., Chapter 3).

Deep soil trace gas fluxes vs. surface soil fluxes

The results for modeled trace gas fluxes at depth can be thought of here as preliminary results: trace gas concentrations measured without concurrent temperature and moisture

measurements (i.e., due to equipment failure) were omitted from the modeled results, and, more generally, substantial uncertainty surrounds the goodness-of-fit of these and other diffusivity models in soil (Koehler *et al.*, 2010). The lack of ^{222}Rn data which can be used as a calibration dataset for similar diffusion models (Davidson *et al.*, 2006; Schwendenmann & Veldkamp, 2006) further demands that these modeled diffusion flux results be considered exploratory and not definitive.

That said, some interesting results emerge that could shed light on patterns of surface greenhouse gas fluxes measured in this system (Table 2.6, O'Connell et al., Chapter 3). During the wet season, soybean agriculture at Tanguro Ranch had significantly higher surface fluxes of CO_2 than forest ($p<0.01$); neither N_2O nor CH_4 surface fluxes differed significantly between land uses. Modeled diffusion flux of CO_2 in agricultural soils was near zero from 4.5 m to 15 cm (Figure 2.4). This could suggest that the high surface fluxes of CO_2 measured in soybean fields were primarily driven by soil and root respiration taking place in the top 15 cm of the soil column, where soybean plants have large portions of their rooting mass. Schwendenmann et al. 2003 (Schwendenmann *et al.*, 2003) found that soil CO_2 efflux from both surface and deep soils in a Costa Rican tropical forest was related to fine root biomass, soil carbon and phosphorus stocks. If we assume that there are relatively few roots below the soybean rooting depths in agricultural fields, this same lack of fine roots could explain the relatively low diffusion flux of CO_2 in agricultural deep soils in comparison to forest sub-soils.

Though surface fluxes of N_2O are not significantly different between land uses during the wet season (Table 2.6), modeled diffusion fluxes of N_2O down the soil profile were much more variable in forest sub-soils than in agricultural sub-soils, though fluxes were alternatively negative and positive depending on pit and month. Similarly, the standard deviation of N_2O surface flux emissions from wet season forest sites was higher than the standard deviation of surface flux emissions from wet season soybean sites (1.81 ng N cm^{-2} h^{-1} in forest and 1.17 ng N cm^{-2} h^{-1} in soybean cropland). That deep soil diffusion fluxes and surface fluxes both have higher variability in forest sites than in soybean sites could be explained by the presence of more frequent hot spots and hot moments of N_2O production in these forest soils, which likely had a more heterogeneous root structure.

Indeed, Figure 2.4 shows that diffusion flux of N_2O can run the gamut from negative fluxes to positive fluxes at the same depth during the same sampling period across soil pits. This could be attributed to that same heterogeneity: perhaps hot spots of N_2O production exist up and down the soil profile such that in some cases (e.g., some soil pits), N_2O is flowing downwards from 150 cm depth towards an N_2O sink and in some cases, due to a different distribution of N_2O production hotspots, N_2O is flowing downwards from 150 cm depth. The homogenous diffusion fluxes in agricultural soils (Figure 2.4) could then imply that hot spots and hot moments down the soil profile are either more rare or produce a lower amount of N_2O than in forests. This same hypothesis could also explain the presence of both positive and negative diffusion flux values for CO_2 and CH_4 in forest soils (Figure 2.4): sub-soils in forests could be more variable

across space due to the presence of roots from multiple species, variability in microbial communities, soil structures that differ between pits and across depths, or other sources of variation down the soil profile that would be limited in an agricultural monoculture.

Methane sub-soil fluxes appeared the least variable of the three trace gases measured. Though there was more variability in sub-soil CH_4 diffusion fluxes in forest than in agriculture, that variability was driven by only two forest observations (Figure 2.4). Otherwise, diffusion flux in sub-soil hovered around 0 in both land uses, reflective of the relatively minor levels of CH_4 uptake observed across land uses in this system (O'Connell et al., Chapter 3).

More broadly, these modeled sub-soil trace gas fluxes seem more relevant for interpreting the relatively large variability in forest surface trace gas fluxes than the difference in magnitudes – where they exist – between forest and agricultural surface trace gas fluxes. Forest sub-soils, with relatively cooler temperatures, much more variable volumetric water content, and presumably differences in roots and microbial communities from agriculture, saw modeled trace gas fluxes that varied more between months, pit locations and depths than agricultural soils, all of which may be contributing to the high variability in forest surface trace gas fluxes which is well established in this literature (Groffman *et al.*, 2006; 2009) and at Tanguro (O'Connell et al., Chapter 3).

Future research needs

Exploring many of the above hypotheses about observed differences between land uses in deep soil trace gas will require an additional key data type – nutrient availability and soil solution nutrient pools down the soil column. In this system, we recently installed tension lysimeters at similar depths in each of these study pits. Those data will enable us to explore relationships between soil C and N and the concentration of N_2O, CO_2 and CH_4, as well as make educated guesses about how plant nutrient use may be interacting with microbial metabolism in agricultural and forest sub-soil. Gas, temperature and moisture sampling and data collection are ongoing, and will contribute to a more robust dataset with better estimates of inter- and intra-annual variability in these dynamics.

Land use impacts and potential implications

Tropical soils are a large reservoir of terrestrial C and N; understanding how global change factors such as drought, burning or land use change alter soil biogeochemistry in both deep and shallow soils will be critical for projecting the implications of global change for plant and microbial productivity, terrestrial C and N balance, and water and nutrient availability across the landscape and through time. Particularly in cropland landscapes, where nutrient balance and losses are of particular concern to land managers, exploring how roots, microbes and soil interact to influence nutrient pools and trace gas fluxes could have important implications for soil sustainability and global change impacts in changing tropical agricultural landscapes.

These results – that trace gas concentrations differ significantly between land uses but do not vary significantly by depth – suggest that the effects of land use on trace gas emissions in this landscape are true throughout the soil profile. Further, these results suggest that intensive soybean agriculture does not dramatically contribute to landscape-level increases in GHG emissions at Tanguro or, perhaps, on similar farms in southeastern Amazonia.

Figures:

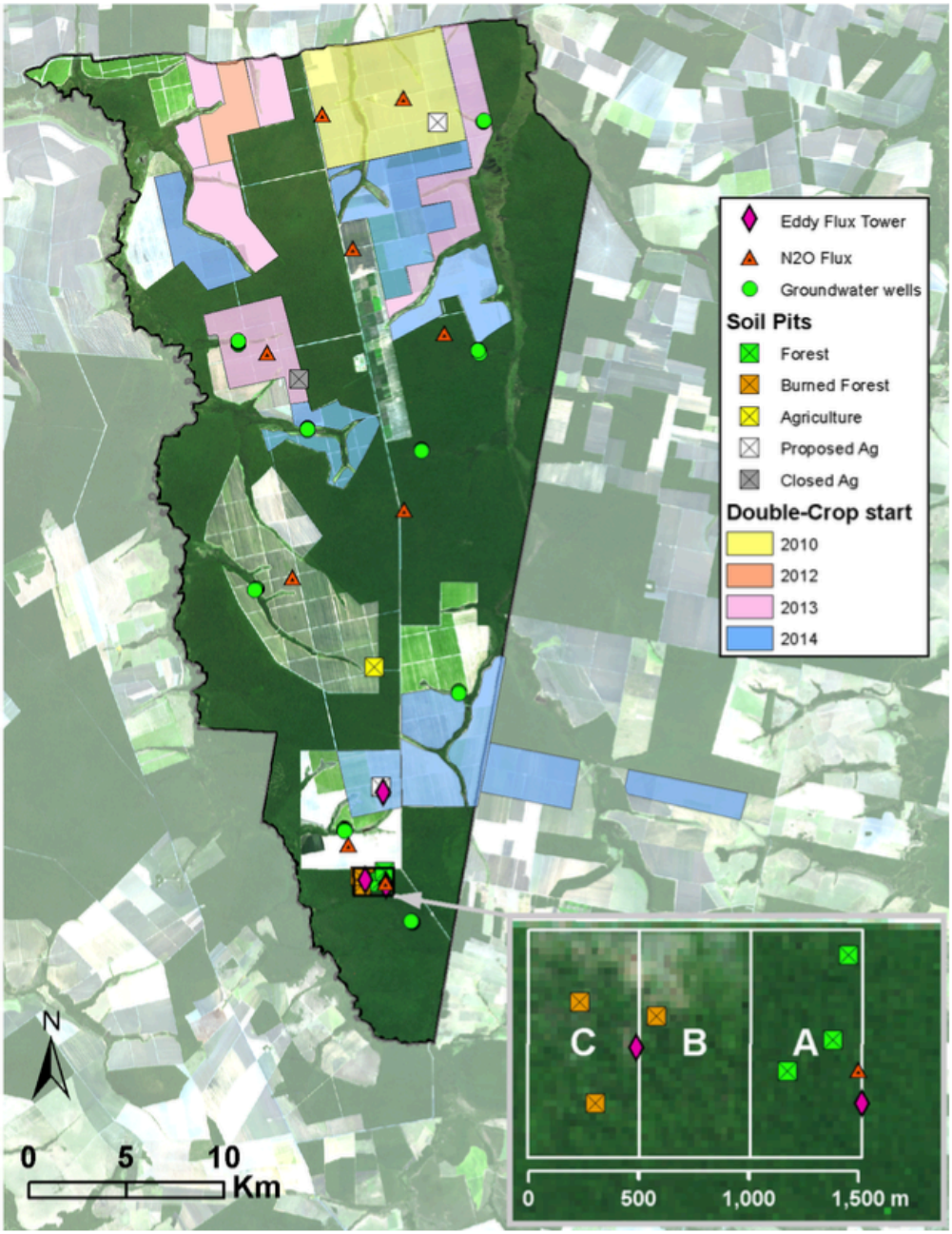

Figure 2.1. Map of study site Tanguro Ranch (courtesy Paul Leferve). Dark areas are forested parcels; light areas are agricultural fields. Soil pits (squares) sampled in this investigation include the southern three forest pits (green squares within forest block "A"

in inset) and an agricultural forest pit (yellow square) in the southern half of the farm. Color overlay indicates what year soy/maize double cropping began, where applicable.

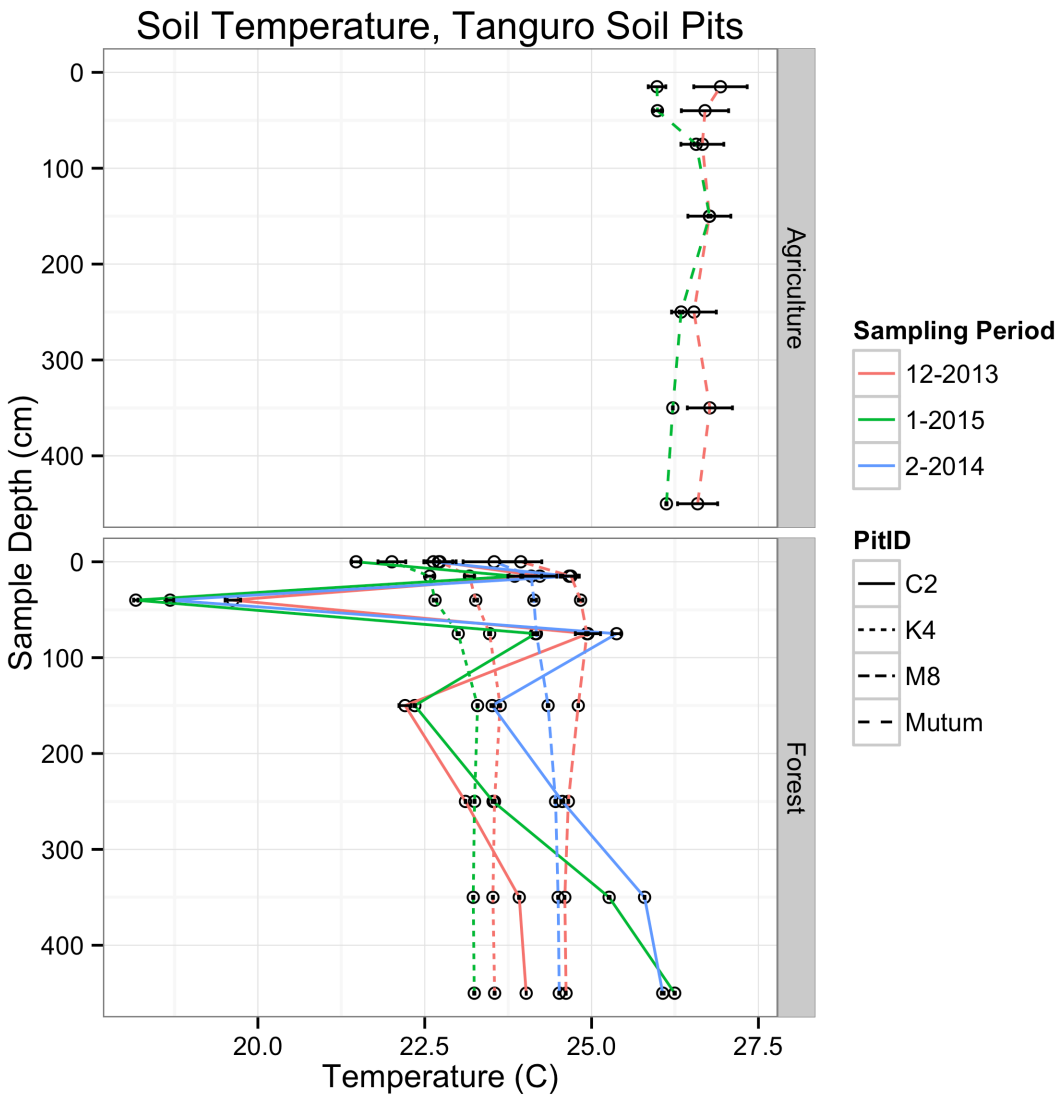

Figure 2.2. Soil temperature (C) in soil pits at Tanguro Ranch. Data are the mean and standard error of a week of thermocouple readings (taken every 6 hours) for the sampling months when gas samples were collected. Line style represents soil pit identification: C2, K4 and M8 are located within intact forest; MU is located within cultivated soybean.

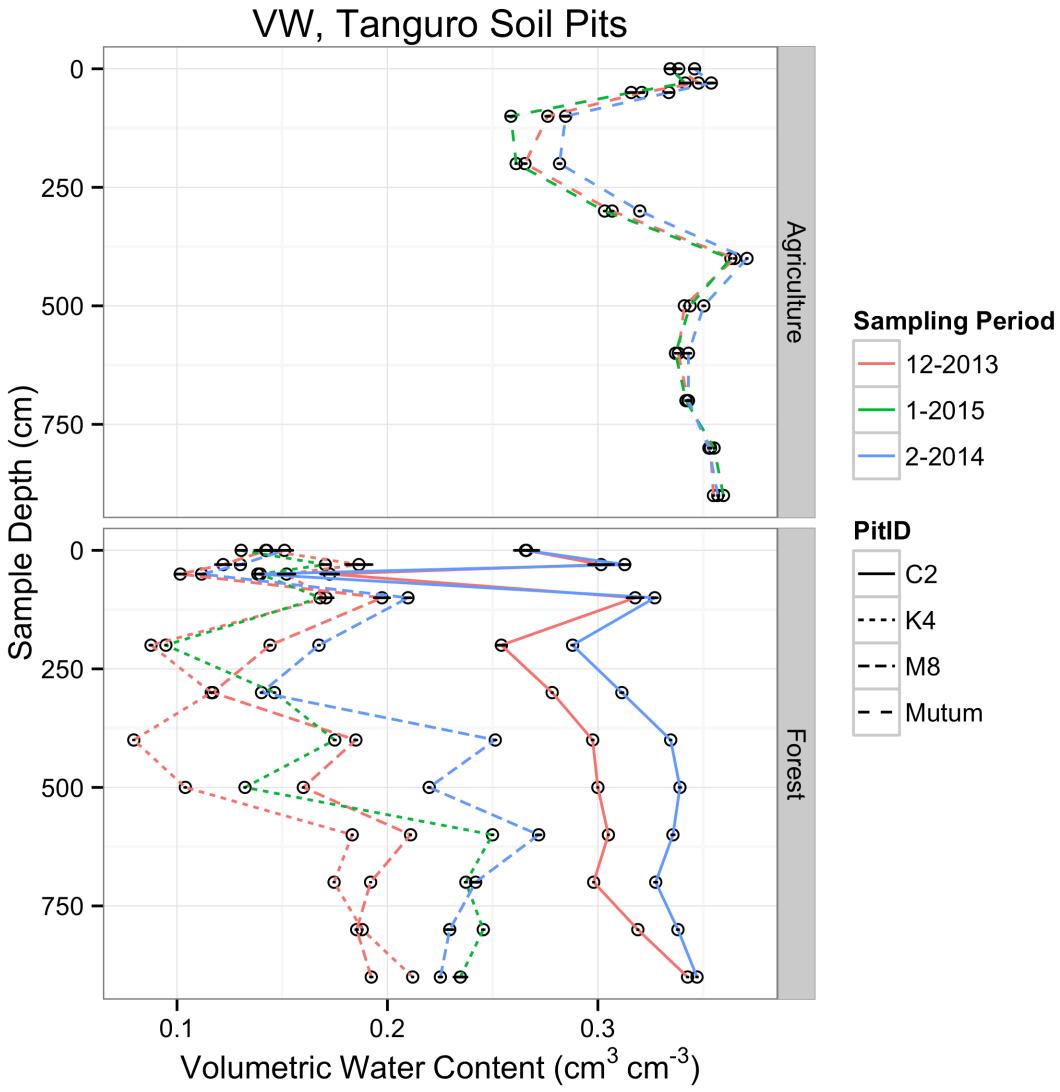

Figure 2.3. Soil volumetric water content (cm^3 cm^{-3}) in soil pits at Tanguro Ranch. Data are the mean and standard error of a week of TDR readings (taken every 6 hours) for the sampling months when gas samples were collected. Line style represents soil pit identification: C2, K4 and M8 are located within intact forest; MU is located within cultivated soybean.

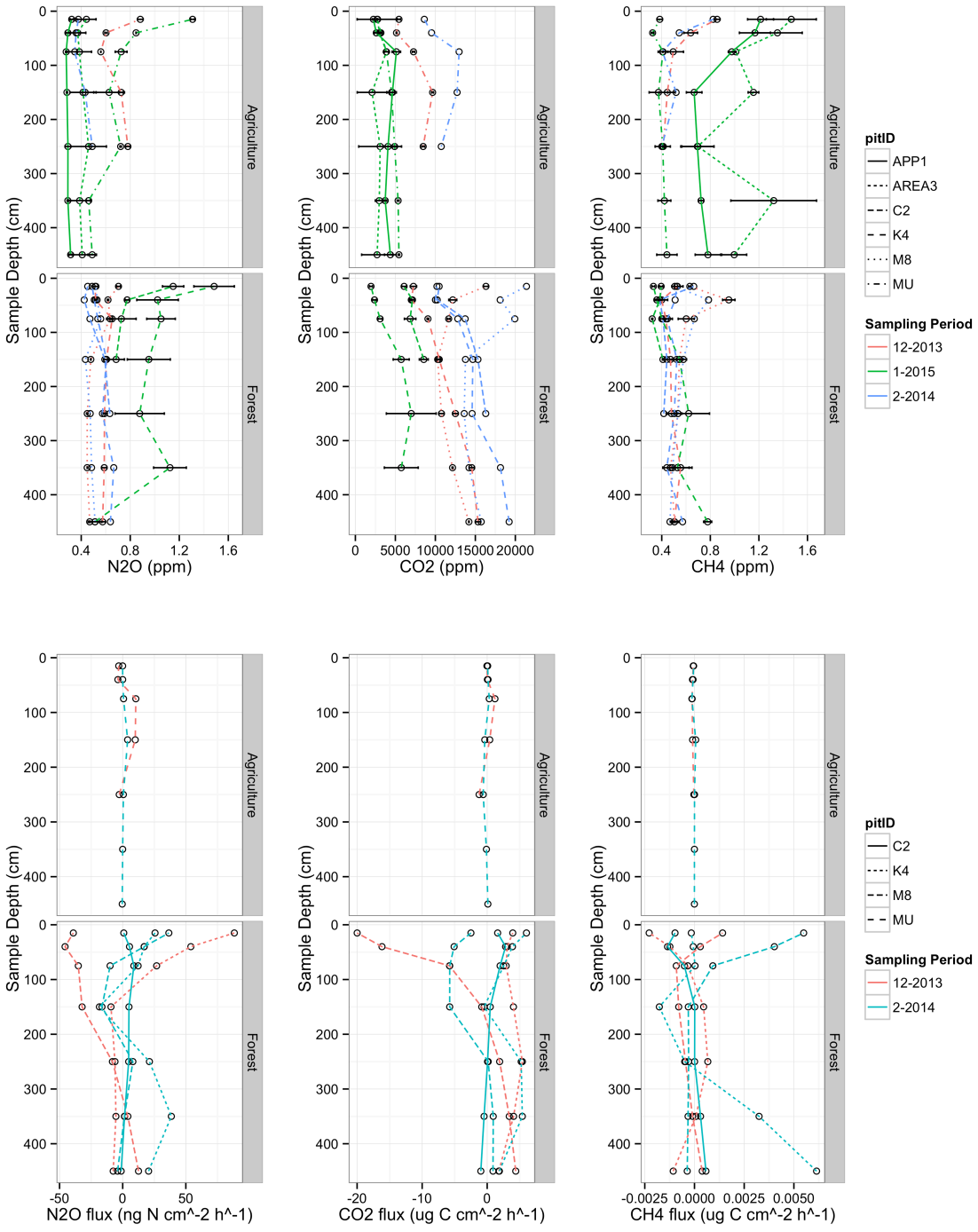

Figure 2.4. Standing concentration (ppm) of trace gases in soil pore space in soil pits at Tanguro Ranch (top panel) and diffusion flux (ng N cm^{-2} h^{-1} or µg C cm^{-2} h^{-1}). Color

indicates sampling month and line type indicates the soil pit identity. Sampling was conducted in December 2013, February 2014 and January 2015. C2, K4 and M8 are located within intact forest, MU and APP1 are located within cultivated soybean, and Area3 is located in soybean/maize double-cropped cultivation. Error bars in the top panel represent the standard error of the multiple vials taken from each gas tube during a given field sampling.

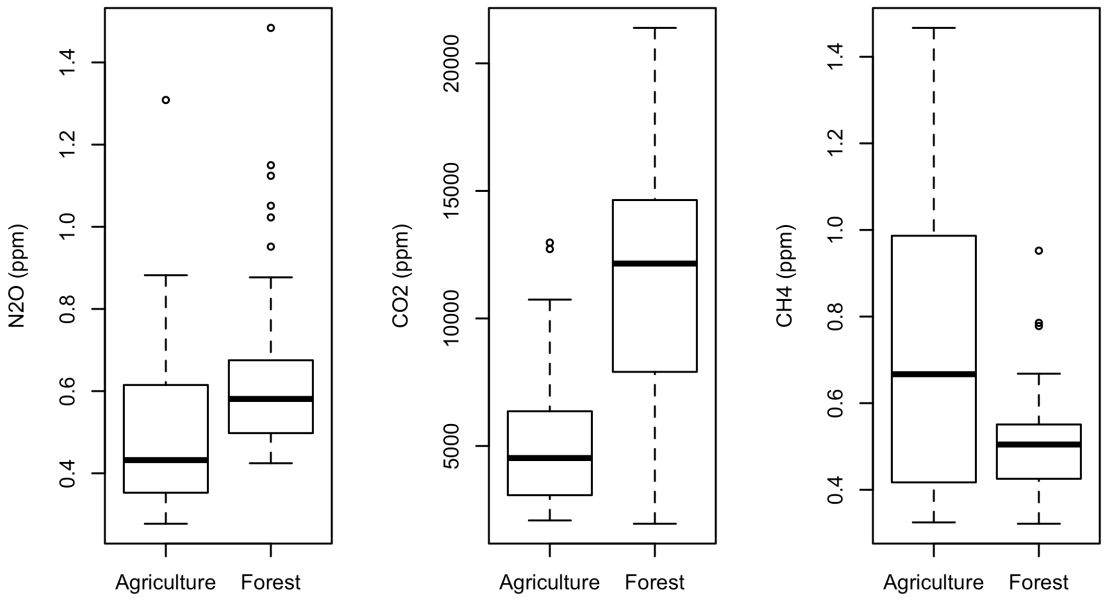

Figure 2.5. Boxplots comparing trace gas concentration between land uses. All three plots have significant differences between land uses ($p < 0.001$).

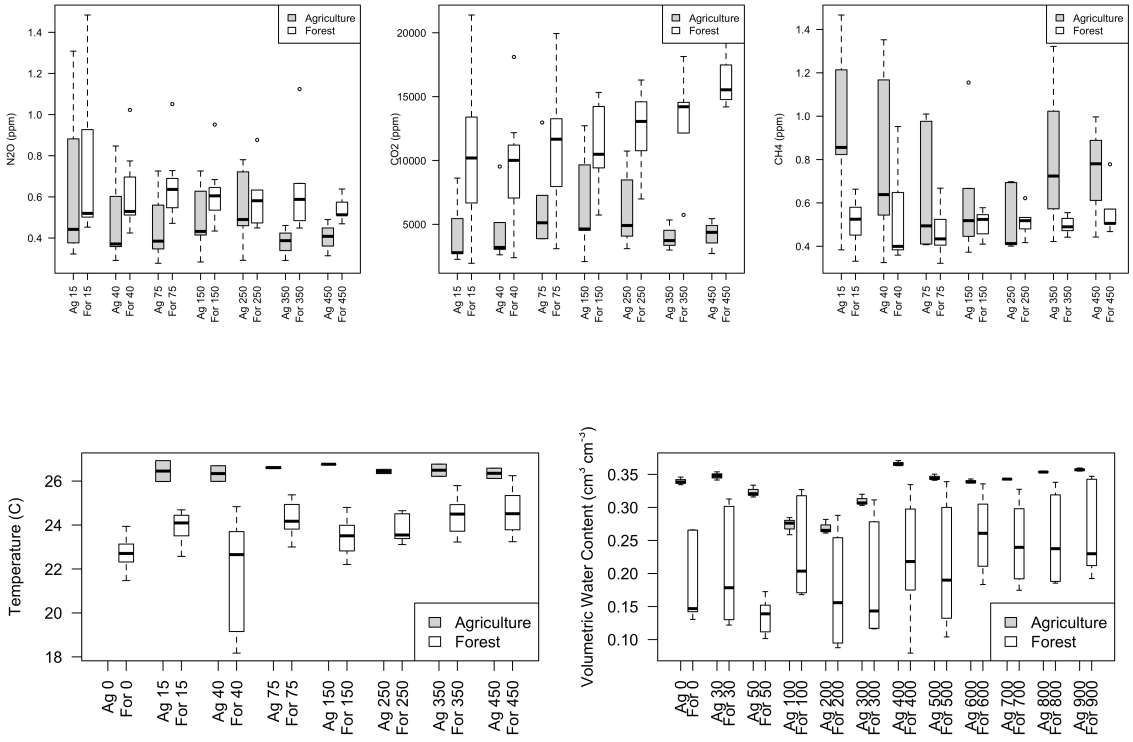

Figure 2.6. Boxplots comparing trace gas concentration, temperature and VWC between land uses, grouped by soil pit depth.

	Df	Sum Sq	Mean Sq	F value	P value
Land Use	1	93.398	93.398	77.445	6.03E-12
Depth	7	40.158	5.737	4.757	0.000334
Land Use:Pit (nested)	2	15.618	7.809	6.475	0.00305
Land Use:Depth (interaction)	6	9.165	1.527	1.267	0.289
Residuals	53	63.917	1.206		
Model details: Temperature predicted by Land Use, Pit nested within Land Use, Depth, and the interaction of Land Use and Depth.					

Table 2.1. Nested ANOVA table comparing the variation in soil temperature between groups.

	Df	Sum Sq	Mean Sq	F value	P value
Land Use	1	0.332	0.332	392.989	5.08E-33
Depth	11	0.0977	0.00888	10.511	9.72E-12
Land Use:Pit (nested)	2	0.254	0.127	150.449	3.63E-28
Land Use:Depth (interaction)	11	0.0339	0.00308	3.647	0.000315
Residuals	82	0.0693	0.000845		
Model details: VWC predicted by Land Use, Pit nested within Land Use, Depth, and the interaction of Land Use and Depth.					

Table 2.2. Nested ANOVA table comparing the variation in VWC between groups.

	Df	Sum Sq	Mean Sq	F value	P value
Land Use	1	1.384	1.384	16.693	0.000139
Depth	6	0.486	0.0810	0.977	0.450
Land Use:Pit (nested)	4	3.046	0.761	9.185	8.47E-06
Land Use:Depth (interaction)	6	0.167	0.0279	0.337	0.915
Residuals	57	4.725	0.0829		
Model details: Log of N_2O concentration predicted by Land Use, Pit nested within Land Use, Depth, and the interaction of Land Use and Depth.					

Table 2.3. Regression table with log of N_2O concentration as the response variable.

	Df	Sum Sq	Mean Sq	F value	P value
Land Use	1	11.225	11.225	53.577	1.03E-09
Depth	6	1.554	0.259	1.236	0.302
Land Use:Pit (nested)	4	6.076	1.519	7.250	8.89E-05
Land Use:Depth (interaction)	6	0.612	0.102	0.487	0.815
Residuals	56	11.733	0.210		
Model details: Log of CO_2 concentration predicted by Land Use, Pit nested within Land Use, Depth, and the interaction of Land Use and Depth.					

Table 2.4. Regression table with log of CO_2 concentration as the response variable.

	Df	Sum Sq	Mean Sq	F value	P value
Land Use	1	1.344	1.344	30.528	8.50E-07
Depth	6	0.498	0.0830	1.885	0.0991
Land Use:Pit (nested)	4	4.927	1.232	27.980	7.11E-13
Land Use:Depth (interaction)	6	0.509	0.0847	1.926	0.0921
Residuals	57	2.509	0.0440		
Model details: Log of CH_4 concentration predicted by Land Use, Pit nested within Land Use, Depth, and the interaction of Land Use and Depth.					

Table 2.5. Regression table with log of CH_4 concentration as the response variable.

Land Use	Season	N_2O Flux (ng N cm^{-2} h^{-1}) NS	CO_2 Flux (µg C cm^{-2} h^{-1}) **	CH_4 Flux (µg C cm^{-2} h^{-1}) NS
Forest	Wet	1.384 (1.813)	13.593 (4.386)[a]	-0.000281 (0.00608)
Soybean/Maize	Wet	1.672 (4.771)	16.846 (12.176)[a]	-0.000462 (0.00139)
Soybean	Wet	0.812 (1.165)	22.226 (20.235)[b]	-0.000468 (0.00536)

Table 2.6. Differences between trace gas fluxes and soil variables between land uses and seasons; data courtesy O'Connell et. al 2015 (Chapter 3 of this document). Responses are reported as mean and standard deviation (in parentheses) values. NS indicated an insignificant difference between groups (one-way ANOVA), while ** indicates a significant model, $p<0.01$. Letters indicate which groups were significantly different (Tukey's HSD post-hoc test).

Supplemental Figures:

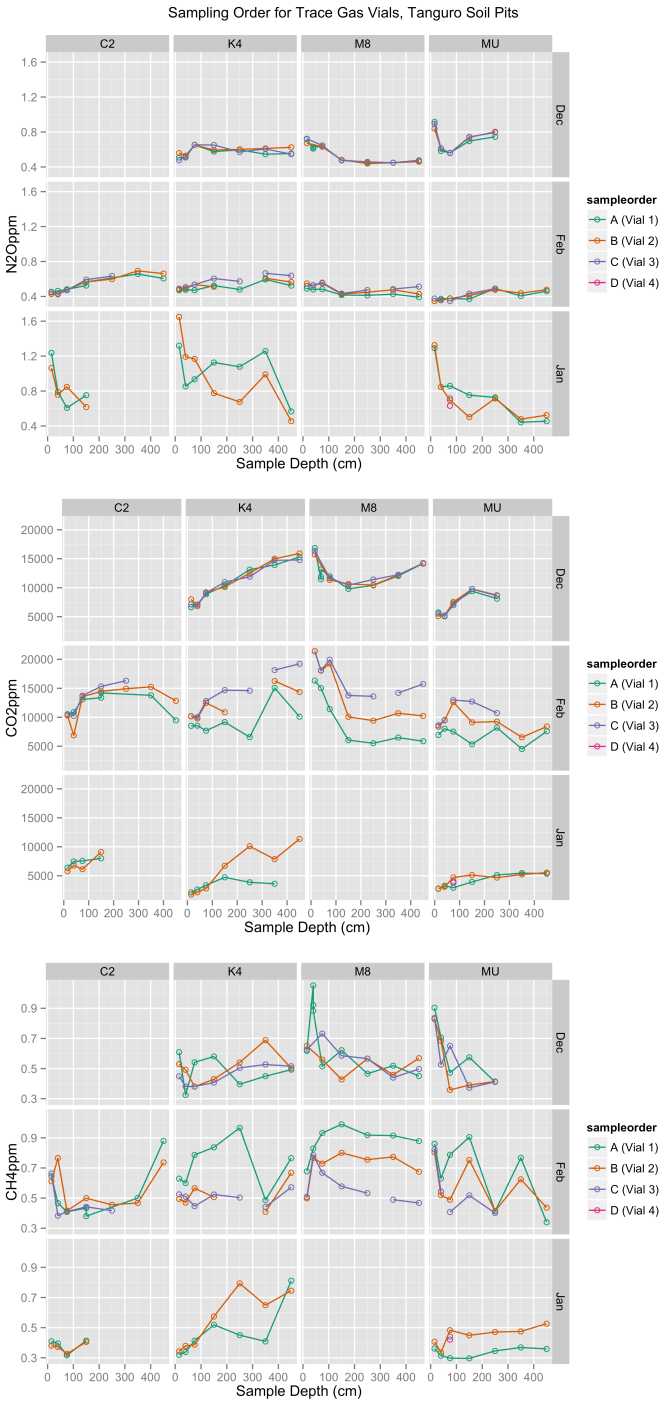

Supplemental Figure S2.1. Standing concentration (ppm) of trace gases in soil pore space in soil pits at Tanguro Ranch. Colors indicate the order in which the vial was

sampled (approximately 1 minute gap between samples), used to assess whether samples were in good agreement.

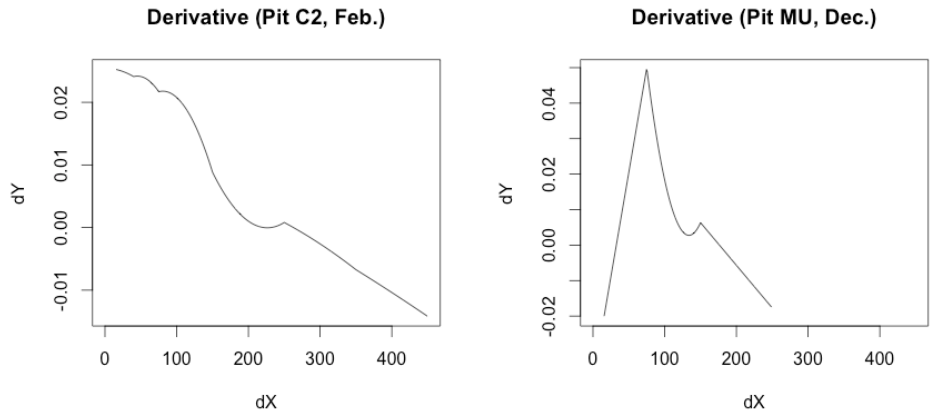

Supplemental Figure S2.2. Examples of the modeled CO_2 concentration gradient, dC/dz, by depth for two pits sampled in a given month. These first derivative values were solved for from a LOESS local regression model to predict μg C cm^{-3} by depth.

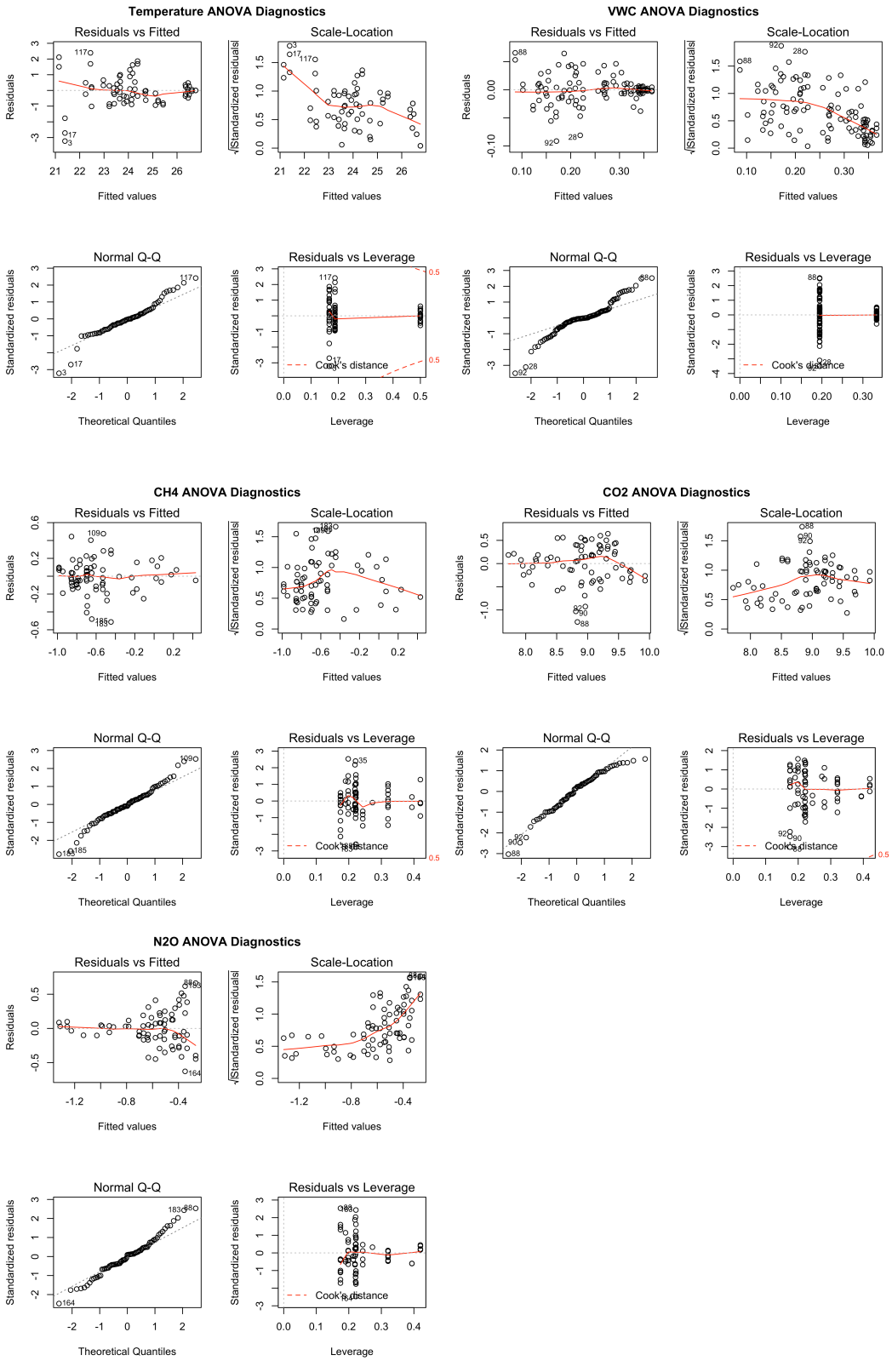
Temperature ANOVA Diagnostics
Residuals vs Fitted
Residuals
Fitted values
Scale-Location
√|Standardized residuals|
Fitted values
Normal Q-Q
Standardized residuals
Theoretical Quantiles
Residuals vs Leverage
Standardized residuals
Cook's distance
Leverage
VWC ANOVA Diagnostics
Residuals vs Fitted
Residuals
Fitted values
Scale-Location
√|Standardized residuals|
Fitted values
Normal Q-Q
Standardized residuals
Theoretical Quantiles
Residuals vs Leverage
Standardized residuals
Cook's distance
Leverage
CH4 ANOVA Diagnostics
Residuals vs Fitted
Residuals
Fitted values
Scale-Location
√|Standardized residuals|
Fitted values
Normal Q-Q
Standardized residuals
Theoretical Quantiles
Residuals vs Leverage
Standardized residuals
Cook's distance
Leverage
CO2 ANOVA Diagnostics
Residuals vs Fitted
Residuals
Fitted values
Scale-Location
√|Standardized residuals|
Fitted values
Normal Q-Q
Standardized residuals
Theoretical Quantiles
Residuals vs Leverage
Standardized residuals
Cook's distance
Leverage
N2O ANOVA Diagnostics
Residuals vs Fitted
Residuals
Fitted values
Scale-Location
√|Standardized residuals|
Fitted values
Normal Q-Q
Standardized residuals
Theoretical Quantiles
Residuals vs Leverage
Standardized residuals
Cook's distance
Leverage

Supplemental Figure S2.3. Diagnostic plots for nested ANOVAs comparing differences measured variables between land uses. The model is a nested design where pit is nested within land use (land use is fixed, pit is random); sample depth and land use are both factors. Sample depth * land use interaction should be included because these are both fixed effects; pit * land use interaction should not be included because that interaction is confounded by the nested pit effect. In all cases, the model is:

aov(Measurement ~ Land Use + Land Use/Pit + Depth + Land Use:Depth (interaction))

Since this experimental design is currently unbalanced, normally we can't trust the p-values from a SS or MS table and we would need to use a Satterthwaite approximation. However, aov() (ANOVA function in R statistical software's base package) handles unbalanced sampling internally and manual corrections for unbalanced sample sizes are unnecessary.

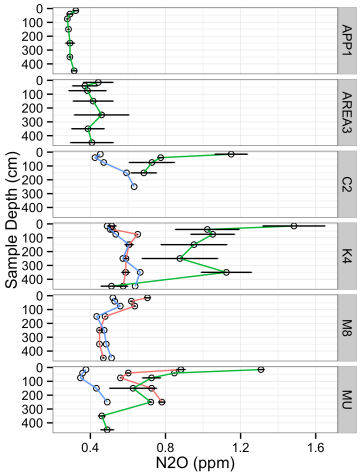
APP1
AREA3
C2
K4
M8
MU
Sample Depth (cm)
0
100
200
300
400
0.4
0.8
1.2
1.6
N2O (ppm)

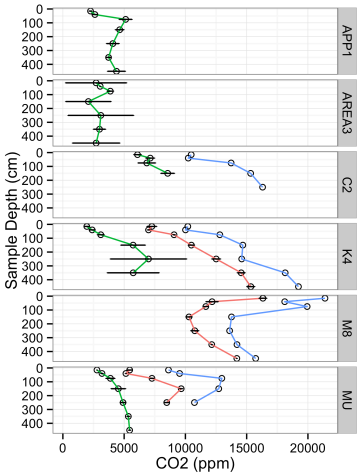
APP1
AREA3
C2
K4
M8
MU
Sample Depth (cm)
0
100
200
300
400
0
5000
10000
15000
20000
CO2 (ppm)

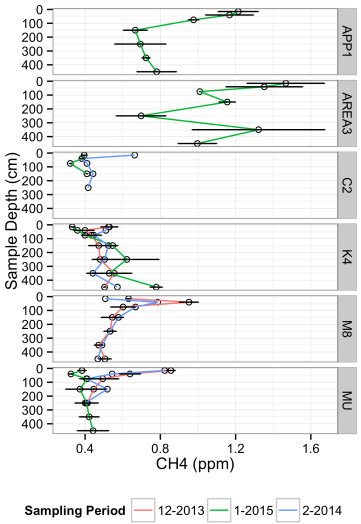
APP1
AREA3
C2
K4
M8
MU
Sample Depth (cm)
0
100
200
300
400
0.4
0.8
1.2
1.6
CH4 (ppm)
Sampling Period
12-2013
1-2015
2-2014

Supplemental Figure S2.4. Standing concentration (ppm) of trace gases in soil pore space in soil pits at Tanguro Ranch. Sampling was conducted in December 2013, February 2014 and January 2015. C2, K4 and M8 are located within intact forest, MU and APP1 are located within cultivated soybean, and Area3 is located in soybean/maize double-cropped cultivation. Error bars represent the standard error of the multiple vials taken from each gas tube during a given field sampling.

Supplemental Text S2.1. While this dissertation is written by the dissertation author, the manuscript version of this chapter will have the following authorships and affiliations:

Authors: Christine S. O'Connell[1,2]*, Michael Coe[3], Eric Davidson[4], KathiJo Jankowski[5], Paul Leferve[3], Chris Neill[5], Rodney Venterea[6,7]

Affiliations:

[1]Department of Ecology, Evolution & Behavior, University of Minnesota, Saint Paul, Minnesota, 55108, USA

[2]Institute on the Environment, University of Minnesota, Saint Paul, Minnesota, 55108, USA

[3]Woods Hole Research Center, Falmouth, MA 02450, USA

[4]University of Maryland Center for Environmental Science, Appalachian Laboratory, 301 Braddock Road, Frostburg, MD 21532, USA

[5]The Ecosystems Center, Marine Biological Laboratory, 7 MBL Street, Woods Hole, MA 02543, USA

[6]Department of Soil, Water, and Climate, University of Minnesota, St. Paul, MN 55108, USA

[7]USDA-ARS, Soil and Water Management Unit, 1991 Upper Buford Circle, St. Paul, MN 55108, USA

*Correspondence to: coconn@umn.edu

Chapter 3:

Intensified double-cropping in Southeastern Amazonia has limited effects on soil nitrous oxide emissions and N availability

Abstract

Over the last 30 years, southeastern Amazonia has experienced extraordinary growth in agricultural production, both from agricultural expansion and more intense management on Amazonia's existing croplands. In particular, there has been a marked trend towards intensive management, including nitrogen (N) fertilization and double-cropped soybean/maize systems. It remains unclear how N fertilizer addition impacts soil nutrient cycling and greenhouse gas (GHG) emissions from southeastern Amazonia's soils. We used field measurements to estimate how cropland intensification in Mato Grosso, Brazil affects the emissions of nitrous oxide (N_2O), carbon dioxide (CO_2) and methane (CH_4), with particular focus on soil N dynamics and N_2O emissions after nitrogenous fertilizer application.

Measured N_2O fluxes were similar in forest and intensified croplands and the magnitude of fluxes were lower than other Amazonian forest fluxes reported in the literature and were more similar to annual N_2O fluxes from cerrado ecosystems. Dry season N_2O emissions in single-cropped (soybean only) fields, double-cropped (soybean/maize) fields and reference tropical forest were below 0.5 ng N cm^{-2} hr^{-1}. Wet season emissions rates across land uses were 1-4 ng N cm^{-2} hr^{-1}, with isolated post-fertilization spikes in N_2O emissions (maximum flux of 42 ng N cm^{-2} hr^{-1}). We estimated

annual N_2O flux rates for each land use, and found that forest soils have the highest annual fluxes (0.75 kgN ha^{-1} $year^{-1}$), followed by soybean/maize croplands (0.51 kgN ha^{-1} $year^{-1}$) and soybean croplands (0.45 kgN ha^{-1} $year^{-1}$). The relatively low N_2O emissions from both managed cropland and unmanaged forest in this area suggests that, given similar soil and fertilizer contexts, croplands in southeastern Amazonia can be intensified to double-cropping soybean/maize systems without incurring substantial increases in greenhouse gas emissions.

Keywords: tropical N cycle, greenhouse gases, Amazonia, agricultural intensification

Introduction

Amazonian croplands, particularly those growing commodity crops such as soybean, maize or cotton, increasingly feature mechanized, intensive management practices. Cropland intensification in Amazonia has poorly understood consequences for nutrient cycling and GHG emissions. In contrast, temperate croplands have long featured intensive management practices, including the addition of fertilizer, herbicide, pesticide, fungicide or other additives above baseline levels, employing advanced seed or mechanization technology, or introducing a more frequent cropping schedule (Foley *et al.*, 2005). More recently, the eastern edge of the Brazilian Amazon has been home to similar cropland intensification. In Mato Grosso state, soybean yields per hectare have been increasing steadily since 2000 (Macedo *et al.*, 2012; Ray *et al.*, 2013) and the area of double-cropping increased by 270% between 2001 and 2011 (Spera *et al.*, 2014). The vast majority (92%) of Mato Grosso's double-cropped croplands are a rotation of soybean/maize (Spera *et al.*, 2014) that has the potential to alter several aspects of the terrestrial nitrogen (N) and carbon (C) cycles and in turn soil emissions of GHGs. How this novel, but spreading, land use will influence soil biogeochemistry and GHG dynamics in southeastern Amazonia remains unclear.

Southeastern Amazonia differs dramatically from temperate croplands that more traditionally include intensified soybean/maize rotational systems. Tropical soils are relatively acidic, depleted in base cations and clay rich (Jobbágy & Jackson, 2001; Batjes, 2007), and because the growing season is long, soybean and maize can be planted in

immediate succession (i.e., double cropped) during a single growing season (Galford *et al.*, 2008). It remains unclear how trace gas fluxes and soil N cycling will change as double-cropping is introduced to southeastern Amazonia's croplands.

Surface soil chamber studies of nitrous oxide and other trace gas emissions have occurred patchily across Amazonia (Table 3.1). But to our knowledge this is the first study that occurred both inside Amazonia (e.g., in a forested biome and not cerrado, or tropical savanna) and measured nitrous oxide fluxes from intensified cropland. While other studies have measured N_2O emissions from maize and soybean in Brazil, those have occurred in the cerrado and not Amazonia. Southeastern Amazonia, where this study occurred, is drier than central Amazonia and other wet tropical forests across the globe (much of Amazonia's southeast gets less than 2000 millimeters of rain per year, typical of a seasonally dry tropical forest (Murphy & Lugo, 1986)), but, unlike the drier cerrado, has closed-canopy forests and higher rates of evapotranspiration, suggesting that N cycling in southeastern Amazonia may be affected by land use change differently than in deeper Amazonian forests or in cerrado.

Mato Grosso's agricultural development

Mato Grosso, a heavily agricultural Brazilian state in Southeastern Amazonia, has had several decades of agricultural development that have been linked with demand for beef and animal feed (in the form of soybeans and, increasingly, maize) on the international market; many of these exports go from Brazil to China, the European Union, and Iran

(MacDonald *et al.*, 2015). Soybean cropland yields have increased as this demand increased (Macedo *et al.*, 2012) due to many of the aforementioned intensive cropping practices: seed technology and alternate varietals, lime addition and soil pH management, and increased use of fertilizer, pesticides and herbicides. Other work has argued that soybean intensification in southeastern Amazonia is driven by rising demand in growing urban areas (DeFries *et al.*, 2013) and a study that considered soybean/maize double cropping in Mato Grosso similarly found that double cropping was correlated with access to transportation networks, international markets, and a previously established agricultural region (VanWey *et al.*, 2013). Agricultural intensification in Mato Grosso via a combination of increases in inputs and double cropping is a novel and transformative land use occurring over large areas on tropical soils (Galford *et al.*, 2011). As such, assessing the tradeoffs between agricultural production and ecological impacts in Amazonia will require investigating these recent – and understudied – intensification impacts (Lapola *et al.*, 2014).

Mechanisms of N cycle disruption after intensification

Nitrogenous fertilizer addition can have cascading effects on soil N pools and fluxes depending on the type of fertilizer applied, the timing of fertilizer application and the soil microbial and mineralogical context (Vitousek *et al.*, 1997b; Galloway *et al.*, 2004; 2008). Nitrate (NO_3^-) fertilizers (e.g., calcium nitrate) immediately increase the pool of labile N available to microbial and root uptake, though to what extent depends on the

duration and placement of fertilizer (van Kessel *et al.*, 2012). Denitrifying bacteria reduce nitrate, which leads to the loss of nitric oxide (NO), N_2O, or nitrogen gas (N_2) (Firestone & Davidson, 1989). Alternatively, NO_3^- can be reduced to NO_2^-, which can then be oxidized back to NO_3^- by nitrifying bacteria; some NO_2^- can be converted to N_2O via nitrifier denitrification (Venterea *et al.*, 2012). In this way, nitrate fertilizers can lead to an increase in soil N availability, an increase in gaseous N losses, or some combination, and through multiple pathways. Additionally, nitrifier denitrification can occur both aerobically and anaerobically, while denitrification is an anaerobic process. These two processes, which both produce N_2O, are difficult to distinguish, as both can be happening at once given variation in soil water content and the microbial community across space.

Urea, manure or other fertilizers with organically bound N, as well as biological N fixation, can also lead to increases in soil available N. As decomposition occurs, N is mineralized and subsequently available as ammonium (NH_4^+). Ammonium can also be added directly by cropland managers as fertilizer (e.g., ammonium sulfate). NH_4^+ then undergoes nitrification and, as above, some of the intermediate product NO_2^- is converted to N_2O via nitrifier denitrification. The product of nitrification, NO_3^- is also then available for denitrification. As such, multiple N fertilizer types can contribute to changing N pools, associated changes in the rates of transformations between N pools, and losses of gaseous N.

Finally, cropland intensification can also have effects on the emissions of CO_2 and CH_4 (Smith *et al.*, 2008; Linquist *et al.*, 2011). Land clearing for agriculture increases

decomposition and loss of soil C as CO_2 in tropical forests (Powers *et al.*, 2011), though slow and fast decomposing pools of carbon likely respond differently depending on the system that undergoes land use change (Schwendenmann & Pendall, 2008) and in some cases soil respiration rates might change only slightly after deforestation (Veldkamp, 1994). Methane uptake by methanotrophs or ammonium oxidizers normally reduces the overall GHG profile of Amazonian forests, and decreases in net consumption could eliminate this GHG sink (Mosier *et al.*, 2004). Net methane consumption in tropical forest soils has been shown to fall after clearance for agriculture (Keller *et al.*, 1990), though this trend can perhaps be mitigated through targeted, crop-specific intervention (Cerri *et al.*, 2007). Tillage practices can influence both CO_2 and CH_4 since it alters soil oxygen availability and decomposition rates (Batjes & Sombroek, 1997).

Disruptions to Southeast Amazonian soil biogeochemistry

Rapidly spreading cropland intensification is transforming the Amazon's agricultural frontier. In particular, double cropping's effect on N cycling is poorly understood in southeastern Amazonia (Galford *et al.*, 2010; Lapola *et al.*, 2014). Determining the magnitude of N cycle changes on tropical croplands is critical to accurately determining how tropical land use is contributing to global change writ large. Here, we report the results of a field study in southeast Amazonia that assessed the impact of double-cropped, soybean/maize intensification on soil GHG emissions and N dynamics – specifically, we targeted the effect of cropland intensification on the emissions of nitrous oxide (N_2O),

carbon dioxide (CO_2) and methane (CH_4) from soils. We hypothesized that N_2O emissions, soil N availability and/or rates of soil N transformation would increase significantly in intensified croplands relative to reference forest, since in this system cropland intensification is accompanied by N inputs to the soil via biological N fixation (i.e., during soybean cropping) and via N-fertilizer addition (i.e., during maize cropping). As double-cropped, tropical cropland becomes more common in southeastern Amazonia, questions surround how soil GHG fluxes will change between cropland and forest soils. This work both characterizes N_2O, CO_2 and CH_4 emissions patterns across land-use types and as well as potential drivers of those patterns by evaluating relationships between GHG fluxes and soil properties.

Materials and methods

Site description

Sampling was conducted at Tanguro Ranch, a 32,000 hectare industrial farm located in Mato Grosso, Brazil (Figure 3.1). Tanguro Ranch is surrounded by closed-canopy tropical forest (25m height) typical of southeastern Amazonia, a region of transitional forest between cerrado (tropical savanna) to the east and more diverse, high-statured forests to the northwest. This area of Amazonia is also marked by lower precipitation and higher seasonality than central Amazonia. Mean annual precipitation (MAP) at Tanguro Ranch averaged 1900 mm/year between 1987 and 2007 and ranged from 1500

to 2500 mm yr^{-1} (Tanguro Ranch, unpublished results). The wet season extends from September to April with a dry season between May and August (Figure 3.2). Mean annual temperature (MAT) is 27 °C, but temperatures vary between forested areas and cropland areas both diurnially and on average over the year (Supplemental Figure S3.1). Tanguro Ranch is located on the Brazilian Shield and the underlying parent material is Precambrian gneisses. Upland soils are ustic oxisols (55% sand, 2% silt, and 43% clay mean texture) with high infiltration rates and little lateral water movement in upper soil horizons (depth to water table estimated to be between 20-40m) (Hayhoe *et al.*, 2011). The site features little topographic variation and is generally flat plateaus interspersed with stream channels.

Originally deforested to support a pasture ranch, Tanguro now primarily plants soybeans, an N-fixing legume. Tanguro's croplands are intensively managed, receiving multiple applications per year of fertilizer (phosphorous [P] and potassium [K]), pesticide, herbicide and soil additives (lime) to moderate soil pH (Grupo A. Maggi, pers. comm.). In recent years Tanguro has begun double-cropping with maize after the primary soybean season, necessitating not only higher gross application rates of P and K, but also the addition of N fertilizer. N fertilizer is applied twice per season to maize crops. First, nitrate is applied directly to the line of seeding concurrently with planting (~30 kg N ha^{-1}). Nitrate is applied in an NPK mix of 18N:21P:8K, with the chemical form determined by the least expensive option (Tanguro Ranch management, pers. communication). Approximately 20 days after planting, broadcast N fertilization of urea occurs (~45 kg N ha^{-1}, for ~75 kg N ha^{-1} total N fertilizer). Fields that are not planted with corn after the

soybean harvest remain fallow through the onset of the next soybean planting season, or are seeded with low-quality seed mixes (e.g., grasses, millet).

Single- and double-cropped fields create an intensification contrast, both of which can be compared with neighboring intact tropical forest. All fields included in sampling were originally cleared for pasture in 1982 and 1983 and converted to soybean between 2003 and 2008, with a subset of those fields becoming double-cropped between 2010 and 2013 (Figure 3.1). Double-cropping at this site is relatively new: at Tanguro, double cropping took place on 10% of fields in 2011, on over 25% in 2012, and on over 50% of fields (18,000 of 32,000 hectares) during the 2013 season, though it has since decreased on the farm while farmers pursue more permanent storage for the harvested maize (Grupo A. Maggi, pers. comm.). There have been numerous previous research projects in this system, all with the cooperation of farm leadership (Balch *et al.*, 2008; Riskin *et al.*, 2013; Brando *et al.*, 2014).

Experimental set up description

We chose three forest sites, three soybean sites, and three soybean/maize sites from across Tanguro Ranch for a total of nine site locations across three land uses (Figure 3.1). We limited forest sites to locations that were no less than 0.5 km from an open field so as to limit the edge effects of land use change. We selected fields that we knew had been chosen for either single- or double-cropping in 2012 for the remaining sites. Field selection was done as a convenience sample based on road access.

We established a nested sampling design where site was nested within land-use type and sampling at each site was repeated over time, as follows. One site within each land use was targeted as a high-frequency sampling site: that site was sampled roughly twice per week, while the two other sites in that land use were sampled roughly every two weeks. In this way, at least one forest, one soybean and one soybean/maize site was sampled twice per week throughout each field campaign and could be directly compared. Though these three high-frequency sites were not always sampled on the same day, we attempted when possible to sample all three within a 48-hour period. At each site, a centralized GPS point along either a road bordering the field or the path leading into the forest was established as the site's center point. From there, for each sampling we took a "random walk" (random number draws for a walk between 20-80 meters in two cardinal directions) into the forest or cropland field before installing the static flux chambers.

Trace gas measurements

We used a closed chamber method (*sensu* Venterea 2005 (Venterea *et al.*, 2005)) to measure soil-to-atmosphere fluxes of CO_2, N_2O and CH_4. Rectangular thin-walled (20 gauge) stainless steel chamber bases (53 cm long, 32 cm wide, 10 cm deep) were inserted into the soil with 2-5 cm of space between the soil surface and the lip of the chamber. Bases were inserted prior to measurement each day, as farm activity prevented installation of bases for the entirety of the season. Five bases were then arranged in a

diamond pattern with a central base, with the corner bases 5 m from the central base in the diamond pattern. At cropland sites, bases were randomly chosen to be inter-row or row chambers. Bases were placed parallel with cropland rows, either centered on the row or centered in between rows. When chambers were placed in locations with plants that were larger than the chamber tops (e.g., soybean plants taller than 10 cm), aboveground biomass was either bent or trimmed until the chamber tops were able to close. Near the end of the maize growing season, the maize stalks were cut in order to close the chamber tops over plants, leaving roots intact.

Chamber tops were also constructed from stainless steel rectangular tubs (20 gauge, 53 cm long, 32 cm wide, 12 cm deep). The chamber edges (2 cm wide) were lined with ethylene propylene diene terpolymer (EPDM) weatherproofing material to provide an airtight seal. Chamber tops were sealed to chamber bottoms using 10 metal clamps arranged around these edges. To prevent large temperature increases inside the chamber, chamber tops were covered with reflective insulating material. A vent tube (0.64 cm diameter, 20 cm long, stainless steel) was inserted near the bottom edge of the chamber top. Fluxes were generally measured between 800 and 1200 h local time when soil temperatures were expected to be within one standard deviation of their daily mean values (Supplemental Figure S3.1).

Deployment time was 30 minutes (gas measurements collected at minutes 0, 10, 20 and 30) between May and August 2012 and 45 minutes (gas measurements collected at minutes 0, 15, 30 and 45) for the remainder of the study period. Samples were collected using a polypropylene syringe (Monoject) that withdrew 12 mL of gas from a

port located at the top of the closed chamber system. Samples were then injected into 9-mL glass vials that had been pre-sealed with butyl rubber septa (Grace Davidson). We used un-evacuated vials containing "ambient" (lab) air (*sensu* Venterea 2005 (Venterea *et al.*, 2005)). Sets of vials containing ambient air included four replicate vials with ambient air that were later analyzed for concentrations of CO_2, N_2O and CH_4, which were then used to correct for the gas concentration from samples collected from chambers. Un-evacuated vials were preferred over evacuated vials in this study because of the length of time that prepared evacuated vials would have been sitting at ambient pressure while in the field. During 2012-14, there was no reliable means to evacuate vials on site, and vials would have had to be evacuated prior to the field season; as evacuated vials sat for up to 3 months, there would have been a high risk of inward air leakage.

Flux measurements were taken between June 2013 and November 2014 during three field campaigns – longer periods of field sampling during a dry season period (June-July 2013), a wet season period (December 2013-April 2014), and soon after the onset of the wet season (November 2014, Figure 3.2, Supplemental Table S3.1). Planting and fertilization dates for soybeans and maize varied across sites, but maize was generally planted in January and harvested in March. Maize was planted with 24 hours of soybean harvest at which point the first N fertilization took place. Maize was fertilized again with broadcast fertilizer application approximately 20-30 days after planting and harvested after another 20 days.

Gas samples were analyzed by gas chromatography (model 5890 Agilent/Hewlett-Packard, Santa Clara, CA) using a headspace autosampler (Teledyne

Tekmar, Mason, OH) at the University of Minnesota. Travel standards were carried from Brazil to Minnesota and used when applicable to correct for travel disruption to samples. The autosampler was modified to fill multiple sample loops from each vial. Sample loops fed into a flame ionization detector for CH_4, an electron capture detector for N_2O and a thermal conductivity detector for CO_2. Standard curves and system calibration were done using analytical grade standards (Scott Specialty Gases, Plumsteadville, PA). Gas fluxes were calculated by fitting a linear model to gas samples taken at the four time points in the field and converted to fluxes on a per area basis using soil surface area within the chamber.

Soil property measurements

We measured temperature using soil temperature probes during the chamber deployment period. Probes were inserted to 10 cm depth within 30 cm of the chamber. Air temperature was measured using a temperature probe placed slightly above the ground near the middle of the five chambers underneath crop or forest canopy as applicable.

After every gas measurement for every chamber, we measured soil inorganic N pools, net N mineralization rate, net nitrification rate and percent soil moisture. After the final gas sample was collected for a given static flux measurement, we collected two 0-10 cm soil cores from the inside of each chamber. One of the collected soil cores was weighed within 6 hours, dried in a drying oven (105 °C for 36-48 hours) and then reweighed to calculate percent soil moisture. The other soil core was used to determine

concentrations of nitrate and ammonium, and net N mineralization and nitrification rates. Within 12 hours of collection, soils were sieved (2 mm), approximately 10 g of field-wet soil was extracted in 50 mL of 2 M KCl for 2 minutes, manually shaken, and then left for 24 hours. After 24 hours, extracts were filtered (no. 42; Whatman, Maidstone, UK) and frozen in polyethylene vials (Fisher Scientific) until analysis. An additional ~10 g of field-wet soil was weighed, placed in a specimen cup (Fisherbrand, 4 oz. capacity), covered, and left to incubate at ambient air temperature (~25 ^{o}C) in a shaded area of the lab for 7 days, at which point those samples underwent the same extraction procedure as the soils that underwent immediate extraction. Extracts were frozen until analysis at Centro de Energia Nuclear na Agricultura (University of Sao Paulo) for ammonium and the sum of nitrite and nitrate using a flow injection analyzer and spectrometric detection (Foss). Differences in ammonium- + nitrate-N and in nitrate-N between initial and post-incubation soil samples were used to calculate the mean net N mineralization rates and net nitrification rates, respectively, during the incubation period.

Bulk density (0-10 cm) was determined in July 2013 using a truth bar to excavate a 10 cm x 10 cm x 10 cm pit of soil followed by drying (105 °C, 48 hours) and weighing. Wet season bulk density samples were collected in November 2014 using a bulk density corer (97 ml, 3 cores 0-10 cm were collected) followed by drying (105 °C, 48 hours) and weighing. These two methods had good agreement, though the truth bar method had consistently lower bulk density values in forest (Supplemental Figure S3.2). Below, any bulk density measurements reported are the mean of the truth bar and corer bulk density values for each site.

Statistical Analyses

To analyze differences in trace gas flux rates and soil N pools and transformations between land uses, we conducted a one-way repeated measured analysis of variance (ANOVA), where land use (e.g., forest, soybean or soybean/maize) was a predictor variable for flux rates or soil variables. Repeated measures were conducted on site (i.e., sampling location) as a random effect, with week of measurement nested within site. We nested week of measurement within site because not all sites were measured each sampling day, but sites of every land use were measured every week. Including week of measurement as a nested variable allows forest sites that were measured, for instance, two days after a soybean site was measured to be compared in the same set of repeated measurements. For statistically significant ANOVA models ($p<0.05$), we conducted a Tukey's HSD posthoc test with a bonferroni correction to determine which groups had statistically significantly different means ($p<0.05$).

We also analyzed how land use and season predicted trace gas flux rates and soil N pools and transformations using a two-way repeated measures ANOVA where land use (e.g., forest, soybean or soybean/maize) and season (e.g., wet or dry season) were predictor variables for flux rates or soil variables. As above, repeated measures were conducted on site (i.e., sampling location) as a random effect, with week of measurement nested within site.

Finally, we conducted a two-way repeated measures ANOVA in which land use (e.g., soybean or soybean/maize) and row placement (e.g., row or inter-row locations on the cropping landscape) were predictor variables for flux rates or soil variables; forest was omitted from the two-way ANOVA as its chambers did not have row placement designations. In these tests, an additional "land use" was added, soybean/maize cropland in the 15 days after fertilization. We hypothesized that row/inter-row effects should be strongest in the days after fertilization and wanted to explicitly consider this option by including row placement as a distinct treatment. For both two-way ANOVA analyses, posthoc tests (Tukey's HSD with a bonferroni correction) were conducted for significant models ($p<0.05$). In cases where an interaction term was significant, this precludes interpretation of main effects, so posthoc tests were not conducted.

For all of the above, to ensure that each model met the assumptions of ANOVA, several diagnostic plots were considered: a trellis plot, a Q-Q plot, and two plots visualizing the distribution of model residuals (Supplemental Figure S3.3). When the assumptions of ANOVA were violated, the model's response variable was log transformed and the model recalculated. In all cases where ANOVA assumptions were initially violated, log transformation improved residual distributions substantially.

To analyze whether soil variables correlated with trace gas flux rates, we used linear regression models. Pearson's linear correlation coefficient (*r*, measures correlation on a -1 to +1 scale) was used to determine to what extent soil variables and trace gas fluxes were correlated. All statistical tests were performed in the R statistical software

environment (R version 3.1.2, packages "nlme" for model construction and "multcomp" for posthoc tests).

We calculated the detection limits on measured trace gas fluxes using a methodology that takes into account the chamber deployment time, number of sampling points used to model the flux rate, and analytical precision, among other variables (Parkin *et al.*, 2012). During the first field sampling period (dry season), when we used a 30-minute chamber deployment, detection limits were 0.58 ngN cm^{-2} h^{-1} for N_2O, 0.0095 μgC cm^{-2} h^{-1} for CO_2 and 0.0022 μgC cm^{-2} h^{-1} for CH_4. During subsequent sampling seasons we lengthened the chamber deployment time to 45 minutes and detection limits decreased to 0.44 ngN cm^{-2} h^{-1} for N_2O, 0.0071 μgC cm^{-2} h^{-1} for CO_2 and 0.0017 μgC cm^{-2} h^{-1} for CH_4. Measured fluxes below the detection limit remain in the full dataset so as to represent the very low fluxes that we often observed as transparently as possible. We report these detection limits here to allow readers to interpret these data with more context.

Annual flux estimates

We estimated the annual GHG emissions from each land use based on the measured fluxes during the wet season and the dry season for forest, soybean and soybean/maize double-cropping. In the case of maize, we also considered the post-fertilization "potential spike" period in addition to wet and dry season fluxes when calculating annual emissions. Specifically, we calculated the mean and standard deviation for fluxes of

N_2O, CO_2 and CH_4 measured in the dry season (May-September, 150 days) and wet season (October-April, 215 days) for each land use (Supplemental Table S3.3). The mean and standard deviation calculations for non-forest sites incorporated both row and inter-row chambers. In order to account for N_2O losses taking place following fertilizer application, we further calculated the mean and standard deviation for GHG fluxes measured fewer than 15 days after fertilization (either broadcast or seedline). We calculated the estimated annual flux for each land use per:

$$\text{AnnualFlux}_{\text{forest}} \text{ and } \text{AnnualFlux}_{\text{soybean}} = (\text{wet season mean flux} * 24 \text{ hr/day} * \text{wet season days}) + (\text{dry season mean flux} * 24 \text{ hr/day} * \text{dry season days})$$

and

$$\text{AnnualFlux}_{\text{soybean/maize}} = (\text{wet season mean flux} * 24 \text{ hr/day} * (\text{wet season days}-30)) + (\text{dry season mean flux} * 24 \text{ hr/day} * \text{dry season days}) + (\text{post-fertilization mean flux} * 24 \text{ hr/day} * 30 \text{ days})$$

Thirty days were assigned to the post-fertilization period, as there are two fertilization events annually in soybean/maize croplands. We calculated three annual flux rates, a low, medium and high estimate. The medium estimate was based on flux means in each season and land use, the low estimate was based on flux means minus one standard deviation, and the high estimate was based on flux means plus one standard deviation. This approach bracketed the estimate of total emissions from each land use.

We separated out a post-fertilization period in soybean/maize cropland for two reasons. First, in order to report fluxes from this period as a comparison to other studies that explicitly consider post-fertilization effects. And second, the post-fertilization period had larger variation in fluxes than the wet season generally. Considering post-

fertilization period flux variances independently for wet-season flux variances aside from the post-fertilization period allowed the magnitude of the increase in variance to be represented in the annual estimate.

Results

Trace gas emissions

Dry season N_2O emissions in single-cropped (soybean only) fields, double-cropped (soybean/maize) fields and reference tropical forest were uniformly near zero, ~0-0.5 ngN cm^{-2} hr^{-1} (Figure 3.3). In contrast to our expectations, wet season emissions rates were between 1-4 ngN cm^{-2} hr^{-1}, for both cropland types and reference forest, substantially lower than wet seasons emissions from other Amazonian forest locations (Table 3.1).

N_2O fluxes did not differ significantly by land use in a one-way ANOVA (Table 3.2) or by land use when season was taken into account (Table 3.3). N_2O fluxes were significantly higher during the wet season ($p<0.01$, Table 3.3). CO_2 fluxes in soybean/maize croplands were significantly higher than those in soybean croplands or forest when season was not considered ($p<0.001$, Table 3.2); season and land use had a significant interaction effect for CO_2 fluxes, precluding traditional posthoc tests (Table 3.3). Qualitatively, CO_2 fluxes dropped dramatically from the wet to the dry season in the agricultural land uses and though CO_2 fluxes were lower during the dry season in

forest locations than in the wet season, they only fell by 66%, as opposed to falling by 90% and 92% in soybean and soybean/maize locations, respectively. There was significantly more uptake of CH_4 in forest ($p<0.001$, Table 3.2, Table 3.3) than in cropland.

Isolated post-fertilization spikes in N_2O emissions were large, with a maximum increase of ~820% to a N_2O emissions rate of 17.9 ngN cm^{-2} hr^{-1} at site M4 (Figure 3.3, Figure 3.4). Particularly large N_2O emissions were observed after broadcast fertilizer application of urea, as opposed to the initial nitrate application done along the seeding line when maize was planted. However, these large post-fertilization N_2O spikes were observed at only two of four sites in double-cropped soybean/maize, M1 and M4, and only three spikes were observed in total (Figure 3.4). Despite repeated sampling at sites M2 and M3 between 1 and 12 days of N-rich fertilizer management events (sampling approximately 4 times over a 1.5 week period), measured N_2O fluxes did not differ significantly from background forest N_2O flux rates measured +/- one day from the maize site measurements. We observed no statistically significant increase in N_2O emissions after each type of fertilizer application in at least one case: site M2 was broadcast fertilized on March 6, 2014 and, unlike site M4's response to broadcast fertilizer, did not show large N_2O losses when sampled 0, 1, 4, 7 and 12 days after fertilization (Figure 3.4). Similarly, site M3 was fertilized on February 10, 2014 and exhibited modest N_2O flux increases that were not statistically distinguishable from the background forest emissions rates when sampled 1, 4, 8, and 11 days after fertilization. Also contrary to expectations, N_2O emissions from soil on soybean/maize rows were not significantly

different from soil in between rows (Figure 3.5). N fertilizer added to interrow spaces (as would occur during broadcast fertilization events) could be expected to result in large N_2O fluxes in the absence of maize root N uptake.

Soil nutrient pools and fluxes

Net N mineralization, net ammonification and NO_3^--N differed significantly between land uses. Soybean/maize cropland had significantly higher soil NO_3^--N concentrations than forest ($p<0.01$, Table 3.2) though NH_4^+-N concentrations did not significantly differ between land uses. Net N mineralization rates were significantly lower in soybean croplands than in soybean/maize croplands or forest ($p<0.05$, Table 3.2) and net ammonification rates were significantly lower in soybean croplands than in soybean/maize croplands ($p<0.05$, Table 3.2).

Though overall trends between land uses were only marginally or not significant, inorganic N pools sizes showed the marked effect of N fertilizer addition during the post-fertilization period: in the periods after N fertilization in soybean/maize cropland, there was an order of magnitude increase in concentration of NO_3^--N and NH_4^+-N (Figure 3.5); forest and soybean sites never exhibited inorganic N pool sizes in the same range as these large increases in available inorganic N. Concurrently, net nitrification rate, measured in lab incubations, increased and net ammonification rate decreased (Figure 3.5). This pattern suggests that NH_4^+ was being consumed for nitrification and conversion to NO_3^-. Net N mineralization rate was roughly similar between land uses.

Row-inter-row dynamics were apparent for soil inorganic N pools and fluxes as well (Figure 3.6). Net nitrification rates were significantly higher on the row in maize cropland for the "post-fertilization period" (less than 15 days after N fertilizer application) while net ammonification rates were significantly lower both on and off the row in maize than in forest or soybean.

Physical soil properties differed among land uses. Previous work and our own measurements have shown that forests at Tanguro were more acidic (mean pH of 3.9 in forest, and 5.1 for croplands (Riskin *et al.*, 2013)), had a lower bulk density (mean of 1.22 (forest), 1.53 (soybean), 1.42 (soybean/maize) g cm^{-3}) (Supplemental Figure S3.2, Supplemental Table S3.1) and lower cation exchange capacity than sampled croplands (Riskin *et al.*, 2013). These differences reflect both the legacy of deforestation and subsequent pasture before conversion to cropland, as well as the inputs (e.g., of lime) to the current cropping systems themselves. Phosphorus additions in this system have been shown to increase soil inorganic P stores (Riskin *et al.*, 2013).

Environmental predictors of N_2O emissions

Soil moisture was significantly positively correlated with the log-transformed N_2O emissions rate in all land uses and nitrate pool size was significantly positively correlated with log-transformed N_2O emissions in soybean cropland (Figure 3.7a). In soybean/maize cropland, neither NO_3^--N, NH_4^+-N, net ammonification rate nor net N mineralization rate were significantly correlated with log-transformed N_2O emissions.

Many instances of large NO_3^--N pools at soybean/maize sites were not also instances of large N_2O fluxes, and similarly many relatively large N_2O fluxes were associated with low net nitrification rates. These instances contradict traditional correlative relationships between nitrous oxide production and soil inorganic N.

Soil moisture was significantly positively correlated with log-transformed CO_2 emissions (Figure 3.7b). CH_4 production in soybean/maize was negatively correlated with NO_3^--N and NH_4^+-N pool sizes, net N mineralization and net ammonification rates, meaning that CH_4 uptake was associated with higher concentrations of inorganic N (Figure 3.7c).

Seasonal and annual GHG emissions estimates

The middle estimates of annual N_2O emissions, determined using the mean flux values for each land use during the wet season, dry season and post-fertilization period (in the case of soybean/maize cropland), were 0.75, 0.45 and 0.51 kg N ha^{-1} yr^{-1} from forest, soybean, and maize, respectively, with forest having the largest annual flux (Figure 3.8, Table 3.1, Supplemental Table S3.3). However, the high estimates, determined using flux values for each period of the mean flux plus one standard deviation, were 1.96, 1.31 and 2.44 kg N ha^{-1} yr^{-1} in forest, soybean and maize, respectively, with maize having higher annual fluxes than forest. This change in ranking can be attributed to the fact that maize fluxes had a very large standard deviation for the post-fertilization period and for the wet season (Supplemental Table S3.3). The variation in forest fluxes was much

smaller, leading to higher N_2O fluxes for soybean/maize land use when high estimate assumptions were made.

Estimates of annual CO_2 emissions did not change ranking in the mean, high and low estimate calculations; soybean soil CO_2 emissions were consistently the highest on an annual basis, followed by forest, followed by soybean/maize (mean estimate: 8,678.945, 12,250.436, 9,582.038 kg C ha^{-1} yr^{-1} for F, S, M; Supplemental Table S3.4). These estimates represent the flux of CO_2 from soils and not net ecosystem flux to the atmosphere; emitted soil CO_2 can be offset by photosynthesis instead of contributing to net GHG emissions. The mean estimates for CH_4 annual emissions were negative across land use (e.g., forest, soybean and soybean/maize exhibited net consumption of methane; mean estimate: -0.647, -0.208, -0.584 kg C ha^{-1} yr^{-1} for F, S, M; Supplemental Table S3.4). In the low estimate of the annual methane flux, using the mean minus one standard deviation for wet season, dry season, and post-fertilization fluxes, these soils took up substantial amounts of methane. In the reverse, high estimate scenario (mean plus one standard deviation for each season's estimate), we estimated that these soils emitted large amounts of methane. Uncertainty surrounding methane's annual flux leaves not only the magnitude, but also the direction of net soil methane emissions unknown.

Discussion

N_2O fluxes: Unmanaged ecosystem emissions across Amazonia

Of the closed-chamber studies we surveyed that include an estimate of the annual N_2O flux from Amazonian forest (Table 3.1), this study site had the lowest annual forest N_2O flux estimate (0.75 kg N ha^{-1} y^{-1}, with the next lowest annual flux being 0.815 kg N ha^{-1} y^{-1} (Verchot *et al.*, 2008) and the highest being 6.13 kg N ha^{-1} y^{-1} (Keller *et al.*, 2005)). In comparison, two trace gas studies conducted in cerrado systems estimated an annual N_2O flux of 0.01 kg N ha^{-1} y^{-1} (Cruvinel *et al.*, 2011) and 0.345 kg N ha^{-1} y^{-1} (Carvalho *et al.*, 2014). Though this study's forest sites emitted N_2O at a rate that was more than twice that of the larger cerrado flux rate on an annual basis, the rate of N_2O emissions was only 12% of the highest forest flux rate on an annual basis. In the wet season, only one forest had a lower mean N_2O flux rate (0.562 ng N cm^{-2} h^{-1} (Vasconcelos *et al.*, 2004) vs. 1.38 ng N cm^{-2} h^{-1} in this study), and in that study the forest site used as a control was in its twelfth year of regrowth and not an entirely undisturbed forest as in this study. In the dry season, no forest sites measured a lower seasonal flux estimate than Tanguro's forests (0.1 ng N cm^{-2} h^{-1}).

Mean annual precipitation alone is insufficient to explain Tanguro's low annual N_2O fluxes. Two forest studies with higher annual N_2O flux estimates than this study's were conducted at sites with lower MAP (0.964 kg N ha^{-1} y^{-1} and 1770 mm y^{-1} MAP (Livingston *et al.*, 1988), 2.43 kg N ha^{-1} y^{-1} and 1850 MAP (Verchot *et al.*, 1999); MAP at Tanguro is 1900). The severity of Tanguro's dry season may differentiate these forests: in Verchot et al. (1999) (Verchot *et al.*, 1999), dry season N_2O fluxes were higher than Tanguro's dry season fluxes, despite Tanguro's higher MAP. Tanguro's

pronounced dry season, with very low N_2O fluxes, could explain why we measured a lower annual flux than other sites with even less annual rainfall. Dry season rainfall totals were rarely reported in papers included in the literature review, so comparisons between the severity of Tanguro's dry season and the dry seasons of these other sites were not possible.

Additionally, Tanguro's soils, while clayey, have high infiltration rates that could prevent anoxic soil microsites from readily forming. High clay content is generally associated with higher N_2O emissions because more clayey soils have higher water holding capacity and more microsites in which denitrification can occur (Parkin, 1987). Despite the high percentage clay, in this system clay particles aggregate readily and infiltration rates in Tanguro's forests are high (Hayhoe *et al.*, 2011): soil moisture content in forests was rarely above 50% and was significantly positively correlated with N_2O fluxes (Figure 3.7a). Four other studies that also estimated higher annual N_2O flux estimates than this study measured soils with lower clay content than forest soils at Tanguro (0.815 kg N ha^{-1} y^{-1} and <14% clay (Verchot *et al.*, 2008), 1.23 kg N ha^{-1} y^{-1} and <20% clay (Silver *et al.*, 2005), 1.40 kg N ha^{-1} y^{-1} and 38% clay (Keller *et al.*, 2005), 1.94 kg N ha^{-1} y^{-1} and 23-29% clay (Melillo *et al.*, 2001); Tanguro's soils are 43% clay). Though MAP is higher than some other forests with higher N_2O emissions from our literature review, relatively low MAP combined with rapid infiltration could have created conditions in which Tanguro's forest N_2O emissions were linked primarily to moisture.

N_2O fluxes: Managed ecosystem emissions across Amazonia

N_2O emissions from croplands in this southeastern Amazonian site were generally lower than those seen in other Amazonian studies of both unmanaged and managed systems. Of the managed ecosystems surveyed on former Amazonian forest land (Table 3.1), this study had a higher estimated annual N_2O flux (0.45 kg N ha^{-1} y^{-1} in soybean fields and 0.51 kg N ha^{-1} y^{-1} in soybean/maize fields) than a pasture located within Amazon forest (0.25 kg N ha^{-1} y^{-1}) (Verchot *et al.*, 1999). However, this study's annual estimate of soybean/maize N_2O flux was only 9% of the annual N_2O emissions from an N-fertilized pasture in Amazonian forest (Luizão *et al.*, 1989) and was smaller than the annual fluxes measured from both young and old pasture systems in a wetter Amazonian forest (Melillo *et al.*, 2001). Our soybean/maize and soybean annual N_2O flux estimates were also smaller than any reported unmanaged forest annual estimates (Table 3.1).

Instead, the seasonal and annual N_2O fluxes from Tanguro's soybean/maize and soybean croplands were more similar to flux estimates from managed and unmanaged land uses in the cerrado. Tanguro's cropland annual fluxes were higher than a study conducted in maize or soybean cultivation within cerrado (0.2 kg N ha^{-1} y^{-1} and 0.1 kg N ha^{-1} y^{-1}, respectively) (Cruvinel *et al.*, 2011) and a pasture whose N_2O fluxes were consistently below detection limits (Varella *et al.*, 2004). However, this study's annual flux estimates were similar to a cerrado site that is perhaps the most straightforward comparison between Tanguro and another managed cropland system: Carvalho et al. (2014) (Carvalho *et al.*, 2014) estimated that the annual N_2O flux from measured soybean/maize croplands was 0.568 kg N ha^{-1} y^{-1}, similar to the 0.51 kg N ha^{-1} y^{-1} we

estimated. This system had a similar MAP (1500-1800 mm y^{-1} vs. Tanguro's 1900 mm y^{-1}) and soil clay content (56% vs. Tanguro's 43%) (Carvalho *et al.*, 2014). These comparisons suggest that while some managed Amazonian systems experience large increases in annual N_2O flux following N fertilization – Luizao et al. (1989) saw N_2O emissions in fertilized pasture more than double those in reference forest (Luizão *et al.*, 1989) – this study system has more in common with N-fertilized croplands in cerrado than those in some other Amazonian forests. Indeed, Carvalho et al. (2009) measured N_2O emissions during the wet season in a formerly-cerrado soybean field that was not fertilized with N that are on par with the emissions we measured during the two weeks immediately following N fertilization in soybean/maize fields (Table 3.1) (Carvalho *et al.*, 2009).

N_2O fluxes: Potential drivers

Why might this system have notably low N_2O fluxes relative to other studies of managed systems in Amazonia? One possibility is that N_2O emissions in this system are driven by quickly resolving hot spots and hot moments (places and times of high emissions, respectively), which we failed to capture with this sampling regime. However, that sampling failed to capture the true temporal pattern seems unlikely to be the full explanation for the low mean N_2O fluxes in each land use. Although the post-fertilization spikes in N_2O emissions may have been so short-lived that we did not fully capture them with our targeted sampling in the two weeks after N fertilization, the two

sites in which we did see distinct post-fertilization effects had lower maximum flux rates than seen in other Amazonian studies and, indeed, other studies conducted in N-fertilized, temperate agriculture (Stehfest & Bouwman, 2006) (Table 3.1). Even if these data underrepresent the magnitude of post-fertilization N_2O fluxes, the maximum post-fertilization rates seem to be lower than expected. It is also possible that we failed to capture hot spots on the landscape. However, this explanation is unlikely. The topographic variation across these sites, and across the managed landscapes at Tanguro generally, is very limited. These upland fields see only slight sloping, and topography often drives hot spots of trace gas production. Further, we conducted a random walk to deploy static chambers on each day of sampling, which has the advantage of sampling more broadly within a radius, with the likelihood of sampling a hot spot increasing. While underrepresentation of high rates of microbial activity is a persistent problem in trace gas datasets, here we do not anticipate that underrepresenting hot spots and hot moments fully explains the low N_2O fluxes.

In some instances, N_2O emissions are limited by the availability of labile N, but that does not appear to be the case here. For example, the rate of N fertilizer application is positively correlated with N_2O emissions in many temperate cropland systems (Pérez *et al.*, 2001; Bouwman *et al.*, 2002; Philibert *et al.*, 2012; Shcherbak *et al.*, 2014), tropical cropland systems (Davidson & Matson, 1996; Matson *et al.*, 1998; Panek *et al.*, 2000), and other systems with excess N addition (Lindau *et al.*, 1988). In addition, increases in N_2O emissions after conversion from Panamanian rainforest to pasture or plantation may have been related to N inputs via manure or legumes or the higher frequency of fire in

these managed systems (Pendall *et al.*, 2010). While in this study N addition did lead to emissions peaks in several instances (Figure 3.4), the fact that large surpluses in labile inorganic N and high rates of inorganic N transformation were often present without large N_2O fluxes (Figure 3.7a) suggests that N availability was not acting as a single control over N_2O flux rates at Tanguro.

Alternatively, N_2O fluxes post-fertilization could be low because gaseous N loss is occurring in the form of NO or N_2 gas, both of which were not measured in this study. NO can be produced during nitrification and can be both produced and consumed during denitrification; both types of NO production are promoted by high rates of N cycling through the ecosystem (Firestone & Davidson, 1989). The ratio of NO:N_2O increases in soils with relatively more oxygen-filled pore space, as lower soil moisture allows NO to escape to the atmosphere without reabsorption into soil water and subsequent use by microbes, ensures that nitrification, an aerobic process, dominates over denitrification, an anaerobic process, and promotes the production of the more-oxidized NO (Davidson *et al.*, 2000). At Tanguro, perhaps overall gaseous N losses were high, but the NO:N_2O ratio was also high, leading to the low observed N_2O fluxes.

Several pieces of information suggest that this explanation is insufficient to explain the low N_2O fluxes measured in this study. Of similar investigations in the literature (Table 3.1), 9 of the 15 studies of N_2O in unmanaged systems and 3 of the 9 studies of N_2O in managed systems also measured NO. Several of these studies observed higher annual rates of NO flux than N_2O flux (Verchot *et al.*, 1999; Keller *et al.*, 2005; Silver *et al.*, 2005; Verchot *et al.*, 2008; Cruvinel *et al.*, 2011). However, the studies that

compared flux estimates among seasons all reported higher NO than N_2O fluxes in the dry season, but higher N_2O than NO fluxes in the wet season (Verchot *et al.*, 1999; Garcia-Montiel *et al.*, 2001; Keller *et al.*, 2005; Verchot *et al.*, 2008). (Three studies report higher annual N_2O fluxes than annual NO fluxes in at least one land use (Verchot *et al.*, 1999; Varella *et al.*, 2004; Silver *et al.*, 2005).) Here, the surprisingly low N_2O emissions occurred during the wet season, at both forest sites and at fertilized maize/soybean sites, when soil moisture was relatively high and oxygen availability relatively low. This ought to have diminished the production of NO relative to N_2O, consistent with other studies that showed lower wet season NO emissions than N_2O emissions. Outside of the Amazon, an investigation of the relative rates of NO and N_2O loss using case studies from across Costa Rica (Keller & Reiners, 1994; Veldkamp *et al.*, 1999), Puerto Rico (Erickson *et al.*, 2001) and Brazil (Verchot *et al.*, 1999) found that the only location with NO+N_2O losses dominated by NO was in a forest with a lower MAP (860 mm y^{-1}) than Tanguro and, presumably, more oxygenated soils (Davidson *et al.*, 2000).

N_2O fluxes may be low instead because gaseous N was being lost primarily as N_2 during denitrification. During our wet season sampling, denitrification may have been the dominant pathway of gaseous N loss. In a seasonal tropical forest in Mexico, NO emissions were driven by nitrification and were most ecologically important during wet-up at the end of the dry season (Davidson *et al.*, 1993). Once wet-up was established, denitrification and N_2O emissions dominated; at that point, soil moisture was positively correlated with N_2O emissions, as it was in this study.

During denitrification, N_2 production is favored over N_2O production when organic carbon, the reductant for denitrification, is relatively more available than NO_3^-, the oxidant for the reaction, and under conditions of higher temperatures, higher pH and lower oxygen availability (Firestone & Davidson, 1989). One explanation for the low N_2O fluxes observed in this study is that denitrification consistently reduced NO_3^- fully to N_2. Few studies in comparable systems have measured emissions of N_2, largely due to methodological challenges (Groffman *et al.*, 2006). Garcia-Montiel et al. (2003) amended southwestern Amazonian forest plots with glucose, water, or NO_3^- and observed large increases in N_2O fluxes after glucose addition, while water and labile N addition did not significantly increase fluxes (Garcia-Montiel *et al.*, 2003). Similar results after C addition have been seen in Costa Rica (Nobre *et al.*, 2001). If, even after N fertilizer addition, organic C were available for the complete reduction of NO_3^-, we could observe high rates of soil N transformation without N_2O emissions. This conforms to our observations. Further, in a subsequent study performed at Tanguro, soybean/maize cropland plots were fertilized with varying rates of N fertilizer. N_2O emissions rates rose sharply after fertilizer application of 120 kg N ha^{-1} (K. Jankowski, pers. comm.), a fertilizer application rate that would have increased NO_3^- relative to organic C, favoring N_2O production in comparison to the 30 and 45 kg N ha^{-1} that were applied during the two N fertilizer application periods in these soybean/maize croplands. Other ecosystem factors also play important roles in the emissions of N_2O, NO and N_2, including microbial community composition before and after land use change (Rodrigues *et al.*, 2013), pH (Cuhel *et al.*, 2010), redox conditions (Itoh *et al.*, 2012), and diffusion down the soil

profile (Martinson *et al.*, 2012). However, several of our observed patterns in this system are consistent with the hypothesis that high N_2 fluxes could have accompanied relatively low N_2O fluxes, perhaps due to organic C limitation during denitrification, the explanation that seems most likely at present.

CO_2 and CH_4 fluxes: Potential drivers

Root respiration in soybean fields may have driven the significantly higher soil CO_2 emissions from soybean and soybean/maize croplands, as soil CO_2 efflux was higher from row chambers than inter-row chambers in soybean cultivation (Figure 3.9). Soil moisture also appears to drive CO_2 efflux in all three land uses. Notably, in these productive landscapes, determining land use patterns of net ecosystem CO_2 exchange is not possible without a full carbon cycle accounting. Using the flux rate of a single carbon cycle transformation is insufficient to reach conclusions about how cropland intensification impacts the overall CO_2 emissions profile from soybean or soybean/maize cropland.

These soils appear to be a marginal CH_4 sink across all land uses, though the mean uptake rate from a given chamber flux measurement was rarely statistically different from zero at the site level. Methane consumption by methanotrophs is an aerobic process and tropical forest soils are often net sinks of methane (Mosier *et al.*, 2004). Soils in subtropical and dry tropical regions likely account for more than 50% of global methane consumption (Curry, 2007). Though these uptake rates were only

marginally detectible overall, we did measure statistical differences in uptake between managed and unmanaged sites at Tanguro, suggesting that this CH_4 sink may decrease in southeastern Amazonia as cropland intensification proceeds.

Management implications

Consistently low N_2O emissions despite relatively N-rich soil and biannual additions of labile N suggests that judicious N fertilizer management by farmers in southeastern Amazonia can minimize increases in GHG fluxes after cropland intensification, particularly if our hypothesis is correct that low N_2O fluxes are a consequence of relatively complete dentrification that reduces most NO_3^- all the way to N_2. Higher fertilization levels could shift the ratio of N_2:N_2O emissions towards greater N_2O emissions, a possibility that deserves further evaluation. CH_4 fluxes, while different between land uses, remained close to zero across them, and CO_2 soil fluxes, while higher in soybean croplands, represent a small portion of the tropical terrestrial carbon cycle.

The most important determinant of high N_2O fluxes from these intensified croplands was row/inter-row fertilizer management. Indeed, our high estimate of annual N_2O emissions, in which we considered one standard deviation above the wet and dry season mean flux rates, increased total annual emissions over the baseline estimate largely because soybean/maize inter-row N_2O emissions increased substantially. In this high estimate, soybean/maize double cropping overtook forest as the highest N_2O emitter per hectare. By contrast, in our low estimate, in which soybean/maize inter-row N_2O

emissions were relatively low, soybean/maize double cropping had a smaller GHG emissions profile than intact forest. This suggests that fertilizer management that targets N fertilizer application on the row of planting for one or both N-fertilizer application events can keep N_2O emissions below the annual totals measured in reference forest while still allowing farmers to benefit from the increased agricultural production of soybean/maize double cropping.

Further research

These initial measurements of C and N trace gas emissions revealed high variability in space and time, making broad interpretations about the biogeochemistry of these novel, intensified croplands difficult. CH_4 consumption/production is a primary case in point: despite widespread sampling across seasons and land uses, variability in CH_4 emissions obscures any obvious patterns. As such, one important area of further research is laboratory investigation of controls on trace gas processes. Measuring in situ patterns may not be useful in projecting the impacts of future global change – instead, mechanistic relationships could help parameterize earth system models to make better estimates of GHG emissions under alternate climatic or management scenarios. Specific to the southeastern Amazon and other tropical seasonal forests, laboratory experiments that explore the relative fluxes of N_2O, NO and N_2 could inform how GHG emissions might change on a global scale as global croplands continue to expand in the tropics.

Secondly, as the frontier of intensified agriculture in southeastern Amazonia becomes more entrenched, numerous new management techniques are likely to emerge, including alternate N fertilization regimes. As we saw here with the row-inter-row N_2O emissions, the distribution of N fertilizer across a field can have important effects on overall GHG emissions. Manipulative field tests that vary management decisions (including level, timing and placement of fertilization) could further illuminate how to balance increasing cropland productivity in southeastern Amazonia while keeping GHG emissions below those from intact forest.

Conclusions

Measurements of carbon dioxide, methane and nitrous oxide emissions from croplands and reference forest in the southeastern Amazon indicated N_2O emissions from intensified croplands did not differ significantly from nearby Amazonian forest, while CO_2 emissions from soil were higher in soybean cropland and CH_4 uptake was higher in forest. N_2O emissions remained unexpectedly low in both the managed and unmanaged land uses, particularly given that soybean/maize croplands received labile N additions. These results suggest that cropland intensification on already deforested land in southeastern Amazon may not have large consequences for the landscape's GHG footprint. If higher agricultural output can be achieved along this portion of Brazil's agricultural frontier through cropland intensification rather than cropland expansion, the GHG impacts of doing so may be modest.

Figures:

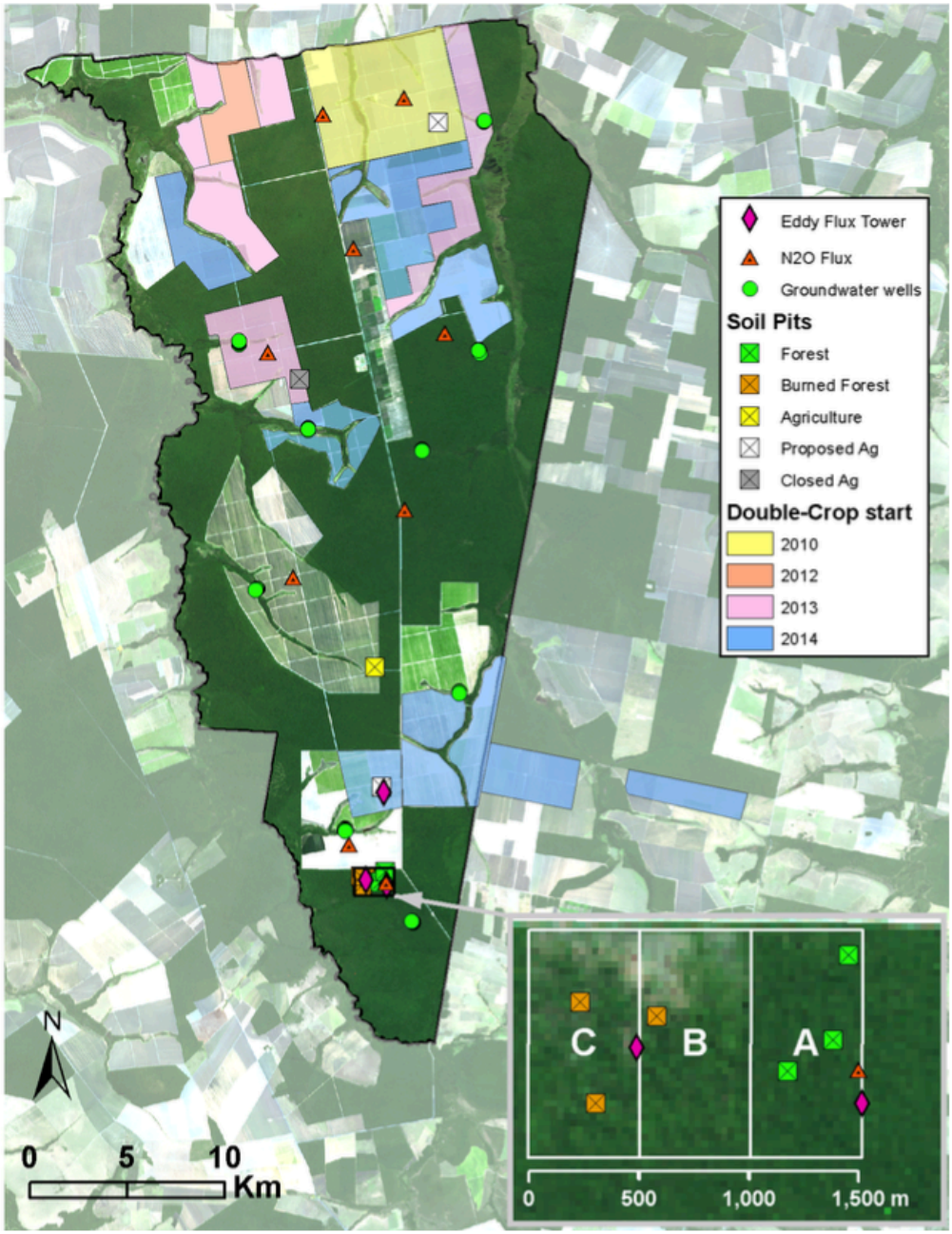

Figure 3.1. Map of study site Tanguro Ranch (courtesy Paul Lefebrve). Dark areas are forested parcels; light areas are agricultural fields. Trace gas sampling locations (orange

triangles) are located in three forest locations, two soybean single-cropping locations and four soybean/maize double cropping locations. Color overlays over cropland areas indicate the year a field was converted from single- to double-cropping (e.g., when maize cropping began).

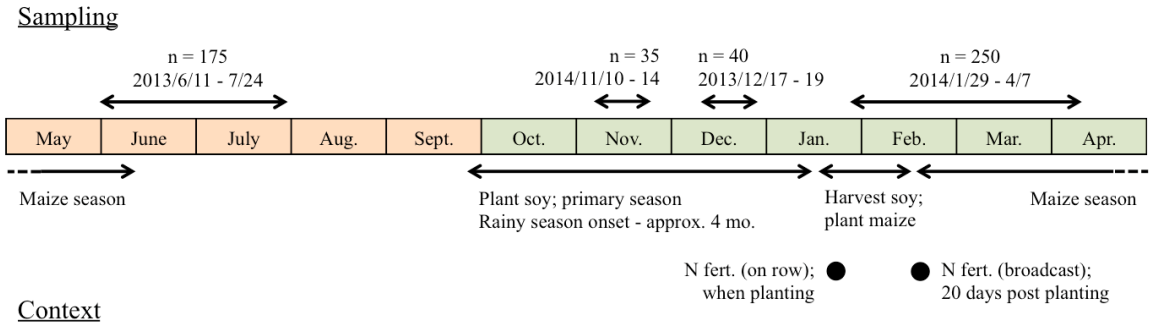

Figure 3.2. Annual timeline of farm management events and of sampling periods conducted at Tanguro Ranch. Wet season months are colored in green, dry season months in orange.

Table 3.1. Nitrous oxide flux comparisons from Amazonian and cerrado sites. Error was reported differently across studies; where error was reported, it is reproduced here with the error metric specified in parentheses. Units have been normalized across studies for annual and seasonal fluxes.

Citation	Location	N_2O Flux (Annual), kg N ha^{-1} y^{-1}	N_2O Flux (Wet Season), ng N cm^{-2} h^{-1}	N_2O Flux (Dry Season), ng N cm^{-2} h^{-1}	MAP	% Clay	Land Use	NO Data?	NO Flux
Unmanaged ecosystems									
Carvalho et al (2009) (Carvalho *et al.*, 2009)	Rondonia, Brazil	NA	-0.68 (1.51) (sd)	1.24 (1.98) (sd)	2170	73	Cerrado	N	
Carvalho et al (2014) (Carvalho *et al.*, 2014)	Goias, Brazil	0.345	NA	NA	1500-1800	56	Cerrado	N	
Cruvinel et al (2011) (Cruvinel *et*	Goias, Brazil	0.01 (1528) (% error)	NA	NA	2078	68	Cerrado	Y	0.1 (11.2) kg N ha^{-1} y^{-1} (% error)

al., 2011)									
Davidson et al (2004) (Davidson *et al.*, 2004)	Para, Brazil	2.6 (1.0) (95%CI)	NA	NA	2000	60-80	Forest	Y	0.9 (1.0) kg N ha^{-1} y^{-1} (95%CI)
Garcia-Montiel et al 2001 (Garcia-Montiel *et al.*, 2001)	Rondonia, Brazil	NA	7.64	0.13	2200	23-29	Forest	Y	0.5 ng N cm^{-2} h^{-1} (wet season), 3.32 ng N cm^{-2} h^{-1} (dry season)
Keller et al (2005) (Keller *et al.*, 2005)	Para, Brazil	6.13 (0.53) (se)	12.8 (1.2) (se)	1.2 (0.3) (se)	2000	80	Forest (oxisol)	Y	7.7 (3.4) ng N cm^{-2} h^{-1} (wet season), 10.4 (4.4) ng N cm^{-2} h^{-1} (dry season), 7.9 (2.5) kg N ha^{-1} y^{-1} (annual) (se)
Keller et al (2005) (Keller *et al.*, 2005)	Para, Brazil	1.40 (0.26) (se)	2.0 (0.4) (se)	1.2 (0.4) (se)	2000	38	Forest (ultisol)	Y	2.3 (1.3) ng N cm^{-2} h^{-1} (wet season), 15.3 (9.9) ng N cm^{-2} h^{-1} (dry season), 7.7 (4.4) kg N ha^{-1} y^{-1} (annual) (se)
Livingston et al	Amazonia,	0.964 (0.201)	NA	NA	1770	NA	Forest (ridge)	N	

(1988) (Livingston *et al.*, 1988)	Brazil	(se)							
Luizão et al (1989) (Luizão *et al.*, 1989)	Amazonia, Brazil	1.9	NA	NA	2200	NA	Forest	N	
Melillo et al (2001) (Melillo *et al.*, 2001)	Rondonia, Brazil	1.94 (0.22) (se)	NA	NA	2200	23-29	Forest	N	
Silver et al (2005) (Silver *et al.*, 2005)	Para, Brazil	11.39 (0.876) (se)	NA	NA	2000	60	Forest (clayey)	Y	2.54 (0.44) kg N ha^{-1} y^{-1} (se)
Silver et al (2005) (Silver *et al.*, 2005)	Para, Brazil	1.23 (0.175) (se)	NA	NA	2000	80% sand	Forest (sandy loams)	Y	3.33 (0.26) kg N ha^{-1} y^{-1} (se)
This study	Mato Grosso, Brazil	0.75 (-0.45, 1.95) (hi, lo est.)	1.38 (0.19) (se)	0.1 (0.1) (se)	1900	43	Forest	N	
Varella et al (2004) (Varella *et al.*, 2004)	Brasilia-DF, Brazil	NA	Below detection limit (0.6)	Below detection limit (0.6)	1500	74	Cerrado	Y	0.6 ng N cm^{-2} h^{-1}

Vasconcelos et al (2004) (Vasconcelos *et al.*, 2004)	Amazonia, Brazil	NA	0.562 (0.050) (se)	0.241 (0.047) (se)	2539 (280) (se)	20	Forest (12yr regrowth)	Y	Mean not reported; visually <0.1 ng N cm^{-2} h^{-1}
Verchot et al (1999) (Verchot *et al.*, 1999)	Para, Brazil	2.43	5.23 (0.40) (se)	1.04 (0.08) (se)	1850	NA	Forest	Y	1.18 (0.15) ng N cm^{-2} h^{-1} (wet season), 2.13 (0.26) ng N cm^{-2} h^{-1} (dry season), 1.52 kg N ha^{-1} y^{-1} (annual) (se)
Verchot et al (2008) (Verchot *et al.*, 2008)	Para, Brazil	0.815	1.44 (0.57) (se)	0.80 (0.30) (se)	2500	86% sand	Forest	Y	0.99 (0.57) ng N cm^{-2} h^{-1} (wet season), 1.58 (1.31) ng N cm^{-2} h^{-1} (dry season), 0.946 kg N ha^{-1} y^{-1} (annual) (se)
Managed ecosystems									
Carvalho et al (2009) (Carvalho *et al.*, 2009)	Rondonia, Brazil	NA	2.18 (1.49) (sd)	1.28 (.94) (sd)	2170	73	Soybean (3yo)	N	

Carvalho et al (2014) (Carvalho *et al.*, 2014)	Goias, Brazil	0.568	NA	NA	1500-1800	56	Soybean/maize	N	
Cruvinel et al (2011) (Cruvinel *et al.*, 2011)	Goias, Brazil	0.2 (35) (% error)	NA	NA	2078	49	Maize	Y	0.3 (21.1) kg N ha^{-1} y^{-1} (% error)
Cruvinel et al (2011) (Cruvinel *et al.*, 2011)	Goias, Brazil	0.1 (28.1) (% error)	NA	NA	2078	72	Soybean	Y	0.2 (13.4) kg N ha^{-1} y^{-1} (% error)
Luizão et al (1989) (Luizão *et al.*, 1989)	Amazonia, Brazil	5.7	NA	NA	2200	NA	Pasture (10yo, fertilized)	N	
Melillo et al (2001) (Melillo *et al.*, 2001)	Rondonia, Brazil	1.45 (0.31) (se)	NA	NA	2200	23-29	Pasture (10yo)	N	
Melillo et al (2001) (Melillo *et al.*, 2001)	Rondonia, Brazil	5.13 (1.84) (se)	NA	NA	2200	23-29	Pasture (2yo)	N	
Metay et al (2007)	Goias,	0.03066	NA	NA	1500	NA	Rice (no till)	N	

(Metay *et al.*, 2007)	Brazil	(0.03919) (sd)							
Metay et al (2007) (Metay *et al.*, 2007)	Goias, Brazil	0.03531 (0.03146) (sd)	NA	NA	1500	NA	Rice (till)	N	
This study	Mato Grosso, Brazil	0.45 (-0.41, 1.3) (hi, lo est.)	0.81 (0.19) (se)	0.09 (0.1) (se)	1900	43	Soybean	N	
This study	Mato Grosso, Brazil	0.51 (-1.4, 2.4) (hi, lo est.)	0.94 (0.33) (se)	-0.05 (0.09) (se)	1900	43	Soybean/maize	N	
This study	Mato Grosso, Brazil	NA	2.2 (0.54) (se)	NA	1900	43	Soybean/maize (post-fertilization)	N	
Varella et al (2004) (Varella *et al.*, 2004)	Brasilia-DF, Brazil	NA	Below detection limit (0.6)	Below detection limit (0.6)	1500	57	Pasture	Y	Mean not reported
Verchot et al (1999) (Verchot *et al.*, 1999)	Para, Brazil	0.25	0.96 (0.23) (se)	-0.20 (0.05) (se)	1850	NA	Pasture	Y	0.62 (0.11) ng N cm^{-2} h^{-1} (wet season), 0.54 (0.12) ng N cm^{-2} h^{-1} (dry

									season), 0.50 kg N ha^{-1} y^{-1} (annual) (se)

Table 3.2. Differences between trace gas fluxes and soil variables between land uses. Responses are reported as mean and standard deviation (in parentheses) values. Repeated measures ANOVA results are marked for each variable at the top of the column as *** when p-value <0.001, ** when p-value <0.01 and * when p-value <0.05. For significant ANOVA results, a Tukey's HSD with a bonferroni correction was calculated; groups that significantly differ ($p<0.05$) are marked with letters. All response variables except for soil moisture were log transformed prior to statistical tests.

Land Use	**N_2O Flux (ng N cm^{-2} h^{-1})^{NS}**	**CO_2 Flux (ug C cm^{-2} h^{-1})****	**CH_4 Flux (ug C cm^{-2} h^{-1})*****	**% Soil Moisture*****	**NO3-N (mg N g^{-1})****	**NH4-N (mg N g^{-1})^{NS}**	**Net N Mineralization (mg N m^{-2} d^{-1})***	**Net Ammonification (mg N m^{-2} d^{-1})***
Forest	0.901 (1.598)	10.245 (5.653)^{a}	-0.000712 (0.00490)^{a}	0.233 (0.0756)^{a}	0.000515 (0.000723)^{a}	0.00245 (0.00171)	0.00902 (0.00406)^{a}	-0.00105 (0.00210)^{ab}
Soybean/Maize	1.201 (4.159)	12.625 (12.468)^{b}	-0.000514 (0.00142)^{b}	0.207 (0.0792)^{b}	0.00475 (0.00496)^{b}	0.00676 (0.0138)	0.0108 (0.0160)^{a}	-0.00539 (0.0144)^{a}
Soybean	0.401 (0.999)	10.862 (16.644)^{a}	-0.000150 (0.00383)^{b}	0.136 (0.0607)^{c}	0.000601 (0.000811)^{ab}	0.000871 (0.000296)	0.00282 (0.00226)^{b}	0.000110 (0.000365)^{b}

Table 3.3. Differences between trace gas fluxes and soil variables between land uses and seasons. Responses are reported as mean and standard deviation (in parentheses) values. Two-way repeated measures ANOVA results are marked for each variable at the top of the column as *** when p-value <0.001, ** when p-value <0.01 and * when p-value <0.05. Main effects are listed as $main_{LU}$ for the main effect of land use and $main_{season}$ for the main effect of season. In cases where an interaction term is significant, this precludes interpretation of main effects, so posthoc tests were not conducted. For significant ANOVA results, a Tukey's HSD with a bonferroni correction was calculated; groups that significantly differ ($p<0.05$) are marked with letters. All response variables except for soil moisture were log transformed prior to statistical tests.

Land Use	**Season**	**N_2O Flux ($ng\ N\ cm^{-2}\ h^{-1}$) $main_{LU}$ NS $main_{season}$ ** interaction NS**	**CO_2 Flux ($\mu g\ C\ cm^{-2}\ h^{-1}$) $main_{LU}$ * $main_{season}$ *** interaction *****	**CH_4 Flux ($\mu g\ C\ cm^{-2}\ h^{-1}$) $main_{LU}$ *** $main_{season}$ NS interaction NS**	**% Soil Moisture $main_{LU}$ *** $main_{season}$ *** interaction NS**
Forest	Wet	1.384 (1.813)[a]	13.593 (4.386)	-0.000281 (0.00608)[a]	0.276 (0.0785)[aLU aS]
	Dry	0.102 (0.758)[b]	4.625 (1.752)	-0.00140 (0.00233)[a]	0.180 (0.0184)[aLU bS]
Soybean/Maize	Wet	1.672 (4.771)[a]	16.846 (12.176)	-0.000462 (0.00139)[b]	0.239 (0.0740)[aLU aS]
	Dry	-0.0509	1.390 (0.920)	-0.000654	0.140 (0.0374)[aLU

		(0.826)[b]		(0.00147)[b]	[bS]
Soybean	Wet	0.812 (1.165)[a]	22.226	-0.000468	0.189 (0.0647)[bLU]
			(20.235)	(0.00536)[ab]	[aS]
	Dry	0.0862 (0.716)[b]	2.172 (2.044)	0.0000937	0.105 (0.0299)[bLU]
				(0.00203)[ab]	[bS]

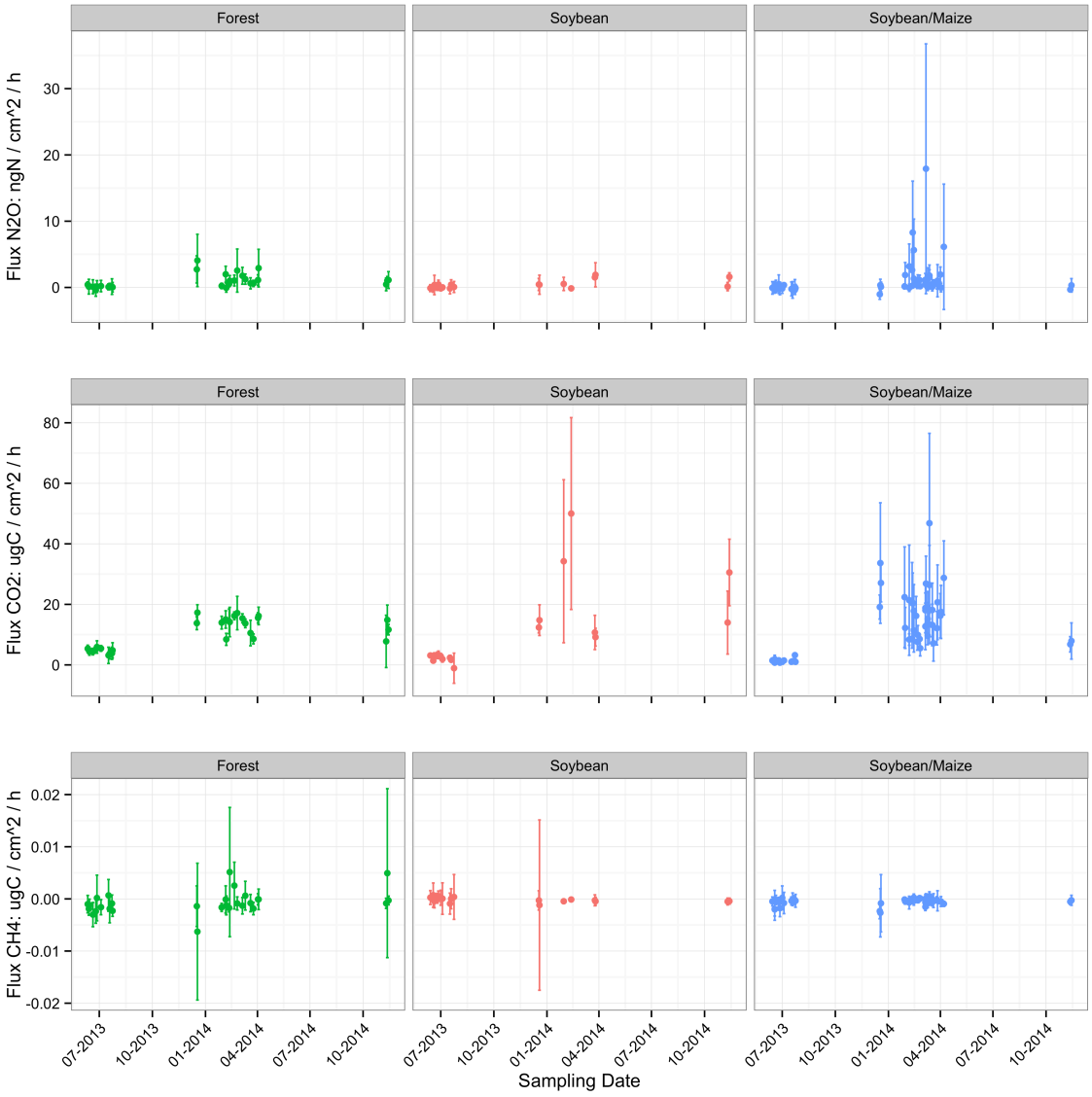

Figure 3.3. Fluxes over time of N_2O, CO_2 and CH_4 in each land use. Points indicate the mean flux of five closed chambers deployed at a given site on a given sampling date; error bars are the standard deviation.

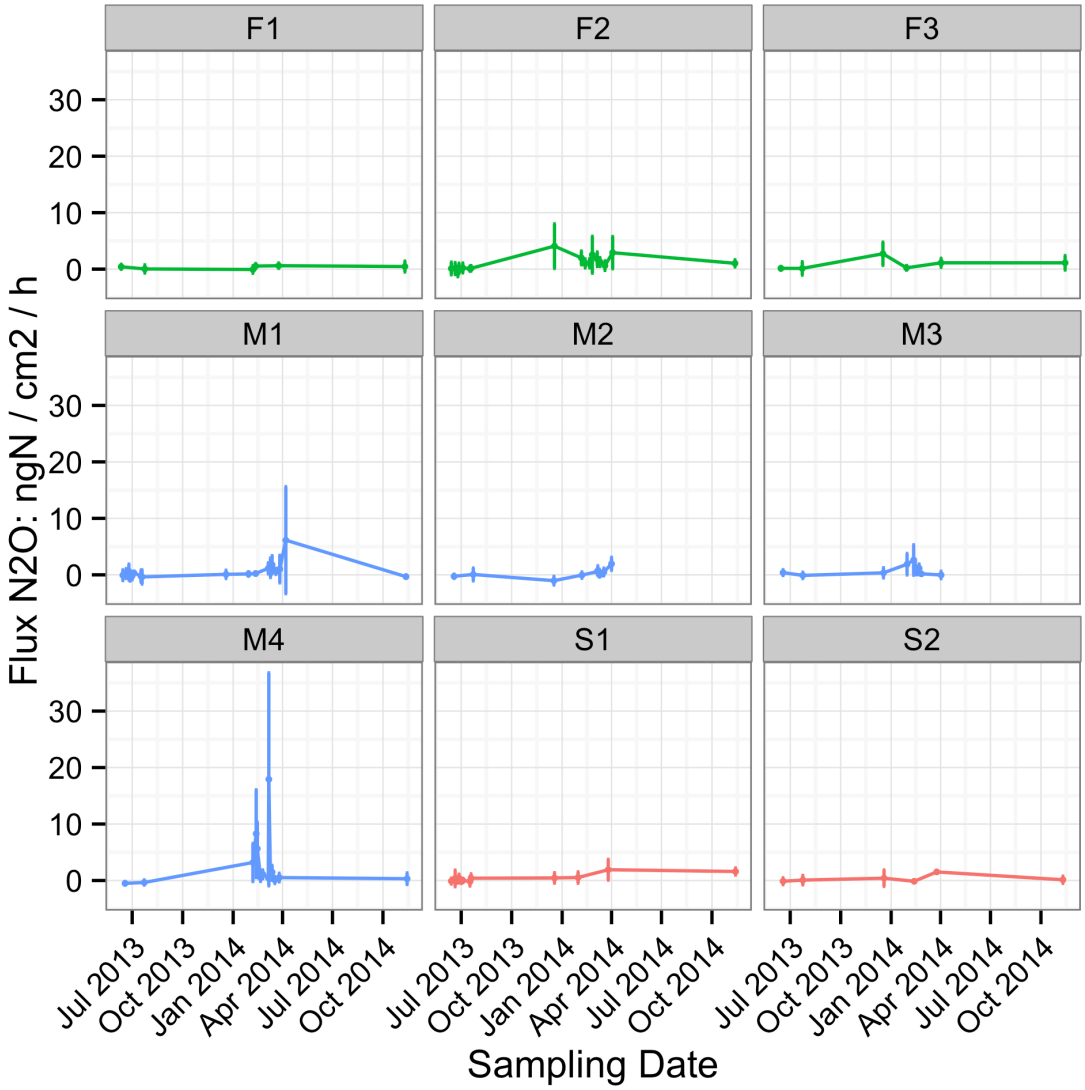

Figure 3.4. Fluxes over time of N_2O, divided by site. Points indicate the mean flux of five closed chambers deployed at a given site on a given sampling date; error bars are the standard deviation.

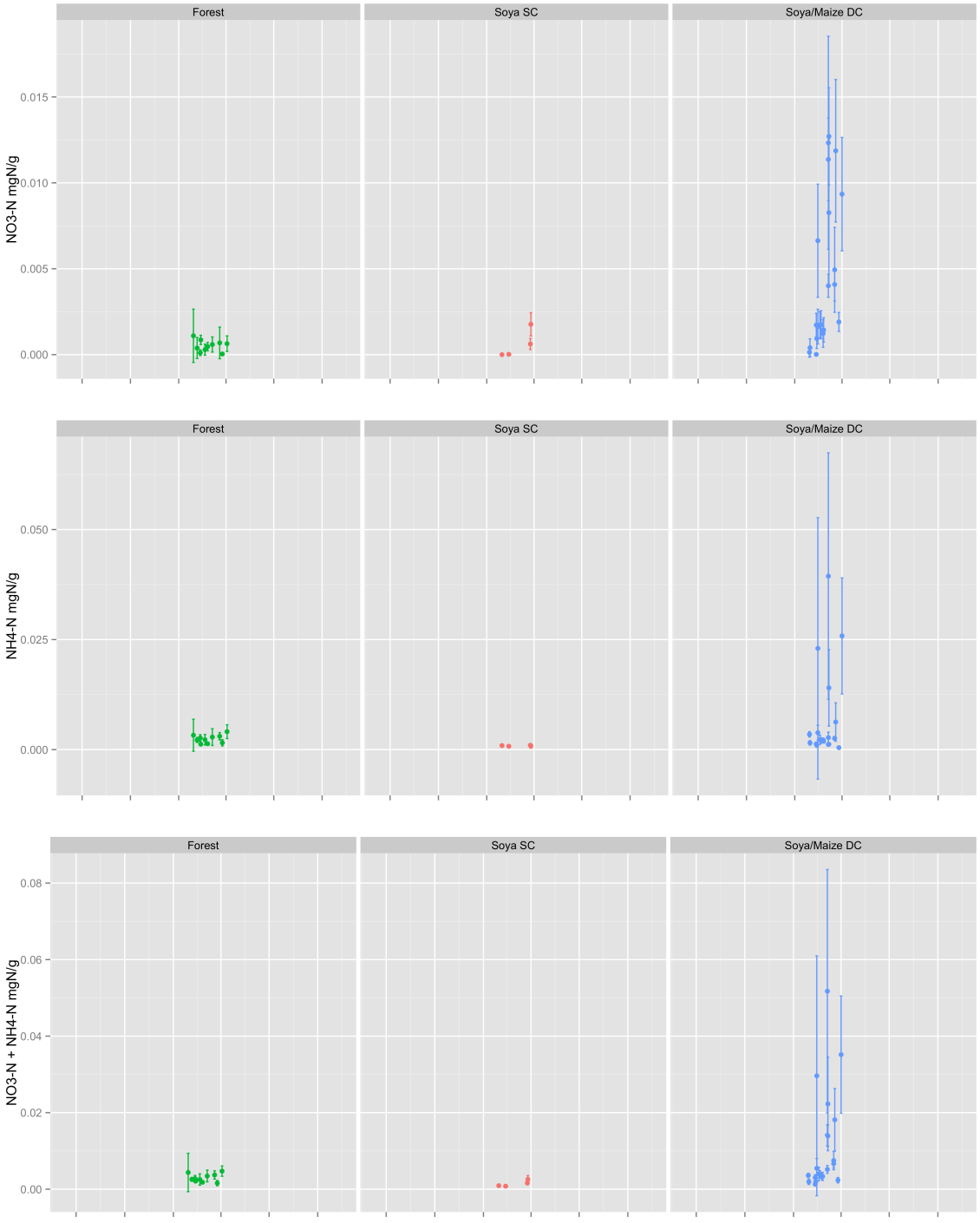

Figure 3.5a. Inorganic N pools across time and between land uses.

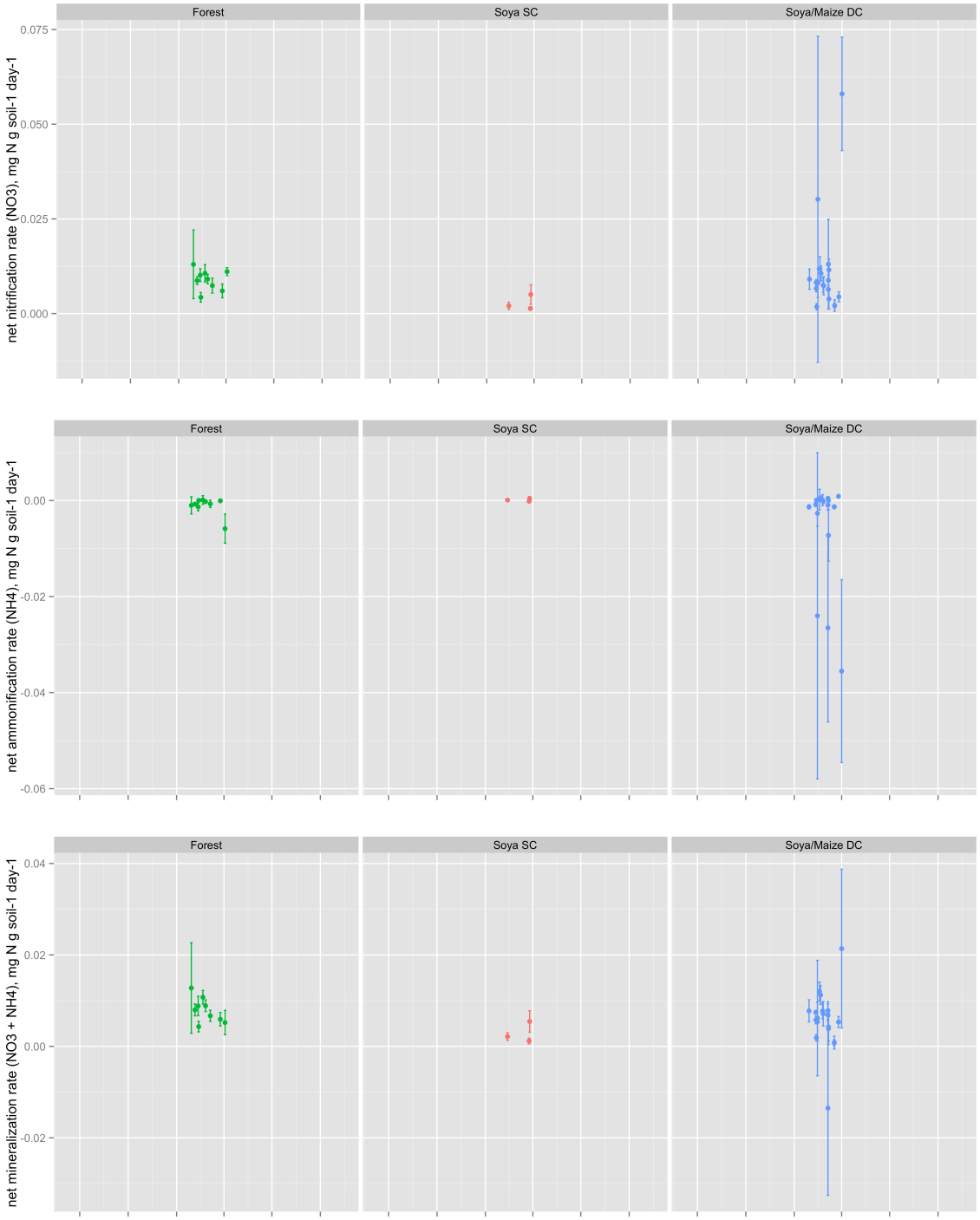

Figure 3.5b. Inorganic N transformations across time and between land uses.

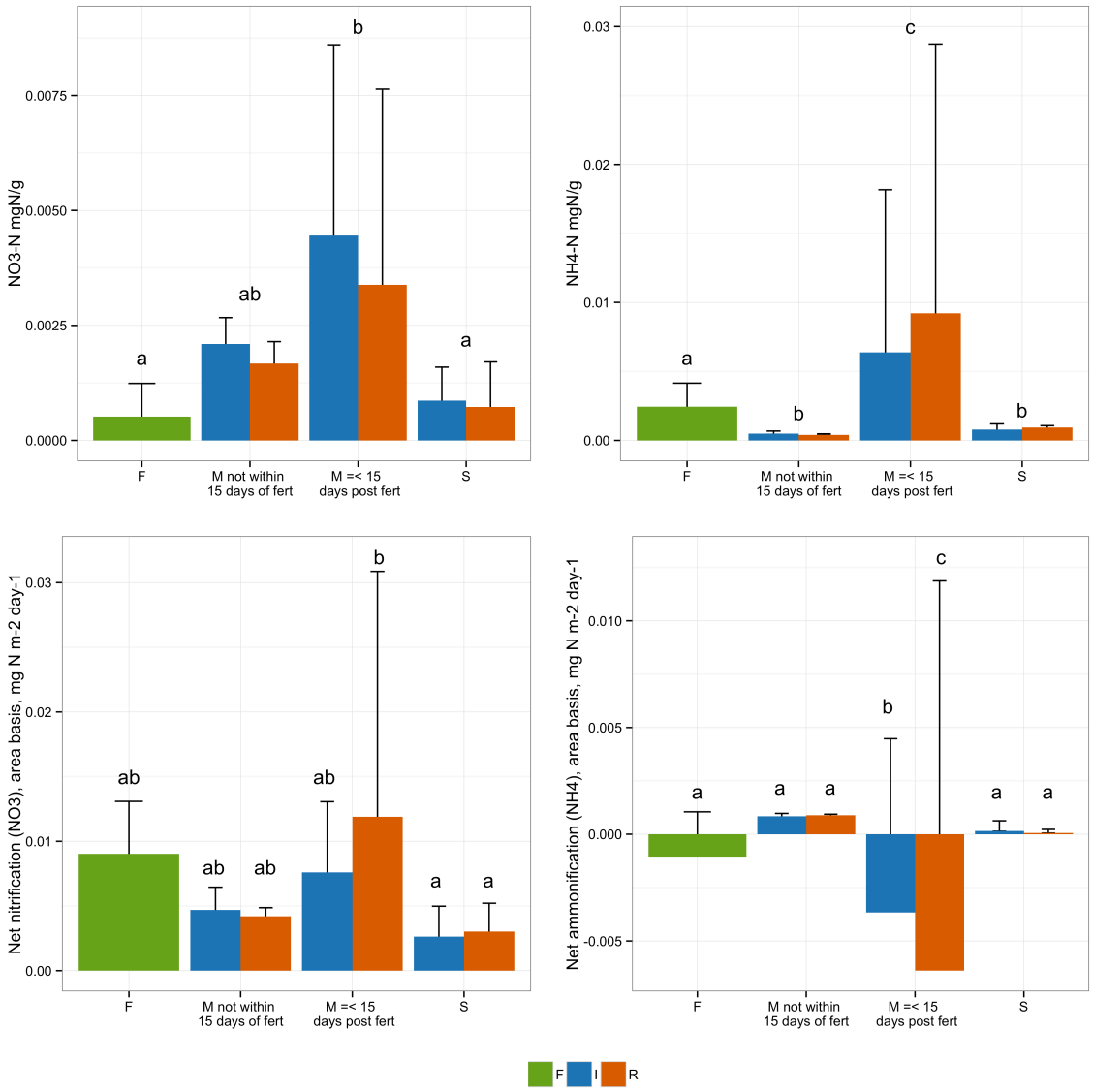

Figure 3.6. Comparison of soil N variables between row and inter-row chamber placements. Blue bars (I) indicate chambers placed on inter-row spaces, while orange bars (R) indicate chambers placed on crop rows. Forest chambers, which do not have a row or inter-row designation, are indicated in green (F).

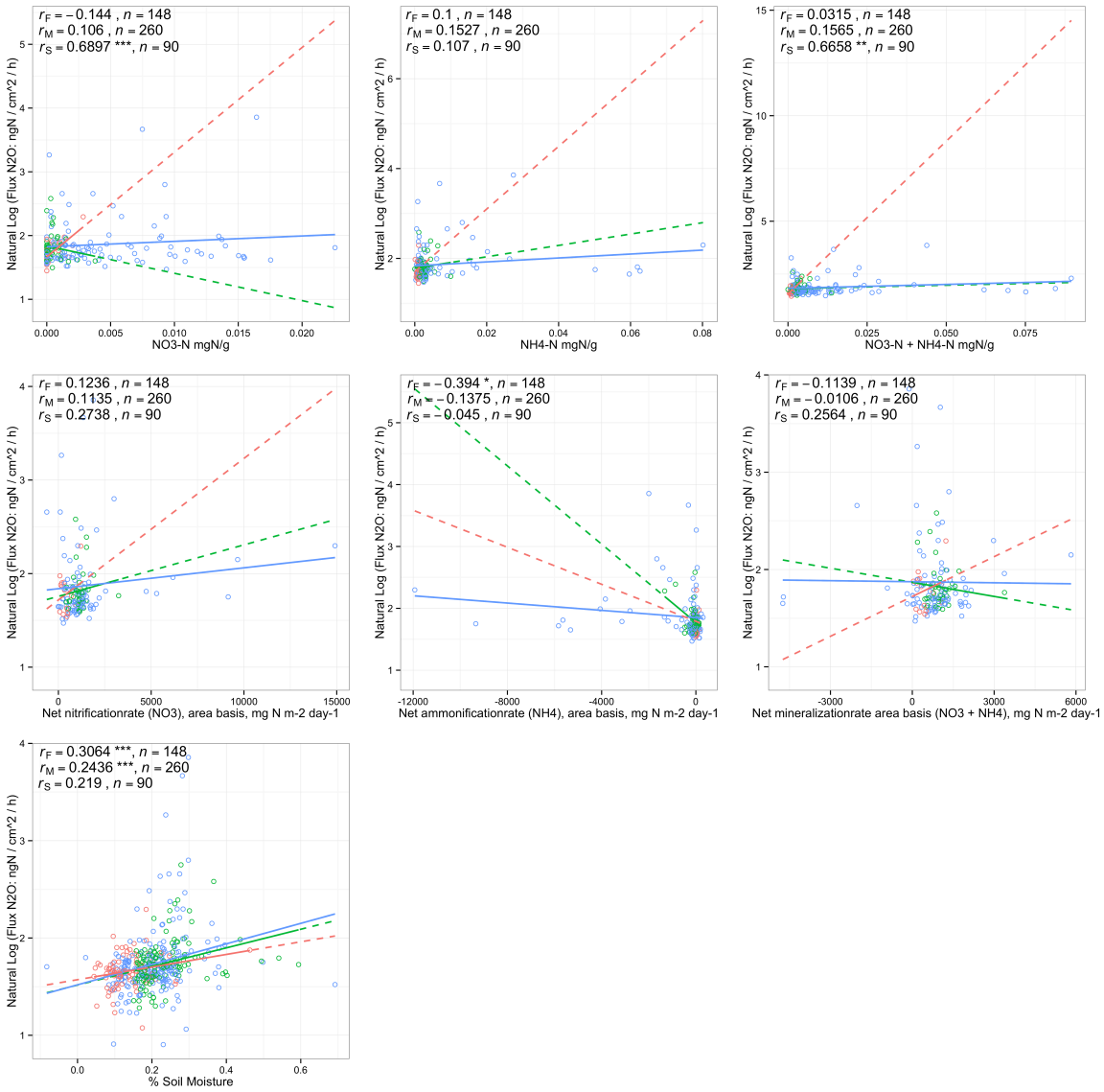

Figure 3.7a. Correlation scatterplots of log-transformed gas fluxes (here, N_2O) and key soil variables. Point color indicates land use (green = forest, blue = soybean-maize double cropping, pink = soybean single cropping). Lines are simple linear regression lines where the dotted portions of the line fall outside of the scope of the data for that land use. Pearson's linear correlation coefficient (*r*, measures correlation on a -1 to +1

scale) is marked as significantly different from zero as *** when p-value <0.001, ** when p-value <0.01 and * when p-value <0.05.

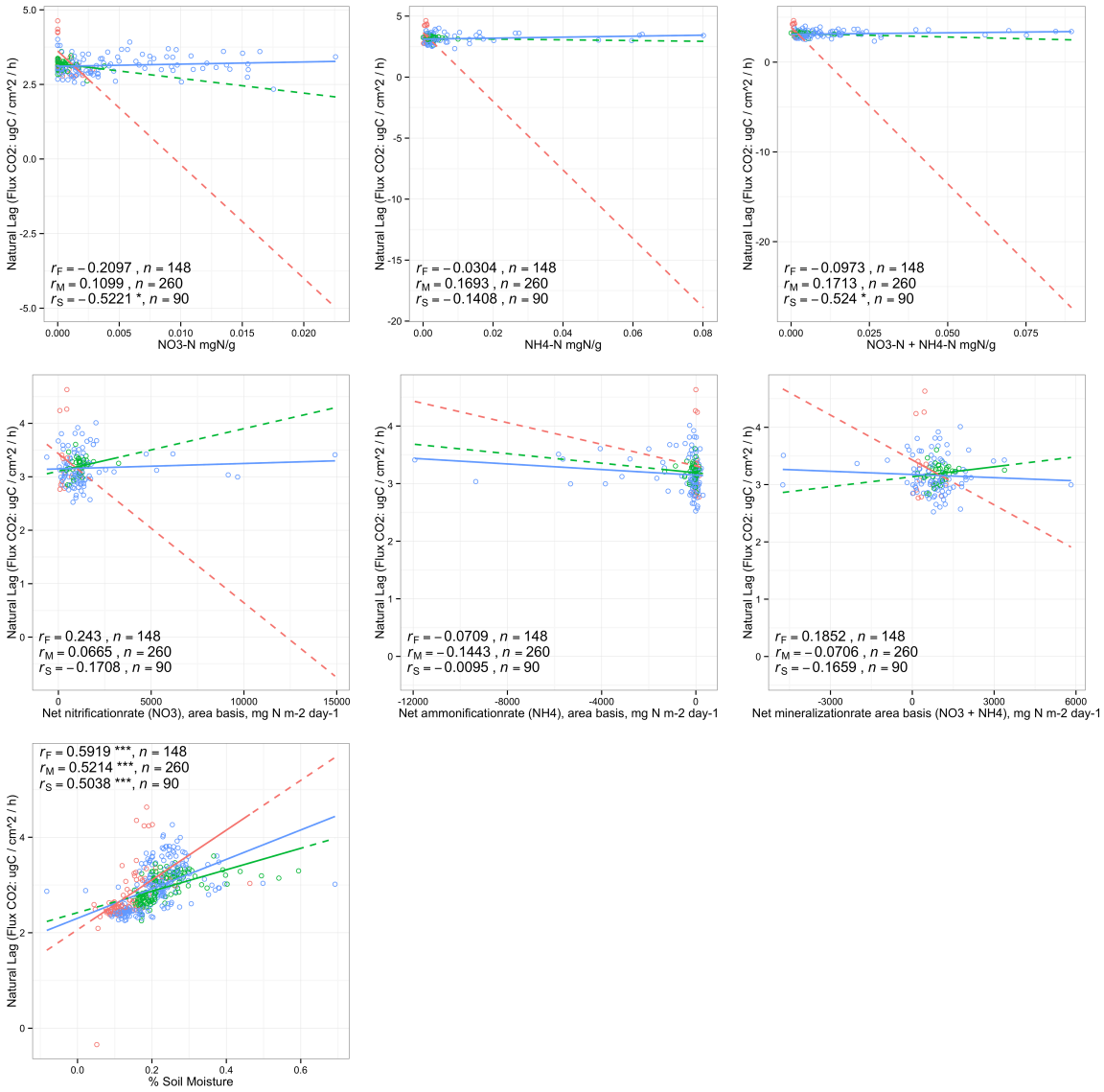

Figure 3.7b. Correlation scatterplots of log-transformed gas fluxes (here, CO_2) and key soil variables. Point color indicates land use (green = forest, blue = soybean-maize double cropping, pink = soybean single cropping). Lines are simple linear regression lines where the dotted portions of the line fall outside of the scope of the data for that land use. Pearson's linear correlation coefficient (*r*, measures correlation on a -1 to +1

scale) is marked as significantly different from zero as *** when p-value <0.001, ** when p-value <0.01 and * when p-value <0.05.

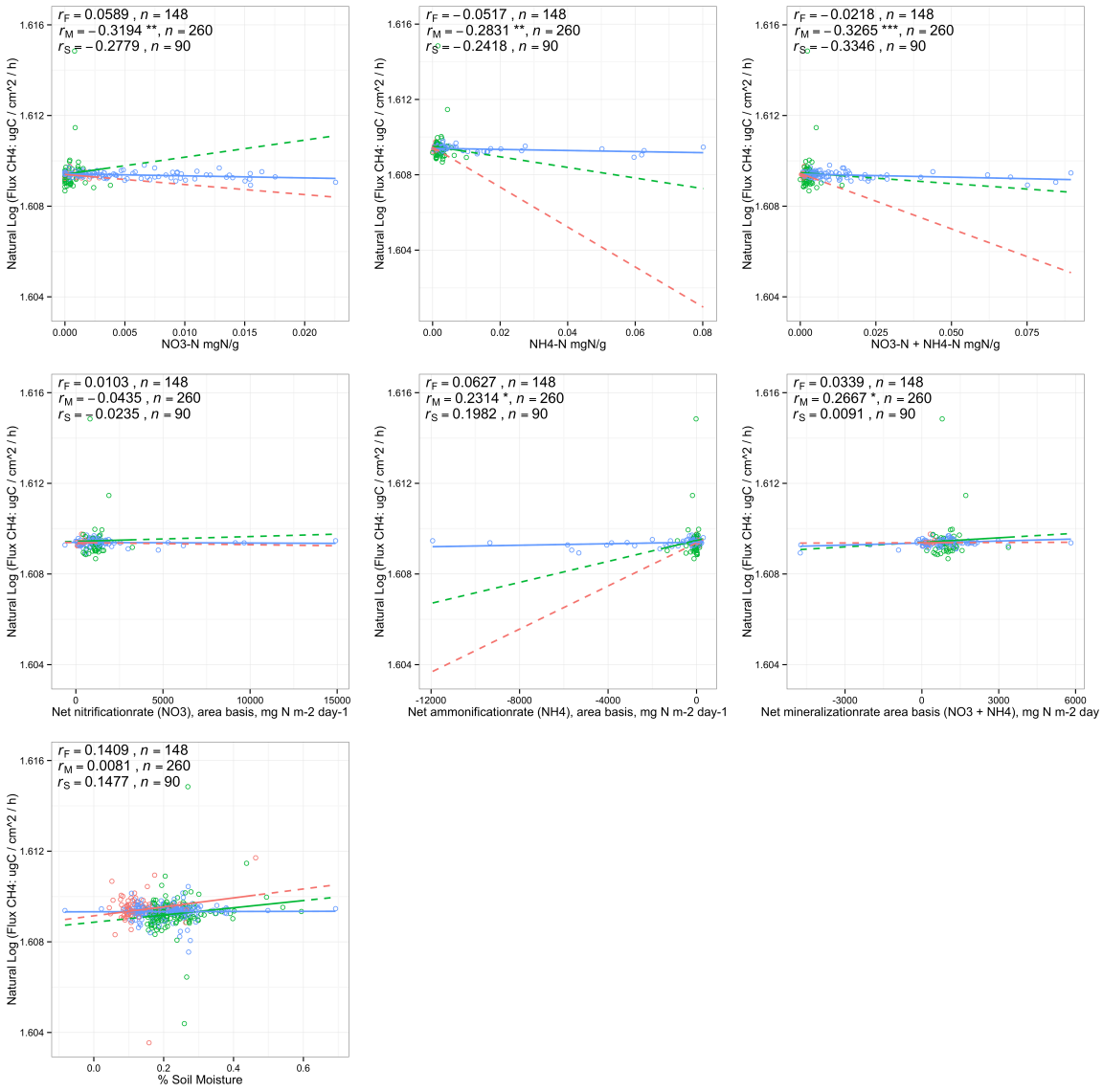

Figure 3.7c. Correlation scatterplots of log-transformed gas fluxes (here, CH_4) and key soil variables. Point color indicates land use (green = forest, blue = soybean-maize double cropping, pink = soybean single cropping). Lines are simple linear regression lines where the dotted portions of the line fall outside of the scope of the data for that land use. Pearson's linear correlation coefficient (*r*, measures correlation on a -1 to +1

scale) is marked as significantly different from zero as *** when p-value <0.001, ** when p-value <0.01 and * when p-value <0.05.

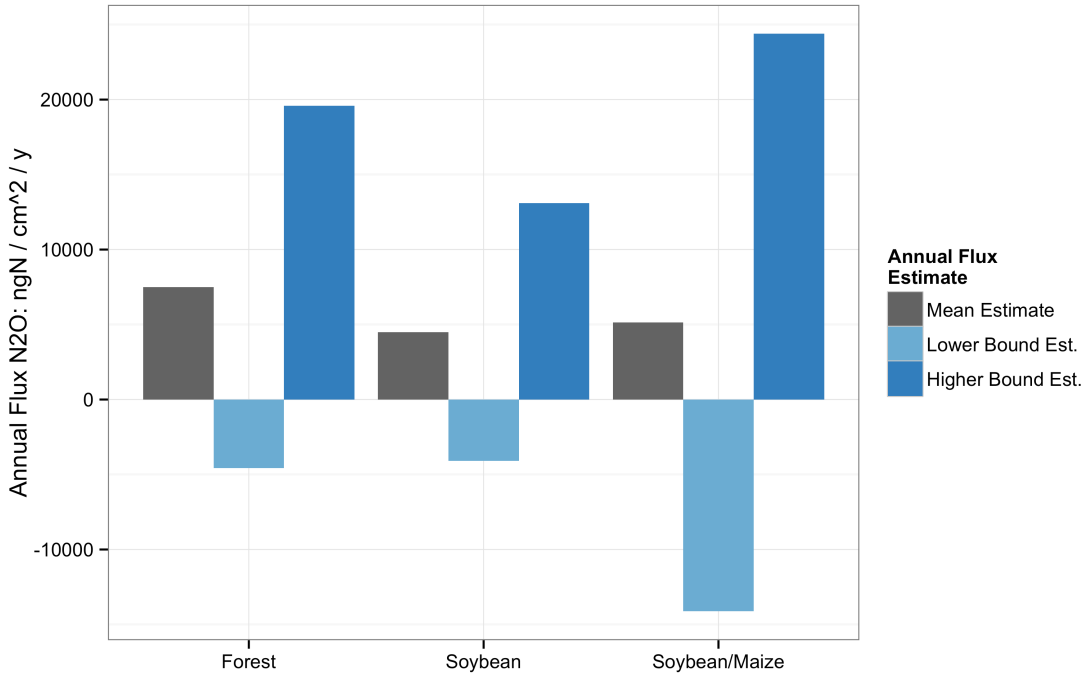

Figure 3.8. Estimated annual flux of N_2O from each land use. The mean estimate combines the mean fluxes during the wet season and the dry season for forest, soybean and the mean fluxes during the wet season, dry season and period after addition of N fertilizer. The low estimate calculates the annual flux using the mean minus one standard deviation for each period; the high estimate uses the mean plus one standard deviation for each period.

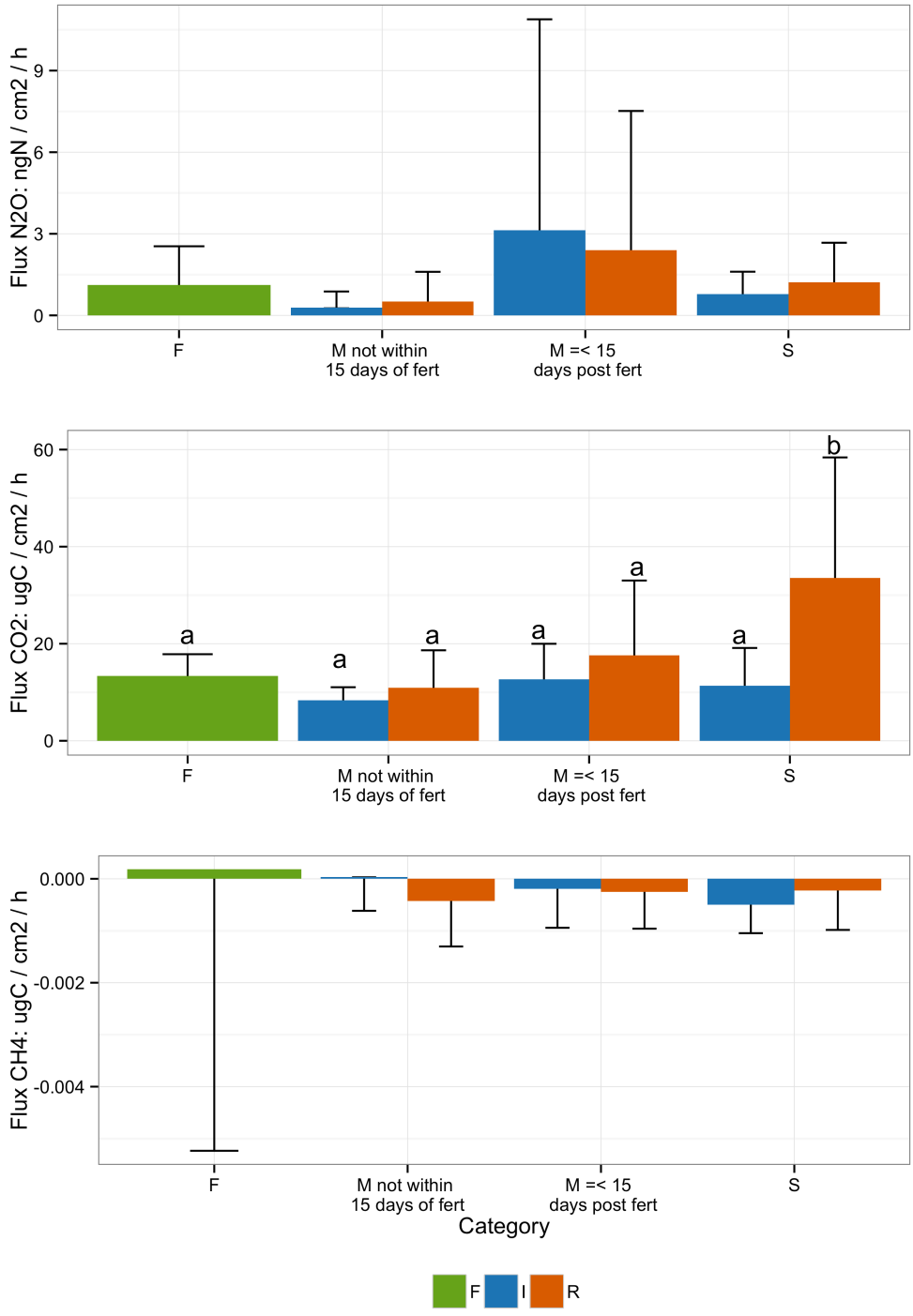

Figure 3.9. Comparison of gas fluxes between row and inter-row chamber placements in cropland land use treatments. Blue bars (I) indicate chambers placed on inter-row spaces,

while orange bars (R) indicate chambers placed on crop rows. Forest chambers, which do not have a row or inter-row designation, are indicated in green (F).

Acknowledgements

This work is heavily indebted to the field team at Tanguro Ranch and the support of Instituto de Pesquisa Ambiental da Amazônia (IPAM), and in particular the following colleagues: Wanderley Rocha da Silva, Claudinei Oliveira-Santos, Adilson Ribeiro Coelho, Darlisson Nunes da Costa, Ebis Pinheiro do Nascimento, Maria Lúcia Nascimento, Raimundo Mota Quintino, Sandro Rocha Pereira and Sebastião Aviz do Nascimento. We thank J. Gerber, P. Engstrom and P. Lefebvre for technical support and assistance with figure creation. We are grateful to M. Dolan and J. Finlay for helpful conversations. Funding was provided by a National Science Foundation Graduate Research Fellowship and a University of Minnesota Graduate Student Fellowship to C.S.O., and grants from the National Science Foundation and the Gordon and Betty Moore Foundation. Stakeholder outreach and public engagement support was provided by the University of Minnesota Institute on the Environment, and contributions by General Mills, Mosaic, Cargill, Pentair, Google, Kellogg's, Mars, and PepsiCo. Funders had no role in study design, data collection and analysis, decision to publish, or preparation of the manuscript.

Supplemental Figures:

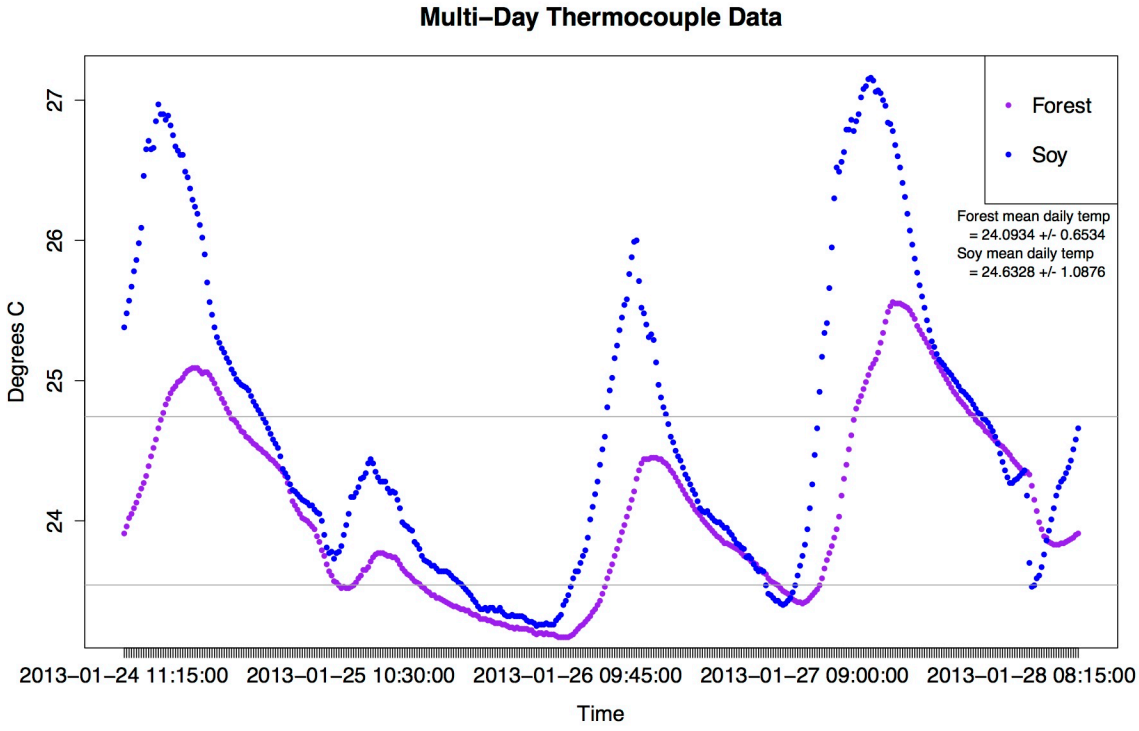

Supplemental Figure S3.1. Daily soil temperature fluctuations; used to determine when during the day to focus gas sampling.

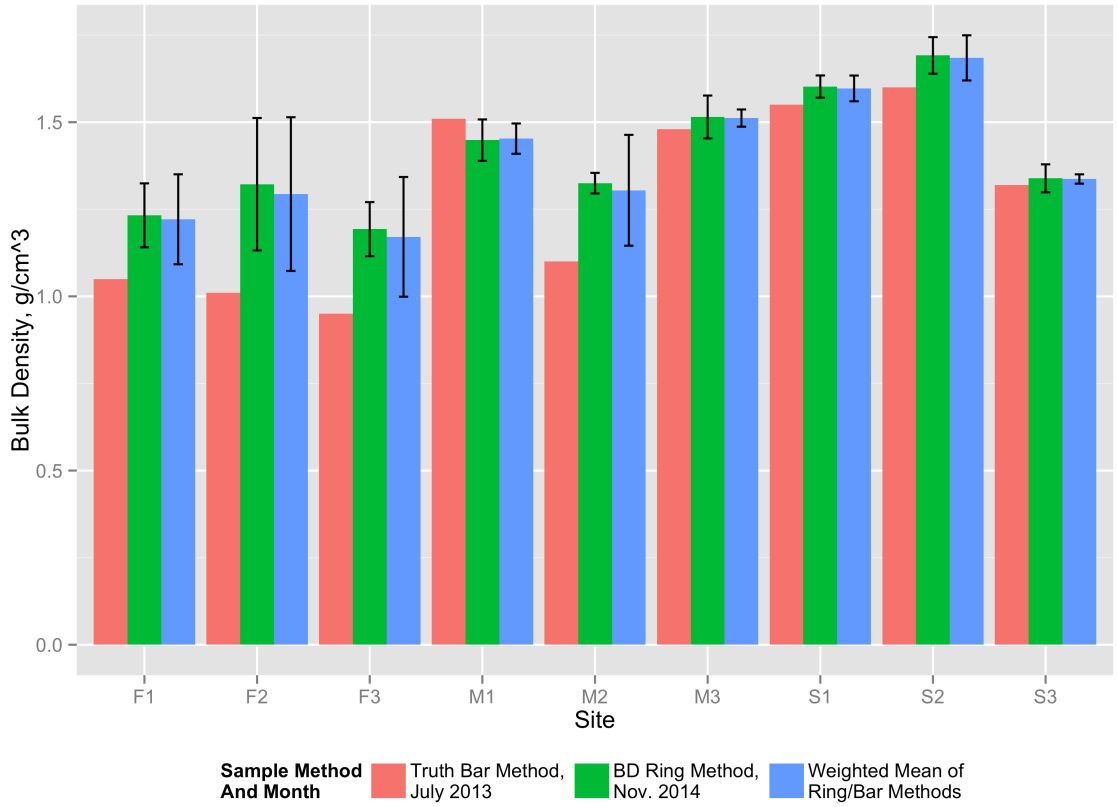

Supplemental Figure S3.2. Bulk density wet and dry season sampling; method comparison.

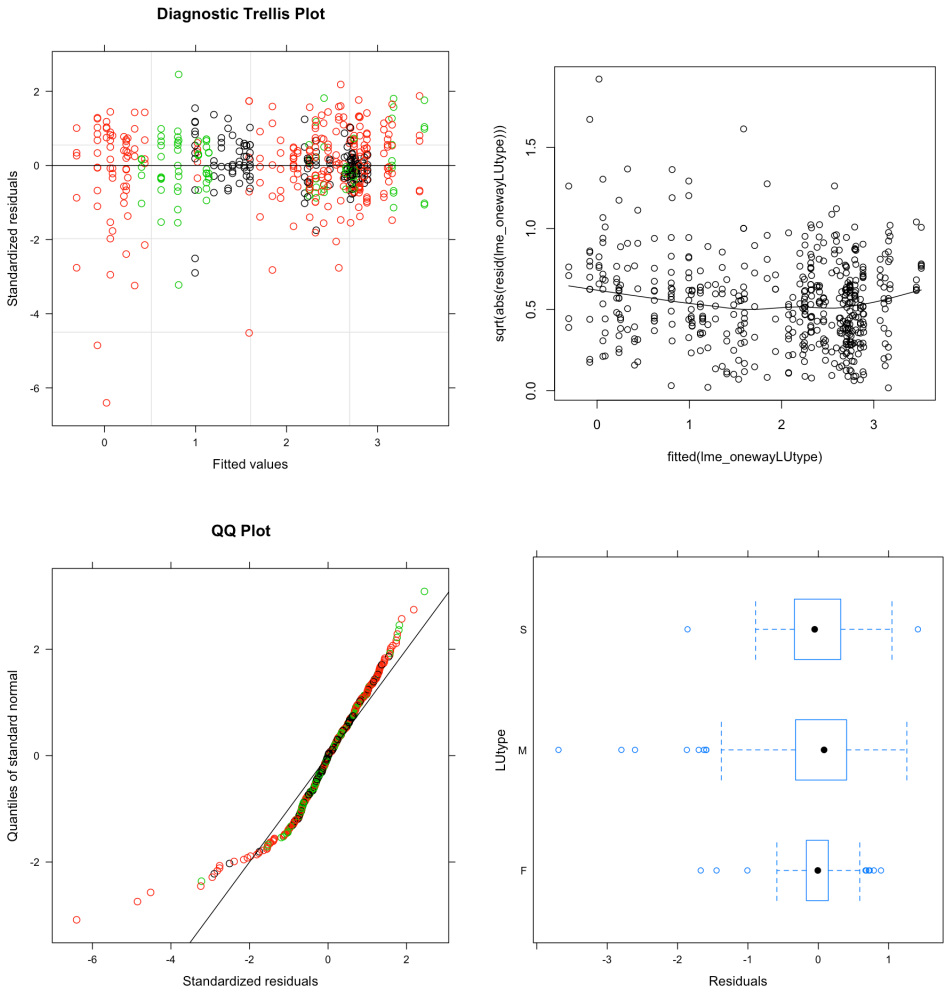

Supplemental Figure S3.3. Diagnostic tests for a one-way repeated measures ANOVA testing whether CO_2 emissions differ across land uses (forest, F, soybean, S or soybean/maize, M). CO_2 emissions have been log transformed to improve the residual distributions. These diagnostic tests roughly mirror the diagnostic tests for the remaining one-way repeated measures ANOVAs conducted.

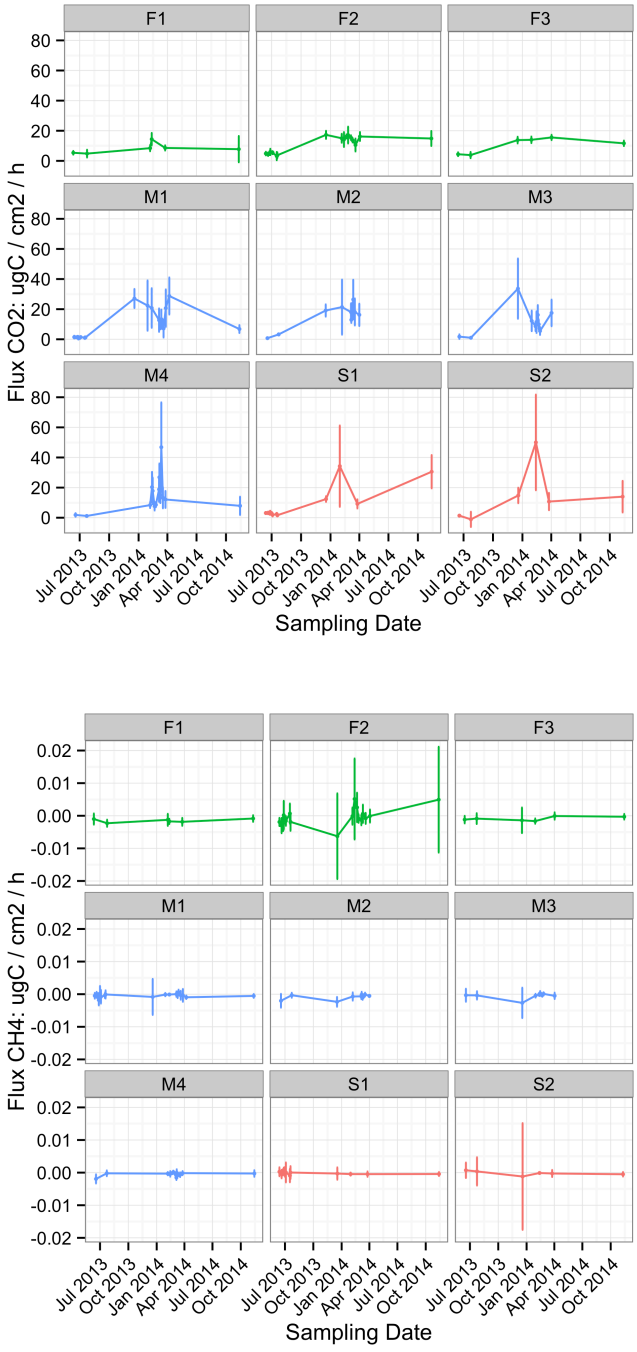

Supplemental Figure S3.4. Fluxes over time of CO_2 and CH_4, divided by site. Points indicate the mean flux of five closed chambers deployed at a given site on a given sampling date; error bars are the standard deviation.

Supplemental Table S3.1. Bulk density values for each site. Land use is either forest (F), single cropped soybean (S) or double-cropped soybean/maize (M).

Site	Bulk density, 0-10 cm, g cm^{-3} (mean)	Bulk density, 0-10 cm, g cm^{-3} (std. dev.)
F1	1.22125	0.129164839
F2	1.293636364	0.220617316
F3	1.170909091	0.171826948
M1	1.452857143	0.043514263
M2	1.304545455	0.159099026
M3	1.511818182	0.024748737
S1	1.597	0.036926687
S2	1.684615385	0.064818122
S3	1.337	0.013356461

Supplemental Table S3.2. All sampling dates included in the dataset in this study. Land use is either forest (F), single cropped soybean (S) or double-cropped soybean/maize (M).

Site	Land use	SampleDate	Season
F1	F	2013.06.11	Dry
F2	F	2013.06.13	Dry
S1	S	2013.06.13	Dry
M1	M	2013.06.14	Dry
F3	F	2013.06.14	Dry
S3	S	2013.06.18	Dry
M3	M	2013.06.18	Dry
S2	S	2013.06.18	Dry
M2	M	2013.06.18	Dry
F2	F	2013.06.20	Dry
S1	S	2013.06.20	Dry
M1	M	2013.06.20	Dry
F2	F	2013.06.25	Dry
M1	M	2013.06.25	Dry
S1	S	2013.06.25	Dry
S1	S	2013.06.27	Dry
M1	M	2013.06.27	Dry
F2	F	2013.06.27	Dry
M1	M	2013.07.01	Dry
S1	S	2013.07.01	Dry

M1	M	2013.07.04	Dry
S1	S	2013.07.04	Dry
F2	F	2013.07.04	Dry
F2	F	2013.07.17	Dry
M1	M	2013.07.17	Dry
S1	S	2013.07.17	Dry
F2	F	2013.07.19	Dry
M1	M	2013.07.19	Dry
S1	S	2013.07.19	Dry
M2	M	2013.07.23	Dry
S3	S	2013.07.23	Dry
F3	F	2013.07.23	Dry
F1	F	2013.07.24	Dry
M3	M	2013.07.24	Dry
S2	S	2013.07.24	Dry
M2	M	2013.12.17	Wet
F3	F	2013.12.17	Wet
F2	F	2013.12.17	Wet
M3	M	2013.12.18	Wet
F2	F	2013.12.18	Wet
S1	S	2013.12.18	Wet
M1	M	2013.12.19	Wet
S2	S	2013.12.19	Wet
F3	F	2014.01.29	Wet
M1	M	2014.01.29	Wet
S1	S	2014.01.30	Wet

M3	M	2014.01.30	Wet
F2	F	2014.02.05	Wet
S3	S	2014.02.06	Wet
M2	M	2014.02.06	Wet
F1	F	2014.02.06	Wet
F1	F	2014.02.11	Wet
M3	M	2014.02.11	Wet
M1	M	2014.02.11	Wet
SD	S	2014.02.12	Wet
F2	F	2014.02.12	Wet
SM	S	2014.02.12	Wet
M3	M	2014.02.14	Wet
SM	S	2014.02.14	Wet
M3	M	2014.02.18	Wet
SM	S	2014.02.20	Wet
F2	F	2014.02.20	Wet
M3	M	2014.02.21	Wet
SM	S	2014.02.24	Wet
F2	F	2014.02.25	Wet
M3	M	2014.02.25	Wet
M1	M	2014.03.06	Wet
M2	M	2014.03.06	Wet
SM	S	2014.03.06	Wet
F2	F	2014.03.06	Wet
M2	M	2014.03.07	Wet
SM	S	2014.03.07	Wet

M2	M	2014.03.10	Wet
SM	S	2014.03.10	Wet
M1	M	2014.03.10	Wet
F2	F	2014.03.11	Wet
M2	M	2014.03.13	Wet
M1	M	2014.03.13	Wet
SM	S	2014.03.13	Wet
M2	M	2014.03.18	Wet
SM	S	2014.03.18	Wet
M1	M	2014.03.20	Wet
F2	F	2014.03.20	Wet
SD	S	2014.03.25	Wet
F1	F	2014.03.25	Wet
SM	S	2014.03.26	Wet
S1	S	2014.03.26	Wet
M1	M	2014.03.27	Wet
M2	M	2014.04.01	Wet
M3	M	2014.04.02	Wet
F3	F	2014.04.02	Wet
F2	F	2014.04.03	Wet
M1	M	2014.04.07	Wet
F1	F	2014.11.10	Wet
SD	S	2014.11.10	Wet
M1	M	2014.11.12	Wet
F2	F	2014.11.12	Wet
S1	S	2014.11.13	Wet

S3	S	2014.11.14	Wet
F3	F	2014.11.14	Wet

Supplemental Table S3.3. Summary statistics for measured trace gas fluxes (in ngN cm^{-2} h^{-1} for N_2O and µgC cm^{-2} h^{-1} for CO_2 and CH_4) from each land use by season (wet vs. dry). Additionally, soybean/maize double-cropping summary statistics are included for fluxes measured within 15 days after fertilization (either broadcast or seedline).

GasType	LUtype	annualest	N	LinearFlux	sd	se	ci
CH4	F	F_dry	56	-0.001395597	0.002333857	0.000311875	0.000625011
CH4	F	F_wet	87	-0.000280905	0.006081409	0.000651995	0.001296124
CO2	F	F_dry	56	4.625395864	1.75221384	0.234149423	0.469245931
CO2	F	F_wet	87	13.59264123	4.386105812	0.470239902	0.934805986
N2O	F	F_dry	56	0.102278725	0.757603072	0.101238969	0.202887427
N2O	F	F_wet	87	1.383691017	1.813256208	0.194401471	0.386457334
CH4	M	M_dry	71	-0.000654005	0.001473769	0.000174904	0.000348835
CH4	M	M_postfert	110	-0.000286495	0.000730605	6.97E-05	0.000138065
CH4	M	M_wet	79	-0.000705195	0.001956435	0.000220116	0.000438218
CO2	M	M_dry	71	1.39029526	0.920418755	0.10923361	0.217859565
CO2	M	M_postfert	110	16.23016205	11.95406314	1.139775199	2.25899739
CO2	M	M_wet	79	17.70259604	12.50511712	1.406935597	2.800993609
N2O	M	M_dry	71	-0.050946414	0.825943026	0.098021403	0.195497525
N2O	M	M_postfert	110	2.195076521	5.684103027	0.541957959	1.074143055
N2O	M	M_wet	79	0.943461091	2.966260822	0.333730416	0.664406221
CH4	S	S_dry	51	9.37E-05	0.002030703	0.000284355	0.000571144
CH4	S	S_wet	39	-0.00046777	0.005359183	0.000858156	0.001737246
CO2	S	S_dry	51	2.171727517	2.044173345	0.286241522	0.574933018
CO2	S	S_wet	39	22.22599605	20.23489978	3.240177144	6.5593957

N2O	S	S_dry	51	0.086180987	0.715545444	0.100196403	0.201250399
N2O	S	S_wet	39	0.811567881	1.165351991	0.186605663	0.377763415

Supplemental Table S3.4. Annual flux measurements (mean, high estimate, low estimate) for each trace gas and land use (ngN cm^{-2} yr^{-1} for N_2O and ugC cm^{-2} yr^{-1} for CO_2 and CH_4).

LUtype	GasType	estmid	estlow	esthigh
F	CH4	-6.47362	-46.25557	33.30833
F	CO2	86789.45386	57849.17804	115729.7297
F	N2O	7508.049058	-4575.72403	19591.82215
S	CH4	-2.076365	-37.04028	32.88755
S	CO2	122504.3587	10733.25179	234275.4656
S	N2O	4497.941818	-4091.23805	13087.12169
M	CH4	-5.842493	-20.80197	9.11698
M	CO2	95820.38228	28178.84986	163461.9147
M	N2O	5135.433693	-14122.29024	24393.15762

Supplemental Text S3.1. While this dissertation is written by the dissertation author, the manuscript version of this chapter will have the following authorships and affiliations:

Authors: Christine S. O'Connell[1,2]*, Paulo Brando[3,4], Carlos Eduardo Cerri[5], Michael Coe[3], Eric Davidson[6], Gillian Galford[7], Sarah E. Hobbie[1], Marcia Macedo[3], Chris Neill[8], Rodney Venterea[9,10]

Affiliations:

[1]Department of Ecology, Evolution & Behavior, University of Minnesota, Saint Paul, Minnesota, 55108, USA

[2]Institute on the Environment, University of Minnesota, Saint Paul, Minnesota, 55108, USA

[3]Woods Hole Research Center, Falmouth, MA 02450, USA

[4]Instituto de Pesquisa Ambiental da Amazônia, 66035-170, Belém, Pará, Brazil

[5]Center for Nuclear Energy in Agriculture, University of São Paulo, Piracicaba, SP, 13416-000, Brazil

[6]University of Maryland Center for Environmental Science, Appalachian Laboratory, 301 Braddock Road, Frostburg, MD 21532, USA

[7]The Gund Institute for Ecological Economics, University of Vermont, 617 Main Street, Burlington, Vermont, 05405, USA

[8]The Ecosystems Center, Marine Biological Laboratory, 7 MBL Street, Woods Hole, MA 02543, USA

[9]Department of Soil, Water, and Climate, University of Minnesota, St. Paul, MN 55108, USA

[10]USDA-ARS, Soil and Water Management Unit, 1991 Upper Buford Circle, St. Paul, MN 55108, USA

*Correspondence to: coconn@umn.edu

Bibliography

Aide TM, Clark ML, Grau HR, et al. (2012) Deforestation and Reforestation of Latin America and the Caribbean (2001-2010). *Biotropica*, **45**, 262–271.

Alencar A, Brando PM, Asner G, Putz FE (2015) Landscape Fragmentation, Severe Drought and the New Amazon Forest Fire Regime. *ESA Pre-print*,, 1–38.

Anderson-Teixeira KJ, Snyder PK, Twine TE, Cuadra SV, Costa MH, DeLucia EH (2012) Climate-regulation services of natural and agricultural ecoregions of the Americas. *Nature Climate Change*, **2**, 177–181.

Baccini A, Goetz SJ, Walker WS, et al. (2012) Estimated carbon dioxide emissions from tropical deforestation improved by carbon-density maps. *Nature Climate Change*, **2**, 182–185.

Bagley JE, Desai AR, Dirmeyer PA, Foley JA (2012) Effects of land cover change on moisture availability and potential crop yield in the world's breadbaskets. *Environmental Research Letters*, **7**, 014009.

Balch JK, Nepstad DC, Brando PM, Curran LM, Portela O, de Carvalho O JR, Lefebvre P (2008) Negative fire feedback in a transitional forest of southeastern Amazonia. *Global Change Biology*, **14**, 2276–2287.

Batjes N (2007) ISRIC-WISE global data set of derived soil properties on a 0.5 by 0.5 degree grid. *Report*, 1–24.

Batjes NH, Sombroek WG (1997) Possibilities for carbon sequestration in tropical and subtropical soils. *Global Change Biology*.

Blasing TJ (2009) Recent Greenhouse Gas Concentrations.

Bonan GB (2008) Forests and Climate Change: Forcings, Feedbacks, and the Climate Benefits of Forests. *Science*, **320**, 1444–1449.

Bouwman AF, Boumans LJM, Batjes NH (2002) Emissions of N 2O and NO from fertilized fields: Summary of available measurement data. *Global Biogeochemical Cycles*, **16**, 6–1–6–13.

Bowman MS, Soares-Filho BS, Merry FD, Nepstad DC, Rodrigues H, Almeida OT (2012) Land Use Policy. *Land Use Policy*, **29**, 558–568.

Brando PM, Balch JK, Nepstad DC, et al. (2014) Abrupt increases in Amazonian tree mortality due to drought-fire interactions. *Proceedings of the National Academy of Sciences*, **111**, 6347–6352.

Brienen R, Helle G, Pons TL (2012) Oxygen isotopes in tree rings are a good proxy for Amazon precipitation and El Niño-Southern Oscillation variability

Carvalho JLN, Cerri CEP, Feigl BJ, Piccolo MC, Godinho VP, Cerri CC (2009) Carbon sequestration in agricultural soils in the Cerrado region of the Brazilian Amazon. *Soil & Tillage Research*, **103**, 342–349.

Carvalho JLN, Raucci GS, Frazão LA, Cerri CEP, Bernoux M, Cerri CC (2014) Agriculture, Ecosystems and Environment. *Agriculture, Ecosystems & Environment*, **183**, 167–175.

Cassidy ES, West PC, Gerber JS, Foley JA (2013) Redefining agricultural yields: from tonnes to people nourished per hectare. *Environmental Research Letters*, **8**, 034015.

Castanho ADA, Coe MT, Costa MH, Malhi Y, Galbraith D, Quesada CA (2013) Improving simulated Amazon forest biomass and productivity by including spatial variation in biophysical parameters. *Biogeosciences*, **10**, 2255–2272.
Cerri C, Sparovek G, Bernoux M, Easterling WE (2007) Tropical agriculture and global warming: impacts and mitigation options. *Scientia.*
Chazdon RL (2008) Beyond Deforestation: Restoring Forests and Ecosystem Services on Degraded Lands. *Science*, **320**, 1458–1460.
Clark ML, Aide TM, Riner G (2012) Land change for all municipalities in Latin America and the Caribbean assessed from 250-m MODIS imagery (2001–2010). *Remote Sensing of Environment*, **126**, 84–103.
Coe MT, Costa MH, Soares-Filho BS (2009) The influence of historical and potential future deforestation on the stream flow of the Amazon River – Land surface processes and atmospheric feedbacks. *Journal of Hydrology*, **369**, 165–174.
Cruvinel ÃBF, da C Bustamante MM, Kozovits AR, Zepp RG (2011) Agriculture, Ecosystems and Environment. *Agriculture, Ecosystems & Environment*, **144**, 29–40.
Cuadra SV, Costa MH, Kucharik CJ, et al. (2011) A biophysical model of Sugarcane growth. *GCB Bioenergy*, **4**, 36–48.
Cuhel J, Simek M, Laughlin RJ, Bru D, Cheneby D, Watson CJ, Philippot L (2010) Insights into the Effect of Soil pH on N2O and N2 Emissions and Denitrifier Community Size and Activity. *Applied and Environmental Microbiology*, **76**, 1870–1878.
Curry CL (2007) Modeling the soil consumption of atmospheric methane at the global scale. *Global Biogeochemical Cycles*.
Daily G, Polasky S, Goldstein J, et al. (2009) Ecosystem services in decision making: time to deliver. *Frontiers in Ecology and the Environment*, **7**, 21–28.
Davidson EA, Matson PA (1996) Nitrous oxide emission controls and inorganic nitrogen dynamics in fertilized tropical agricultural soils. *Soil Science Society of America Journal*.
Davidson EA, Trumbore SE (1995) Gas diffusivity and production of CO2 in deep soils of the eastern Amazon. *Tellus B*.
Davidson EA, de Araújo AC, Artaxo P, et al. (2012a) The Amazon basin in transition. *Nature*, **481**, 321–328.
Davidson EA, de Araújo AC, Artaxo P, et al. (2012b) The Amazon basin in transition. *Nature*, **481**, 321–328.
Davidson EA, Ishida FY, Nepstad DC (2004) Effects of an experimental drought on soil emissions of carbon dioxide, methane, nitrous oxide, and nitric oxide in a moist tropical forest. *Global Change Biology*, 1–13.
Davidson EA, Keller M, Erickson HE, Verchot L, Veldkamp E (2000) Testing a Conceptual Model of Soil Emissions of Nitrous and Nitric Oxides. *BioScience*.
Davidson EA, Matson PA, Vitousek PM, Riley R (1993) Processes Regulating Soil Emissions of NO and N2O in a Seasonally Dry Tropical Forest. *Ecology*.
Davidson EA, Savage KE, Trumbore SE (2006) Vertical partitioning of CO2 production within a temperate forest soil. *Global Change Biology*.
DeFries R, Herold M, Verchot L, Macedo MN, Shimabukuro Y (2013) Export-oriented

deforestation in Mato Grosso: harbinger or exception for other tropical forests? *Philosophical Transactions of the Royal Society B: Biological Sciences*, **368**, 20120173–20120173.

DeFries RS, Rudel T, Uriarte M, Hansen M (2010) Deforestation driven by urban population growth and agricultural trade in the twenty-first century. *Nature Geoscience*, **3**, 178–181.

Del Grosso S, Parton W, Stohlgren T, et al. (2008) Global potential net primary production predicted from vegetation class, precipitation, and temperature. *Ecology*, **89**, 2117–2126.

Dirzo R, Raven P (2003) Global state of biodiversity and loss. *Annual Review Of Environment And Resources*, **28**, 137–167.

Eilers KG, Debenport S, Anderson S, Fierer N (2012) Soil Biology & Biochemistry. *Soil Biology and Biochemistry*, **50**, 58–65.

Erickson H, Keller M, Davidson EA (2001) Nitrogen Oxide Fluxes and Nitrogen Cycling during Postagricultural Succession and Forest Fertilization in the Humid Tropics. *Ecosystems*, **4**, 67–84.

Fearnside PM, Barbosa RI (1998) Soil carbon changes from conversion of forest to pasture in Brazilian Amazonia. *Forest Ecology and Management*.

Feeley KJ, Rehm EM (2012) Amazon's vulnerability to climate change heightened by deforestation and man-made dispersal barriers. *Global Change Biology*, **18**, 3606–3614.

Feeley KJ, Silman MR (2009) Extinction risks of Amazonian plant species. *Proceedings of the National Academy of Sciences*, **106**, 12382–12387.

Feeley KJ, Malhi Y, Zelazowski P, Silman MR (2012a) The relative importance of deforestation, precipitation change, and temperature sensitivity in determining the future distributions and diversity of Amazonian plant species. *Global Change Biology*, **18**, 2636–2647.

Feeley KJ, Malhi Y, Zelazowski P, Silman MR (2012b) The relative importance of deforestation, precipitation change, and temperature sensitivity in determining the future distributions and diversity of Amazonian plant species. *Global Change Biology*, **18**, 2636–2647.

Feldpausch TR, Rondon MA, Fernandes EC, Riha SJ, Wandelli E (2004) Carbon and nutrient accumulation in secondary forests regenerating on pastures in central Amazonia. *Ecological applications: a publication of the Ecological Society of America*, **14**, 164–176.

Firestone MK, Davidson EA (1989) Microbiological basis of NO and N2O production and consumption in soil. *Exchange of trace gases.*

Foley J, Asner G, Costa M, et al. (2007) Amazonia revealed: forest degradation and loss of ecosystem goods and services in the Amazon Basin. *Frontiers in Ecology and the Environment*, **5**, 25–32.

Foley J, DeFries R, Asner G, et al. (2005) Global consequences of land use. *Science*, **309**, 570.

Foley JA, Levis S, Prentice IC, Pollard D, Thompson SL (1998) Coupling dynamic models of climate and vegetation. *Global Change Biology*, **4**, 561–579.

Foley JA, Ramankutty N, Brauman KA, et al. (2012) Solutions for a cultivated planet. *Nature*, **478**, 337–342.
Fujisaki K, Perrin A-S, Desjardins T, Bernoux M, Balbino LC, Brossard M (2015) From forest to cropland and pasture systems: a critical review of soil organic carbon stocks changes in Amazonia. *Global Change Biology*, **21**, 2773–2786.
Galford GL, Melillo JM, Kicklighter DW, Cronin TW, Cerri CEP, Mustard JF, Cerri CC (2010) Greenhouse gas emissions from alternative futures of deforestation and agricultural management in the southern Amazon. *Proceedings of the National Academy of Sciences*, **107**, 19649–19654.
Galford GL, Melillo JM, Kicklighter DW, Mustard JF, Cronin TW, Cerri CEP, Cerri CC (2011) Historical carbon emissions and uptake from the agricultural frontier of the Brazilian Amazon. *Ecological applications: a publication of the Ecological Society of America*, **21**, 750–763.
Galford GL, Mustard JF, Melillo JM, Gendrin A, Cerri CC, Cerri CEP (2008) Wavelet analysis of MODIS time series to detect expansion and intensification of row-crop agriculture in Brazil. *Remote Sensing of Environment*, **112**, 576–587.
Galloway JN, Dentener FJ, Capone DG, Boyer EW (2004) Nitrogen cycles: past, present, and future. *Biogeochemistry*.
Galloway JN, Townsend AR, Erisman JW, et al. (2008) Transformation of the Nitrogen Cycle: Recent Trends, Questions, and Potential Solutions. *Science*, **320**, 889–892.
Garcia-Montiel DC, Melillo JM, Steudler PA, Cerri CC, Piccolo MC (2003) Carbon limitations to nitrous oxide emissions in a humid tropical forest of the Brazilian Amazon. *Biology and Fertility of Soils*, **38**, 267–272.
Garcia-Montiel DC, Steudler PA, Piccolo MC, Melillo JM, Neill C, Cerri CC (2001) Controls on soil nitrogen oxide emissions from forest and pastures in the Brazilian Amazon. *Global Biogeochemical Cycles*, **15**, 1021–1030.
Gatti LV, Gloor M, Miller JB, et al. (2014) Drought sensitivity of Amazonian carbon balance revealed by atmospheric measurements. *Nature*, **506**, 76–80.
Gloor M, Brienen RJW, Galbraith D, et al. (2013) Intensification of the Amazon hydrological cycle over the last two decades. *Geophysical Research Letters*, **40**, 1729–1733.
Goldstein JH, Caldarone G, Duarte TK, et al. (2012) Integrating ecosystem-service tradeoffs into land-use decisions. *Proceedings of the National Academy of Sciences*, **109**, 7565–7570.
Groffman PM, Altabet MA, Böhlke JK, et al. (2006) Methods for measuring denitrification: diverse approaches to a difficult problem. *Ecological applications : a publication of the Ecological Society of America*, **16**, 2091–2122.
Groffman PM, Butterbach-Bahl K, Fulweiler RW, et al. (2009) Challenges to incorporating spatially and temporally explicit phenomena (hotspots and hot moments) in denitrification models. *Biogeochemistry*, **93**, 49–77.
Harris NL, Brown S, Hagen SC, et al. (2012) Baseline Map of Carbon Emissions from Deforestation in Tropical Regions. *Science*, **336**, 1573–1576.
Harrison RB, Footen PW, Strahm BD (2011) Deep soil horizons: contribution and importance to soil carbon pools and in assessing whole-ecosystem response to

management and global change. *Forest Science*.
Hayhoe SJ, Neill C, Porder S, McHorney R (2011) Conversion to soy on the Amazonian agricultural frontier increases streamflow without affecting stormflow dynamics. *Global Change Biology*.
Hiederer R, Kochy M (2012) Global Soil Organic Carbon Estimates and the Harmonized World Soil Database. 1–90.
Hijmans RJ, Cameron SE, Parra JL, Jones PG, Jarvis A (2005) Very high resolution interpolated climate surfaces for global land areas. *International Journal of Climatology*, **25**, 1965–1978.
Hubbell SP, He F, Condit R, Borda-de-Agua L, Kellner J, Steege ter H (2008) How many tree species are there in the Amazon and how many of them will go extinct? *Proceedings of the National Academy of Sciences*, **105**, 11498–11504.
INPE (Brazilian National Institute for Space Research) Program for the Estimation of Amazon Deforestation (Projeto PRODES Digital). *dpi.inpe.br*.
Isbell F, Tilman D, Polasky S, Loreau M (2014) The biodiversity-dependent ecosystem service debt (R Bardgett, Ed.). *Ecology Letters*, **18**, 119–134.
Itoh M, Kosugi Y, Takanashi S, et al. (2012) Effects of soil water status on the spatial variation of carbon dioxide, methane and nitrous oxide fluxes in tropical rain-forest soils in Peninsular Malaysia. *Journal of Tropical Ecology*, **28**, 557–570.
Jackson RB, Randerson JT, Canadell JG, et al. (2008) Protecting climate with forests. *Environmental Research Letters*, **3**, 044006.
Jobbágy E, Jackson R (2000) The vertical distribution of soil organic carbon and its relation to climate and vegetation. *Ecological Applications*, **10**, 423–436.
Jobbágy EG, Jackson RB (2001) The distribution of soil nutrients with depth: global patterns and the imprint of plants. *Biogeochemistry*.
Karp DS, Ziv G, Zook J, Ehrlich PR, Daily GC (2011) Resilience and stability in bird guilds across tropical countryside. *Proceedings of the National Academy of Sciences*, **108**, 21134–21139.
Keller M, Reiners WA (1994) Soil-atmosphere exchange of nitrous oxide, nitric oxide, and methane under secondary succession of pasture to forest in the Atlantic lowlands of Costa Rica. *Global Biogeochemical Cycles*, **8**, 399–409.
Keller M, Mitre ME, Stallard RF (1990) Consumption of atmospheric methane in soils of central Panama: effects of agricultural development. *Global Biogeochemical Cycles*.
Keller M, Varner R, Dias JD, Silva H, Crill P, de Oliveira RC Jr, Asner GP (2005) Soil-atmosphere exchange of nitrous oxide, nitric oxide, methane, and carbon dioxide in logged and undisturbed forest in the Tapajos National Forest, Brazil. *Earth Interactions*, **9**, 1–28.
Koehler B, Zehe E, Corre MD, Veldkamp E (2010) An inverse analysis reveals limitations of the soil-CO_2 profile method to calculate CO_2 production and efflux for well-structured soils. *Biogeosciences*, **7**, 2311–2325.
Kucharik CJ (2003) Evaluation of a Process-Based Agro-Ecosystem Model (Agro-IBIS) across the U.S. Corn Belt: Simulations of the Interannual Variability in Maize Yield. *Earth Interactions*, **7**, 1–33.
Lapig-Database - Periódicos - Detecção De Desmatamentos No Bioma Cerrado Entre

2002 E 2009: Padrões, Tendências E Impactos. Lapig-Database - Periódicos - Detecção De Desmatamentos No Bioma Cerrado Entre 2002 E 2009: Padrões, Tendências E Impactos. *LAPIG (Laboratorio de Processamento de Imagens e Geoprocessamento) Deforestation Alerts.*

Lapola DM, Martinelli LA, Peres CA, et al. (2014) Pervasive transition of the Brazilian land-use system. *Nature Climate Change*, **4**, 27–35.

Lenzen M, Moran D, Kanemoto K, Foran B, Lobefaro L, Geschke A (2012) International trade drives biodiversity threats in developing nations. *Nature*, **486**, 109–112.

Lindau CW, De Laune RD, Jones GL (1988) Fate of added nitrate and ammonium-nitrogen entering a Louisiana gulf coast swamp forest. *Journal (Water Pollution Control Federation)*.

Linquist B, Groenigen KJ, Adviento-Borbe MA, Pittelkow C, Kessel C (2011) An agronomic assessment of greenhouse gas emissions from major cereal crops. *Global Change Biology*, **18**, 194–209.

Livingston GP, Vitousek PM, Matson PA (1988) Nitrous oxide flux and nitrogen transformations across a landscape gradient in Amazonia. *Journal of Geophysical Research*.

Luizão F, Matson PA, Livingston G, Luizão R, Vitousek P (1989) Nitrous oxide flux following tropical land clearing. *Global Biogeochemical Cycles*, **3**, 281–285.

MacDonald GK, Brauman KA, Sun S, Carlson KM, Cassidy ES, Gerber JS, West PC (2015) Rethinking Agricultural Trade Relationships in an Era of Globalization. *BioScience*, **65**, 275–289.

Macedo MN, DeFries RS, Morton DC, Stickler CM, Galford GL, Shimabukuro YE (2012) Decoupling of deforestation and soy production in the southern Amazon during the late 2000s. *Proceedings of the National Academy of Sciences*, **109**, 20120171–20120171.

Madsen EL (2011) Microorganisms and their roles in fundamental biogeochemical cycles. *Current Opinion in Biotechnology*, **22**, 456–464.

Malhi Y, Roberts JT, Betts RA, Killeen TJ, Li W, Nobre CA (2008) Climate Change, Deforestation, and the Fate of the Amazon. *Science*, **319**, 169–172.

Malhi Y, Wood D, Baker TR, et al. (2006) The regional variation of aboveground live biomass in old-growth Amazonian forests. *Global Change Biology*, **12**, 1107–1138.

Marin-Spiotta E, Silver WL, Swanston C, ostertag R (2009) Soil organic matter dynamics during 80 years of reforestation of tropical pastures. *Global Change Biology*.

Martinson GO, Corre MD, Veldkamp E (2012) Responses of nitrous oxide fluxes and soil nitrogen cycling to nutrient additions in montane forests along an elevation gradient in southern Ecuador. *Biogeochemistry*, **112**, 625–636.

Matson PA, Naylor R, Ortiz-Monasterio I (1998) Integration of environmental, agronomic, and economic aspects of fertilizer management. *Science*, **280**, 112–115.

Melillo JM, Steudler PA, Feigl BJ, et al. (2001) Nitrous oxide emissions from forests and pastures of various ages in the Brazilian Amazon. *Journal of Geophysical Research*, **106**, 34179–34–188.

Melo VS, Desjardins T, Silva ML Jr, Santos ER, Sarrazin M, Santos MMLS (2012) Consequences of forest conversion to pasture and fallow on soil microbial biomass

and activity in the eastern Amazon. *Soil Use and Management*, **28**, 530–535.
Metay A, Oliver R, Scopel E, et al. (2007) N2O and CH4 emissions from soils under conventional and no-till management practices in Goiânia (Cerrados, Brazil). *Geoderma*, **141**, 78–88.
Morton DC, DeFries RS, Shimabukuro YE, et al. (2006) Cropland expansion changes deforestation dynamics in the southern Brazilian Amazon. *Proceedings of the National Academy of Sciences*, **103**, 14637–14641.
Mosier A, Wassmann R, Verchot L, King J (2004) Methane and nitrogen oxide fluxes in tropical agricultural soils: sources, sinks and mechanisms. *Environment, Development and Sustainability*.
Mueller ND, Gerber JS, Johnston M, Ray DK, Ramankutty N, Foley JA (2012a) Closing yield gaps through nutrient and water management. *Nature*.
Mueller ND, Gerber JS, Johnston M, Ray DK, Ramankutty N, Foley JA (2012b) Closing yield gaps through nutrient and water management. *Nature*, **490**, 254–257.
Murphy PG, Lugo AE (1986) Ecology of tropical dry forest. *Annual Review of Ecology and Systematics*.
Murty D, Kirschbaum M, Mcmurtrie R, Mcgilvray H (2002) Does conversion of forest to agricultural land change soil carbon and nitrogen? A review of the literature. *Global Change Biology*, **8**, 105–123.
Nachtergaele F, van Velthuizen H, Verelst L (2012) Harmonized World Soil Database. *FAO-IIASA-ISRIC-ISSCAS-JRC*,, 1–50.
Neill C, Piccolo MC, Cerri CC, Steudler PA, Melillo JM (2006) Soil Solution Nitrogen Losses During Clearing of Lowland Amazon Forest for Pasture. *Plant and Soil*, **281**, 233–245.
Neill C, Piccolo MC, Melillo JM, Steudler PA (1999) Nitrogen dynamics in Amazon forest and pasture soils measured by 15 N pool dilution. *Soil Biology and Biochemistry*.
Neill C, Piccolo MC, Steudler PA, Melillo JM, Feigl BJ, Cerri CC (1995) Nitrogen dynamics in soils of forests and active pastures in the western Brazilian Amazon Basin. *Soil Biology and Biochemistry*, **27**, 1167–1175.
Nelson E, Mendoza G, Regetz J, et al. (2009) Modeling multiple ecosystem services, biodiversity conservation, commodity production, and tradeoffs at landscape scales. *Frontiers in Ecology and the Environment*, **7**, 4–11.
Nepstad DC, Boyd W, Stickler CM, Bezerra T, Azevedo AA (2013) Responding to climate change and the global land crisis: REDD+, market transformation and low-emissions rural development. *Philosophical Transactions of the Royal Society B: Biological Sciences*, **368**, 20120167–20120167.
Nepstad DC, de Carvalho CR, Davidson EA, Jipp PH (1994) The role of deep roots in the hydrological and carbon cycles of Amazonian forests and pastures.
Nepstad DC, McGrath DG, Stickler C, et al. (2014) Slowing Amazon deforestation through public policy and interventions in beef and soy supply chains. *Science*, **344**, 1118–1123.
Nobre AD, M K, P C, R H (2001) Short-term nitrous oxide profile dynamics and emissions response to water, nitrogen and carbon additions in two tropical soils.

Biology and Fertility of Soils, **34**, 363–373.
Oliveira LJC, Costa MH, Soares-Filho BS, Coe MT (2013) Large-scale expansion of agriculture in Amazonia may be a no-win scenario. *Environmental Research Letters*, **8**, 024021.
Olson D, Dinerstein E, Wikramanayake ED, et al. (2001) Terrestrial Ecoregions of the World: A New Map of Life on Earth. *BioScience*,, 1–6.
Panek JA, Matson PA, Ortiz-Monasterio I, Brooks P (2000) Distinguishing nitrification and denitrification sources of N2O in Mexican wheat systems using 15N as a tracer.
Parkin TB (1987) Soil microsites as a source of denitrification variability. *Soil Science Society of America Journal*.
Parkin TB, Venterea RT, Hargreaves SK (2012) Calculating the Detection Limits of Chamber-based Soil Greenhouse Gas Flux Measurements. *Journal of Environment Quality*, **41**, 705.
Pendall E, Schwendenmann L, Rahn T (2010) Land use and season affect fluxes of CO2, CH4, CO, N2O, H2 and isotopic source signatures in Panama: evidence from nocturnal boundary layer profiles. *Global Change Biology*.
Pérez T, Trumbore SE, Tyler SC (2001) Identifying the agricultural imprint on the global N2O budget using stable isotopes. *Journal of Geophysical Research*.
Philibert A, Loyce C, Makowski D (2012) Quantifying Uncertainties in N2O Emission Due to N Fertilizer Application in Cultivated Areas (CJ Bernacchi, Ed.). *PLoS ONE*, **7**, e50950.
Piccolo MC, Andreux F, Cerri CC (2011) HYDROCHEMISTRY OF SOIL SOLUTION COLLECTED WITH TENSION-FREE LYSIMETERS IN NATIVE AND CUT-AND-BRUNED TROPICAL RAIN FOREST. *Geochimica Brasiliensis*.
Pimm SL, Jenkins CN, Abell R, et al. (2014) The biodiversity of species and their rates of extinction, distribution, and protection. *Science*, **344**, 1246752–1246752.
Powers JS, Corre MD, Twine TE, Veldkamp E (2011) Geographic bias of field observations of soil carbon stocks with tropical land-use changes precludes spatial extrapolation. *Proceedings of the National Academy of Sciences*, **108**, 6318–6322.
Ramankutty N, Foley J, Norman J, McSweeney K (2002) The global distribution of cultivable lands: current patterns and sensitivity to possible climate change. *Global Ecology and Biogeography*, **11**, 377–392.
Ray DK, Mueller ND, West PC, Foley JA (2013) Yield Trends Are Insufficient to Double Global Crop Production by 2050 (JP Hart, Ed.). *PLoS ONE*, **8**, e66428.
Riskin SH, Porder S, Neill C, Figueira AMES, Tubbesing C, Mahowald N (2013) The fate of phosphorus fertilizer in Amazon soya bean fields. *Philosophical Transactions of the Royal Society B: Biological Sciences*, **368**, 20120154–20120154.
Rodrigues JL, Pellizari VH, Mueller R, et al. (2013) Conversion of the Amazon rainforest to agriculture results in biotic homogenization of soil bacterial communities. *Proceedings of the National Academy of Sciences*, **110**, 988–993.
Rudel TK, Defries R, Asner GP, Laurance WF (2009) Changing Drivers of Deforestation and New Opportunities for Conservation. *Conservation Biology*, **23**, 1396–1405.
Rumpel C, Kögel-Knabner I (2010) Deep soil organic matter—a key but poorly understood component of terrestrial C cycle. *Plant and Soil*, **338**, 143–158.

Saatchi SS, Harris NL, Brown S, et al. (2011) Benchmark map of forest carbon stocks in tropical regions across three continents. *Proceedings of the National Academy of Sciences*, **108**, 9899–9904.
Sano EE, Rosa R, Brito JLS, Ferreira LG (2009) Land cover mapping of the tropical savanna region in Brazil. *Environmental Monitoring and Assessment*, **166**, 113–124.
Schwendenmann L, Pendall E (2006) Effects of forest conversion into grassland on soil aggregate structure and carbon storage in Panama: evidence from soil carbon fractionation and stable isotopes. *Plant and Soil*.
Schwendenmann L, Pendall E (2008) Response of soil organic matter dynamics to conversion from tropical forest to grassland as determined by long-term incubation. *Biology and Fertility of Soils*, **44**, 1053–1062.
Schwendenmann L, Veldkamp E (2006) Long-term CO2 production from deeply weathered soils of a tropical rain forest: Evidence for a potential positive feedback to climate warming. *Global Change Biology*.
Schwendenmann L, Veldkamp E, Moser G (2010) Effects of an experimental drought on the functioning of a cacao agroforestry system, Sulawesi, Indonesia. *Global Change Biology*.
Schwendenmann L, Veldkamp E, Brenes T, O'Brien JJ (2003) Spatial and temporal variation in soil CO2 efflux in an old-growth neotropical rain forest, La Selva, Costa Rica. *Biogeochemistry*.
Setälä H, Bardgett RD, Birkhofer K, et al. (2013) Urban and agricultural soils: conflicts and trade-offs in the optimization of ecosystem services. *Urban Ecosystems*, **17**, 239–253.
Shcherbak I, Millar N, Robertson GP (2014) Global metaanalysis of the nonlinear response of soil nitrous oxide (N2O) emissions to fertilizer nitrogen. *Proceedings of the National Academy of Sciences*, **111**, 9199–9204.
Silver WL, Thompson AW, McGroddy ME, et al. (2005) Fine root dynamics and trace gas fluxes in two lowland tropical forest soils. *Global Change Biology*, **11**, 290–306.
Smith P, Martino D, Cai Z, et al. (2008) Greenhouse gas mitigation in agriculture. *Philosophical Transactions of the Royal Society B: Biological Sciences*, **363**, 789–813.
Soares-Filho BS, Moutinho P, Nepstad DC, et al. (2010) Role of Brazilian Amazon protected areas in climate change mitigation. *Proceedings of the National Academy of Sciences*, **107**, 10821–10826.
Soares-Filho BS, Nepstad DC, Curran LM, et al. (2006) Modelling conservation in the Amazon basin. *Nature*, **440**, 520–523.
Soares-Filho BS, Rajao R, Macedo M, et al. (2014) Cracking Brazil's Forest Code. *Science*, **344**, 363–364.
Sotta ED, Veldkamp E, Schwendenmann L (2007) Effects of an induced drought on soil carbon dioxide (CO2) efflux and soil CO2 production in an Eastern Amazonian rainforest, Brazil. *Global Change Biology*.
Spera SA, Cohn AS, VanWey LK, Mustard JF, Rudorff BF, Risso J, Adami M (2014) Recent cropping frequency, expansion, and abandonment in Mato Grosso, Brazil had selective land characteristics. 1–13.

Stehfest E, Bouwman L (2006) N2O and NO emission from agricultural fields and soils under natural vegetation: summarizing available measurement data and modeling of global annual emissions. *Nutrient Cycling in Agroecosystems*, **74**, 207–228.
Stickler C, Nepstad DC, Coe M, et al. (2009) The potential ecological costs and cobenefits of REDD: a critical review and case study from the Amazon region. *Global Change Biology*, **15**, 2803–2824.
Stickler CM, Coe MT, Costa MH, et al. (2013) Dependence of hydropower energy generation on forests in the Amazon Basin at local and regional scales. *Proceedings of the National Academy of Sciences*, **110**, 9601–9606.
Tallis H, Polasky S (2009) Mapping and Valuing Ecosystem Services as an Approach for Conservation and Natural-Resource Management. *Annals of the New York Academy of Sciences*, **1162**, 265–283.
Tilman D, Balzer C, Hill J, Befort BL (2011) Global food demand and the sustainable intensification of agriculture. *Proceedings of the National Academy of Sciences*, **108**, 20260–20264.
van Kessel C, Venterea R, Six J, Adviento-Borbe MA, Linquist B, van Groenigen KJ (2012) Climate, duration, and N placement determine N 2O emissions in reduced tillage systems: a meta-analysis. *Global Change Biology*, **19**, 33–44.
VanWey LK, Spera S, de Sa R, Mahr D, Mustard JF (2013) Socioeconomic development and agricultural intensification in Mato Grosso. *Philosophical Transactions of the Royal Society B: Biological Sciences*, **368**, 20120168–20120168.
Varella RF, Bustamante M, Pinto AS (2004) Soil fluxes of CO2, CO, NO, and N2O from an old pasture and from native savanna in Brazil. *Ecological Applications.*
Vasconcelos SS, Zarin DJ, Capanu M, et al. (2004) Moisture and substrate availability constrain soil trace gas fluxes in an eastern Amazonian regrowth forest. *Global Biogeochemical Cycles*, **18**, n/a–n/a.
Veldkamp E (1994) Organic carbon turnover in three tropical soils under pasture after deforestation. *Soil Science Society of America Journal*.
Veldkamp E, Becker A, Schwendenmann L (2003) Substantial labile carbon stocks and microbial activity in deeply weathered soils below a tropical wet forest. *Global Change Biology*.
Veldkamp E, Davidson E, Erickson H, Keller M, Weitz A (1999) Soil nitrogen cycling and nitrogen oxide emissions along a pasture chronosequence in the humid tropics of Costa Rica. *Soil Biology and Biochemistry*, **31**, 387–394.
Venterea RT, Burger M, Spokas KA (2005) Nitrogen Oxide and Methane Emissions under Varying Tillage and Fertilizer Management. *Journal of Environment Quality*, **34**, 1467.
Venterea RT, Halvorson AD, Kitchen N, et al. (2012) Challenges and opportunities for mitigating nitrous oxide emissions from fertilized cropping systems. *Frontiers in Ecology and the Environment*, **10**, 562–570.
Verchot L, Krug T, Lasco R, et al. (2012) IPCC Guidelines for National Greenhouse Gas Inventories: Agriculture, Forestry and Other Land Use; Chapter 6: Grasslands. 1–49.
Verchot LV, Brienza S Júnior, de Oliveira VC, Mutegi JK, Cattânio JH, Davidson EA (2008) Fluxes of CH4, CO2, NO, and N2O in an improved fallow agroforestry

system in eastern Amazonia. *Agriculture, Ecosystems & Environment*, **126**, 113–121.
Verchot LV, Davidson EA, Cattânio H, ackerman I, Erickson H, Keller M (1999) Land use change and biogeochemical controls of nitrogen oxide emissions from soils in eastern Amazonia. *Global Biogeochemical Cycles*.
Vitousek P, Mooney H, Lubchenco J, Melillo JM (1997a) Human domination of Earth's ecosystems. *Science*, **277**, 494.
Vitousek PM, Aber J, Howarth RW, Likens GE (1997b) Human alteration of the global nitrogen cycle: causes and consequences.
West P, Gibbs H, Monfreda C, Wagner J, Barford C, Carpenter S, Foley J (2010) Trading carbon for food: Global comparison of carbon stocks vs. crop yields on agricultural land. *Proceedings of the National Academy of Sciences*,, 1–4.
West PC, Narisma GT, Barford CC, Kucharik CJ, Foley JA (2011) An alternative approach for quantifying climate regulation by ecosystems. *Frontiers in Ecology and the Environment*, **9**, 126–133.
Wick B, Veldkamp E, De Mello WZ (2005) Nitrous oxide fluxes and nitrogen cycling along a pasture chronosequence in Central Amazonia, Brazil. *Biogeosciences*.
Williams MR, Fisher TR, Melack JM (1997) Solute dynamics in soil water and groundwater in a central Amazon catchment undergoing deforestation. *Biogeochemistry*.